SYNTHESIS OF A NON-LINEAR FEEDBACK SYSTEM WITH SIGNIFICANT PLANT-IGNORANCE FOR PRESCRIBED TIME-DOMAIN TOLERANCES

by
K. R. KRISHNAN
and
I. M. HOROWITZ

This research was supported by the National Aeronautics and Space Administration under Research Grant NGR 06-003-083, and by the National Science Foundation under Grant GK-33485.

DEPARTMENT OF ELECTRICAL ENGINEERING
UNIVERSITY OF COLORADO
BOULDER, COLORADO
JANUARY 1, 1973

SYNTHESIS OF A NON-LINEAR FEEDBACK SYSTEM WITH SIGNIFICANT PLANT-IGNORANCE FOR PRESCRIBED TIME-DOMAIN TOLERANCES

by

K. R. KRISHNAN

and

I. M. HOROWITZ

This research was supported by the National Aeronautics and Space Administration under Research Grant NGR 06-003-083, and by the National Science Foundation under Grant GK-33485.

DEPARTMENT OF ELECTRICAL ENGINEERING

UNIVERSITY OF COLORADO

BOULDER, COLORADO

TABLE OF CONTENTS

		Page
I.	STATEMENT OF THE PROBLEM	3
	1.1 Introduction	3
	1.2 Principle of Linear Design	4
	1.3 Design with Non-Linear Elements	7
II.	ANALYSIS OF NON-LINEAR RESPONSE	8
	2.1 The Clegg Integrator	8
	2.2 Stability in the Absence of Input	10
	2.3 Equations for Calculation of Forced-Response	12
	2.4 A Modified Non-Linear Device	19
	2.5 Equations for Calculation of Forced-Response with Modified Non-Linear Device	21
	2.6 Second-Order Non-Linear Step- and Disturbance-Response	23
	2.7 Noise Response of the Clegg Integrator and the Modified Non-Linear Device	26
III.	PROCEDURE FOR NON-LINEAR DESIGN	35
	3.1 The Design Problem	35
	3.2 Design Procedure	36
	3.2.1 Outline of Procedure for Linear Design	37
	3.2.2 Development of Procedure for Non-Linear Design	39
	3.2.3 Steps in Non-Linear Design	45
IV.	A DESIGN EXAMPLE	48
	4.1 The Problem	48
	4.2 Linear Design	49
	4.3 Non-Linear Design	50

Table of Contents (Continued)

Page

4.4 Results 52

4.5 Conclusion 53

FIGURES 54

REFERENCES 101

APPENDIX 102

ABSTRACT

The problem considered is the design of a feedback system containing a linear, time-invariant, minimum-phase plant, whose parameters are known only within given bounds, such that the time-response of the system remains within specified limits. A quasi-optimal design, for given design constraints, is one which minimizes the effect of white sensor-noise on the input to the plant. Horowitz and Sidi have presented a method for the design of such a quasi-optimal, linear time-invariant system.

This report investigates the use of the non-linear device known as the Clegg Integrator in the design of such a system. The describing-function of the Clegg Integrator has the same magnitude characteristic, apart from a scale factor, as the linear integrator, but has 52° less phase-lag, at all frequencies, than the linear integrator; thus, when used in a feedback system, it provides a larger stability margin than the linear integrator. This property allows the non-linear feedback system to be designed so that the sensor-noise is attenuated more than in the linear design.

The non-linear time-response is calculated in terms of an equivalent linear representation, and the reduced phase-lag in the frequency-domain is seen to correspond, in general, to smaller overshoot in the time-response. In order to obtain satisfactory steady-state response, the non-linear device is modified by putting a linear integrator in parallel with it.

It is shown that for given bounds on plant-ignorance and time-response tolerances, the non-linear feedback system can be designed such that the effect of white sensor-noise on the plant-input is smaller than in a linear design. A method is developed for implementing the non-linear design in terms of an equivalent linear design by Horowitz and Sidi's method.

CHAPTER I

STATEMENT OF THE PROBLEM

1.1 Introduction

An important, fundamental problem in control is the design of a system whose performance remains within specified limits despite the uncertainty in the parameters of a vital system portion denoted as the plant. In Fig. 1.1, let P(s) be the transfer-function of a linear, time-invariant, minimum-phase plant whose parameters assume values within a given range. Note that we are not considering the case of a time-varying plant whose parameters change during the time an input signal is present; rather, we suppose the plant to be constant while a signal is being applied, but allow it to change between successive applications of the input; or else, we may take the plant parameters to be fixed but known only within certain tolerances.

Given such a plant P(s) with the range of values of its parameters, and given a range of acceptable overall system performance, such as, for example, bounds for its step-response as in Fig. 1.2, the problem (for design with linear, time-invariant elements) is to find fixed compensating functions G(s) and F(s), such that the response of the closed-loop system of Fig. 1.1 lies within the specified bounds for all values of the plant-parameters within the given range.

1.2 Principle of Linear Design[1]

The general principle underlying a linear design for this problem can be described as follows: the closed-loop transfer-function in Fig. 1.1 is

$$T(s) \triangleq \left.\frac{C(s)}{R(s)}\right|_{N(s)=0} = \frac{F(s)\,L(s)}{1+L(s)}$$

where

$$L(s) \triangleq P(s)\,G(s)$$

With $s = j\omega$, if $|L(j\omega)| >> 1$, then $T(j\omega) \approx F(j\omega)$, and is thus quite insensitive to changes in $L(j\omega)$ (caused by changes in $P(j\omega)$), so long as $|L(j\omega)|$ remains much larger than 1. In a linear design, a minimum-phase $G(s)$ is so chosen that $|L(j\omega)| >> 1$ for all possible plant-conditions, over a frequency-range $0 \leq \omega \leq \omega_c$ whose width ω_c depends on the response specifications. Thus $T(j\omega) \approx F(j\omega)$ for $0 \leq \omega \leq \omega_c$, independent of the actual plant condition, and if ω_c is properly chosen, the closed-loop time-response essentially depends on $F(j\omega)$ and can be made quite insensitive to changes in the plant.

We note from Fig. 1.1, however, that the transfer-function between the noise-source $n(t)$ in the feedback sensor and the input $z(t)$ to the plant is

$$B(s) \triangleq \left.\frac{Z(s)}{N(s)}\right|_{R(s)=0} = -\frac{1}{P(s)}\left[\frac{L(s)}{1+L(s)}\right] .$$

If $S_{nn}(\omega)$ = spectral density of n(t)

$S_{zz}(\omega)$ = spectral density of z(t), then,

$S_{zz}(\omega) = S_{nn}(\omega)\ |B(j\omega)|^2$, and

$$z_{rms} = \left[\frac{1}{2\pi}\int_{-\infty}^{\infty} S_{zz}(\omega)d\omega\right]^{1/2} .$$

Considering $B(j\omega)$ for $\omega >> \omega_c$, where $|L(j\omega)| << 1$, $|B(j\omega)|^2 \approx \left|\frac{L(j\omega)}{P(j\omega)}\right|^2 = |G(j\omega)|^2$, and if $|G(j\omega)| > 1$, the sensor noise-components at such frequencies are amplified at the input to the plant and tend to produce saturation.

$|G(j\omega)| > 1$ implies that $|L(j\omega)| > |P(j\omega)|$, a condition that occurs when the plant is unable to provide the required loop-gain which must then be supplied by the compensation $G(j\omega)$. The condition $|L(j\omega)| > |P(j\omega)|$ can occur over a wide frequency-range even when $|L(j\omega)| < 1$ over that range, as illustrated in Fig. 1.3 with $P(s) = \frac{1}{s}$ and

$$L(s) = P(s)G(s) = 2048\ \frac{(s+1)}{s(s+8)(s+16)^2} .$$

$|L(j\omega)| < 1$ for all $\omega > 8$ rad/sec but $|G(j\omega)| \geq 1$ until ω exceeds about 40 rad/sec. Fig. 1.4 shows $|G(j\omega)|^2$ as a function of ω on linear scales, and it is seen that the frequency-range $8 \leq \omega < 40$ (throughout which $L(j\omega) < 1$) is, in fact, the significant range for the amplification of sensor-noise at the plant-input.

It is, therefore, desirable to reduce $|L(j\omega)|$ as rapidly as possible beyond the frequency-range $0 \leq \omega \leq \omega_c$, in which sensitivity-specifications require it to be large. However,

in a minimum-phase transfer-function, rapid attenuation in the magnitude characteristic is accompanied by a large phase-lag, and a limit is set to the rate of attenuation of $|L(j\omega)|$ by the stability requirement that the phase-lag of $L(j\omega)$ cannot exceed 180° till $|L(j\omega)|$ has become less than 1, for all possible plant-parameter values. Thus, as a result of the relation between the magnitude and phase functions of $L(j\omega)$, the attenuation of $|L(j\omega)|$ has to be gradual until $|L(j\omega)|$ has become less than 1 at a phase-lag less than 180°, for all plant-conditions.

We may define an optimal design L(s) for the above problem as one which satisfies the specifications on closed-loop response while minimizing the effect of sensor noise on the input to the plant. This definition takes into account the power spectrum of the noise source. This problem has not yet been solved. Another problem, which approximates the above when the sensor-noise is white, is defined as follows: Let q = (number of finite poles - number of finite zeros) of L(s). Then, for large $|s|$, L(s) has the asymptotic form

$$L(s) \approx \frac{k}{s^q} \tag{1.1}$$

For a given q, the optimal L(s) is defined as that which meets the specifications on closed-loop response and has the smallest possible value of k in Equation (1.1).

This problem of optimal linear design has been investigated by Horowitz and Sidi[1,2], who have established the existence and properties of the optimal design for a class of problems, and developed a procedure for its implementation.

1.3 Design with Non-Linear Elements

The fixed relation that exists between the magnitude and phase of a transfer-function sets a limit to the maximum rate of attenuation of $|L(j\omega)|$ possible in a stable linear system, over a frequency-range that is important in regard to amplification of sensor-noise. Can this limitation, inherent in a linear design, be overcome by the use of non-linear devices in the compensation? Suppose there is a non-linear device with a describing-function in which the magnitude characteristic is associated with a smaller phase-lag than that due to the same magnitude characteristic in a linear, time-invariant device. Such a device would appear to permit a sharper reduction in the magnitude of the loop describing function than that allowed in a linear design. We are then led to the question, "Using such a non-linear device, can the specifications on response, in the problem stated above, be met with a compensation which produces a smaller noise output than the optimal linear design for the same problem?"

This report presents the results of an investigation of this question, in which the non-linear device is the Clegg Integrator[3,4]. It is shown that the non-linear device leads to a design with a smaller effect of sensor noise than in the optimal linear design, for problems of two-degree-of-freedom design.

CHAPTER II

ANALYSIS OF NON-LINEAR RESPONSE

2.1 The Clegg Integrator

This device[3,4] is a non-linear integrator obtained from a linear integrator merely by arranging its output to be reset to zero whenever the input signal crosses zero and changes sign. Between consecutive zero-crossings of the input, the device is just a linear integrator. It can be simulated on the analogue computer by using logic circuits to detect zero-crossings of the input and to switch a linear integrator between "reset" and "compute" modes. The simulation we used is shown in Fig. 2.1.

Describing Function of the Clegg Integrator

If a non-linear device produces a periodic output $y(t)$ to the sinusoidal input $x(t) = A \sin\omega t$, its describing-function is defined as the complex ratio

$$\frac{Be^{j\theta}}{A} ,$$

where $B \sin(\omega t+\theta)$ is the fundamental component in the Fourier series expansion of $y(t)$.

When the input to the Clegg Integrator is $x(t) = A \sin\omega t$, its output $y(t)$ has the periodic waveform shown in Fig. 2.2, and is given, over the first period, by the expression

$$y(t) = \begin{cases} -\frac{A}{\omega}\cos\omega t + \frac{A}{\omega} & , \quad 0 \leq \omega t < \pi \\ -\frac{A}{\omega}\cos\omega t - \frac{A}{\omega} & , \quad \pi \leq \omega t < 2\pi \end{cases}$$

i.e. $y(t) = -\frac{A}{\omega}\cos\omega t + f(t)$, where $f(t)$ is a square wave of amplitude $\frac{A}{\omega}$ and period $\frac{2\pi}{\omega}$.

The Fourier series for $f(t)$ is

$$f(t) = \frac{4A}{\pi\omega}\left[\sin\omega t + \frac{1}{3}\sin 3\omega t + \frac{1}{5}\sin 5\omega t + \ldots\right]$$

and, therefore, $y(t)$ has the Fourier series

$$y(t) = \left[\frac{4A}{\pi\omega}\sin\omega t - \frac{A}{\omega}\cos\omega t\right] + \frac{4A}{\pi\omega}\left[\frac{1}{3}\sin 3\omega t + \frac{1}{5}\sin 5\omega t + \ldots\right] .$$

The fundamental component of $y(t)$ is

$$\frac{A}{\omega}\left[\frac{4}{\pi}\sin\omega t - \cos\omega t\right] = \frac{A}{\omega}\left[1 + \frac{16}{\pi^2}\right]^{1/2}\sin\left(\omega t - \tan^{-1}\frac{\pi}{4}\right)$$

$$= \frac{1.62A}{\omega}\, e^{-j38^\circ}$$

$$\triangleq Be^{j\theta}$$

Therefore, the describing function $D(j\omega)$ of the Clegg Integrator is given by

$$D(j\omega) = \frac{B}{A}\, e^{j\theta} = \frac{1.62}{\omega}\, e^{-j38^\circ} = 1.62\left(\frac{1}{j\omega}\right) e^{j52^\circ} \quad ,$$

while the transfer function of a linear integrator, for $s = j\omega$, is $\left(\frac{1}{j\omega}\right)$. We note that the describing function of the non-linear integrator has the same magnitude characteristic as the linear integrator, apart from a scale factor of 1.62, but has a lag of 38° at all frequencies, which is a lead of 52° over the phase of the linear integrator. The describing-function is independent of the input amplitude A, a fact which makes closed-loop calculations as simple as open-loop calculations.

2.2 Stability in the Absence of Input

From the describing-function of the Clegg Integrator, it appears that a closed-loop system that is unstable with a linear integrator might be stable when a Clegg Integrator replaces the linear integrator. For example, in the linear system shown in Fig. 2.3-a, the loop transmission $L(s) = \frac{k}{s^2}$ and the condition for free oscillations is $1 + L(j\omega) = 0$, whose solution is $\omega = k^{1/2}$; hence, the system is unstable for all k, the frequency of oscillations depending on k. The result of analogue simulation for $k = 1$ is shown in Fig. 2.3-b.

The system of Fig. 2.4-a is obtained by replacing a linear integrator in the system of Fig. 2.3-a by the Clegg Integrator. Since the loop-describing function $L_d(j\omega) = \frac{1.62ke^{j52°}}{(j\omega)^2}$, the equation $1 + L_d(j\omega) = 0$ is not satisfied by any real ω and k. Thus, according to

describing-function theory, in the absence of external input, the non-linear system should be stable for all k. This is borne out by the results of analogue simulation for k = 10 and k = 100, shown in Figures 2.4-b and 2.4-c, respectively.

As another example, consider the linear system of Fig. 2.5-a. The loop-transmission $L(s) = \frac{k}{s(s+1)^2}$ and the equation $1 + L(j\omega) = 0$ has the solution $\omega = 1$, $k = 2$. Thus, the system is stable for $0 < k < 2$ and breaks into unstable oscillations of frequency 1 rad/sec at $k = 2$. The result of analogue simulation for $k = 2.1$ is shown in Fig. 2.5-b.

On replacing the linear integrator in the system of Fig. 2.5-a by the Clegg Integrator, the non-linear system of Fig. 2.6-a is obtained. The loop-describing function $L_d(j\omega) = \frac{1.62ke^{j52^\circ}}{j\omega(j\omega+1)^2}$, and the equation $1 + L_d(j\omega) = 0$ has the solution $\omega = 2.9$ and $k = 17$. The non-linear system is thus stable for $0 < k < 17$ and breaks into unstable oscillations of frequency 2.9 rad/sec at $k = 17$. Figures 2.6-b and 2.6-c show the non-linear system responses at $k = 5$ and $k = 16$ respectively, and there is evidence of a stable limit cycle, with an amplitude of about 0.15 volts for the case $k = 16$, while Fig. 2.7 shows the unstable oscillations at $k = 18$.

The stable limit cycle occurring in Fig. 2.6-c, for example, is not predicted by the single input describing-function of the Clegg Integrator. It occurs in a situation

where the oscillations at the input to the Clegg Integrator have a non-zero mean value and a dual-input describing-function of the Clegg Integrator must be investigated to account for it. This point is considered again in Sections 2.3 and 2.4.

2.3 Equations for Calculation of Forced Response

The verification of stability in the absence of input, however, gives no indication of the forced-response of the non-linear system, such as, for example, its response to a step-input. We now consider the calculation of forced-response of a system containing the Clegg Integrator, assuming that all other elements of the system are linear and time-invariant.

We have the following relation between the input x(t) to the Clegg Integrator and its output y(t):

$$y(t) = \int_{t_z}^{t} x(p)dp \qquad (2.1)$$

where t_z is the instant of the last zero-crossing of the input x prior to t. It is thus clear that the zero-crossings of the input have a decided effect on the output. Consider now the interval $[t_o, t_f]$ and suppose that $t_1, \ldots, t_n$ are the instants of zero-crossing of x(t) in this interval, with $t_o \leq t_1 < t_2 \ldots < t_n \leq t_f$. Then, over the sub-interval $t_i \leq t < t_{i+1}$,

$(i = 0,1,\ldots,n-1)$, we have

$$y(t) = \int_{t_i}^{t} x(p)dp \qquad , \qquad t_i \le t < t_{i+1}$$

$$= \int_{t_o}^{t} x(p)dp - \int_{t_o}^{t_i} x(p)dp$$

$$= \int_{t_o}^{t} x(p)dp - \sum_{k=1}^{i} \int_{t_{k-1}}^{t_k} x(p)dp \qquad ;$$

and, $y(t_{i+1}) = 0$, the output being reset to zero as $x(t)$ crosses zero at t_{i+1}. Using the unit-step function $u(t)$, we may write a single expression for $y(t)$ for the entire interval $[t_o, t_f]$ as follows:

$$y(t) = \int_{t_o}^{t} x(p)dp - \sum_{k=1}^{n} \left[\int_{t_{k-1}}^{t_k} x(p)dp \right] u(t-t_k); \; t_o \le t \le t_f \qquad (2.2)$$

We note that $y(t)$ is discontinuous at the instants t_i of zero-crossing of $x(t)$, being reset to zero at t_i from the value

$$y(t_i-) = \int_{t_{i-1}}^{t_i} x(p)dp \triangleq y_i \qquad (2.3)$$

Substituting from (2.3) into (2.2),

$$y(t) = \int_{t_o}^{t} x(p)dp - \sum_{i=1}^{n} y_i \, u(t-t_i)$$

$$= \int_{t_o}^{t} \left[x(p) - \sum_{i=1}^{n} y_i \delta(p-t_i) \right] dp \; , \quad t_o \le t \le t_f \qquad (2.4)$$

which can be represented as the output of a linear integrator to which is applied the sum of $x(t)$ and an impulse-train $a(t) = -\sum_i y_i \delta(t-t_i)$. We thus arrive at the equivalence shown in Fig. 2.8, in which the Clegg Integrator is replaced by a linear integrator and the resets are represented by the addition of a suitable impulse-train at its input.

With this linear representation of the Clegg Integrator, we may calculate the response as the sum of the linear responses to the actual input and to the "equivalent input" consisting of a train of impulses.

Thus the closed-loop non-linear system of Fig. 2.9 may be represented by the linear system of Fig. 2.10, and the forced-response calculated by adding the response due to the input $r(t)$ to that due to the impulse-train. We thus obtain the pair of equations

$$c(t) = \int_o^t r(p)h(t-p)dp - \sum_i y_i h(t-t_i) \qquad (2.5)$$

$$y(t) = \int_o^t r(p)v(t-p)dp - \sum_i y_i v(t-t_i) \qquad (2.6)$$

where

$$\left.\begin{aligned} H(s) &= \mathcal{L}h(t) = \frac{C(s)}{R(s)} = \frac{C(s)}{A(s)} \\ V(s) &= \mathcal{L}v(t) = \frac{Y(s)}{R(s)} = \frac{Y(s)}{A(s)} \end{aligned}\right\} \quad \text{for the } \underline{\text{linear}} \text{ system of Fig. 2.10;}$$

and, $y_i \triangleq \lim_{t \to t_i-} y(t)$, with the t_i's being the instants at

which $e(t) = 0$, i.e. $r(t_i) = c(t_i)$, $i = 1,2,\ldots$; these are the instants at which the Clegg Integrator is reset. We note that for $t < t_i$, $h(t-t_i) = v(t-t_i) = 0$.

Equations (2.5) and (2.6) do not seem to admit of a general analytical solution for $c(t)$ and $y(t)$ but a numerical solution may always be constructed in the following manner: for $0 \leq t < t_1$ (i.e. till the first reset), $c(t)$ and $y(t)$ are given by just the integral terms in Equations (2.5) and (2.6):

$$\left.\begin{aligned} c(t) &= \int_0^t r(p)h(t-p)dp \qquad (2.7) \\ y(t) &= \int_0^t r(p)v(t-p)dp \qquad (2.8) \end{aligned}\right\} \quad 0 \leq t < t_1 \quad .$$

Expression (2.7) for $c(t)$, in fact, determines whether, at all, there is an instant $t_1 > 0$ at which $e(t_1) = r(t_1)-c(t_1) = 0$. If that condition never occurs, then the input to the Clegg Integrator never changes sign and it is never reset; in that case, $c(t)$ and $y(t)$ are identical with the corresponding linear responses (those obtained when a linear integrator is used in place of the Clegg Integrator), and are given by Equations (2.7) and (2.8) for all $t \geq 0$. If, however, Equation (2.7) does give a $t_1 > 0$ at which $r(t_1) - c(t_1) = 0$, then Equation (2.8) determines the value of $y_1 \triangleq y(t_1-)$, and the terms $-y_1h(t-t_1)$ and $-y_1v(t-t_1)$ are added to the right-hand side of Equations (2.7) and (2.8) respectively, enabling the non-linear response to be calculated for $t \geq t_1$.

In general, Equation (2.5) determines whether there is a reset at t_{j+1} following a reset at t_j. If no reset occurs

after t_j, then, for all $t \geq t_j$.

$$c(t) = \int_0^t r(p)h(t-p)dp - \sum_{i=1}^{j} y_i h(t-t_i)$$

$$y(t) = \int_0^t r(p)v(t-p)dp - \sum_{i=1}^{j} y_i v(t-t_i)$$

If another reset does occur at t_{j+1}, then Equation (2.6) determines $-y_{j+1} \triangleq -y(t_{j+1}-)$, the strength of the impulse to be added at the input to the integrator at t_{j+1} in order to calculate $c(t)$ and $y(t)$ for $t \geq t_{j+1}$.

Setting $r(t) = u(t)$ in Equations (2.5) and (2.6), we get equations for the step-response of the system of Fig. 2.9. It is obvious that if the step-response of the corresponding linear system (obtained upon replacing the Clegg Integrator by a linear integrator) has no overshoot, then the condition $c(t) = r(t) = 1$ never occurs for finite t; thus t_1 does not exist and the non-linear step-response is identical with the corresponding linear step-response.

What is the nature of the non-linear step-response in the case when the corresponding linear step-response has overshoot? The instant of the first overshoot in the linear step-response is the instant t_1 of the first reset of the Clegg Integrator in the non-linear case, and for $0 \leq t \leq t_1$, the linear and non-linear responses are identical. Equations (2.5) and (2.6) enable the further calculation of the non-linear response. It is instructive to carry out the calculations for a second-order system in which the corresponding linear step-response

can have overshoot. An analytical solution of Equations (2.5) and (2.6) is possible in this special case.

Let us consider the step-response of the non-linear system shown in Fig. 2.11. The corresponding linear system, shown in Fig. 2.12, has the transfer-function $H(s) = \frac{C(s)}{R(s)} = \frac{k}{s^2+as+k}$, and will have overshoot in its step-response if $k > \frac{a^2}{4}$. The linear step-response is given by

$$c(t) = 1 - \frac{1}{\sqrt{1-\delta^2}} e^{-\omega_n \delta t} \sin\left(\omega_n \sqrt{1-\delta^2}\, t + \cos^{-1}\delta\right) \qquad (2.9)$$

where

$$\omega_n = \sqrt{k}$$

$$\delta = \frac{a}{2\sqrt{k}} = \frac{a}{2\omega_n} \quad ;$$

the instant of first overshoot, which is the instant t_1 of the first reset of the Clegg Integrator in the non-linear case, is given by

$$t_1 = \frac{\pi - \cos^{-1}\delta}{\omega_n \sqrt{1-\delta^2}} \qquad (2.10)$$

On calculating the expressions in Equations (2.5) and (2.6), it is found that

$$t_i = t_1 + \frac{(i-1)\pi}{\omega_n \sqrt{1-\delta^2}} \quad , \quad i = 1,2,3,\ldots$$

$$= \frac{i\pi - \cos^{-1}\delta}{\omega_n \sqrt{1-\delta^2}} \quad , \quad i = 1,2,3,\ldots \qquad (2.11)$$

and

$$c(t) = \begin{cases} 1 - \dfrac{e^{-\omega_n \delta t}}{\sqrt{1-\delta^2}} \sin\left(\omega_n \sqrt{1-\delta^2}\, t + \cos^{-1}\delta\right) & , \; 0 \le t \le t_1 \\ 1 - \dfrac{2\delta e^{-\omega_n \delta (t-t_1)}}{\sqrt{1-\delta^2}} \sin\left[\omega_n \sqrt{1-\delta^2}\, (t-t_1)\right] & , \; t_1 \le t \le t_2 \\ c\left(t - \dfrac{\pi}{\omega_n \sqrt{1-\delta^2}}\right) & , \; t \ge t_2 \end{cases} \qquad (2.12)$$

Equation (2.12) describes a step-response with a periodic undershoot, and the result of analogue simulation shown in Fig. 2.13 confirms this conclusion.

We thus find that while the non-linear system of Fig. 2.11 is stable without an input, as one expects from the describing-function of the loop, its response to a step-input contains forced oscillations and does not reach a steady state. This result is not explained by the single-input sinusoidal describing function of the Clegg Integrator for the simple reason that it is inadequate for the situation in which a step-input is applied. The actual input to the Clegg Integrator is $e(t) = 1 - c(t)$ and it is seen to oscillate about a <u>non-zero</u> mean value. The sinusoidal describing-function is not applicable in this situation.

We have shown earlier that the non-linear step-response is identical with the corresponding linear step-response whenever the latter has no overshoot. In the second-order example above, we also find that if the linear step-response

does have overshoot, the non-linear response contains sustained oscillations. Simulation of several higher-order systems suggests that, in general, the non-linear step-response contains sustained oscillations whenever the corresponding linear step-response has overshoot. An analytical proof of this fact has not been found, but the instances in which it has been verified are themselves sufficient to show that the Clegg Integrator cannot be used without some modification.

2.4 A Modified Non-Linear Device

It has been found that when a linear integrator is put in parallel with the Clegg Integrator, the sustained oscillations in the step-response are eliminated. The modified non-linear device, shown in Fig. 2.14-a, has the describing-function $\left(\frac{1.62e^{j52^\circ}+b}{j\omega} \right)$, which has less phase-lag than the corresponding linear transfer-function $\left(\frac{1+b}{j\omega} \right)$.

The phase lead obtained in the non-linear device over the corresponding linear transfer-function is plotted as a function of b in Fig. 2.14-b.

Step-Response

Fig. 2.15 shows a closed-loop system with this non-linear device and Fig. 2.16 shows its step-response. The corresponding linear system is shown in Fig. 2.17 and its step-response in Fig. 2.18. The non-linear response now attains the same steady-state as the linear response but with much less oscillation than the linear response. By simulation of a third-order

system, it was also verified that the limit of stable operation of the non-linear system corresponds to the sinusoidal describing-function $\left(\frac{1.62e^{j52^\circ}+b}{j\omega} \right)$ of the non-linear device, both in the absence of input and the presence of a step-input. In explanation of this result, we note that due to the linear integrator in parallel with the Clegg Integrator, any sustained oscillations at the input to the Clegg Integrator must have zero mean, whether or not there is an input (unless the response itself is unbounded). The sinusoidal describing-function is applicable in this situation and the results agree with conclusions based on it. In other words, within the stability limit set by the describing-function, the step-response cannot have sustained oscillations.

Ramp-Response

While the presence of a linear integrator in parallel with the Clegg Integrator inside a closed-loop removes sustained oscillations from the step-response of the closed-loop, the nature of the ramp-response remains to be considered. Of course, with the device (Clegg Integrator + $\frac{b}{s}$) at the error-junction, if the corresponding linear ramp-response has no overshoot, then the non-linear ramp-response is identical with the linear ramp-response and is thus free of sustained oscillations. However, if the corresponding linear loop-transmission is of Type-0 or Type-1 and the corresponding linear ramp-response has overshoot, it turns out that the non-linear ramp-response contains sustained oscillations, as demonstrated by Fig. 2.20, the ramp-response of the system of Fig. 2.19.

This happens because, with a ramp input, oscillations at the input to the Clegg Integrator do not have zero mean-value if the loop-transmission is of Type-0 or Type-1, but must have a non-zero mean value to give rise to the ramp in the output. The sinusoidal describing-function of the Clegg Integrator is inapplicable in this situation. Following this train of thought, we are led to conclude that if the loop-transmission is of Type-2 (or higher) the ramp-response should be free of sustained oscillations, and, in general, if a steady-state condition requires that at large t, the input to the Clegg Integrator has zero mean, then the sinusoidal describing-function is applicable, and the non-linear system response will be free of sustained oscillations within the stability limit determined by describing-function theory. This conclusion is borne out by Fig. 2.22, the ramp-response of Fig. 2.21. We note that since the linear system corresponding to the system of Fig. 2.21 is unstable, the corresponding linear ramp-response is, in fact, unstable, while the non-linear response is stable.

2.5 Equations for Calculation of Forced-Response with Modified Non-Linear Device

The calculation of time-response with the modified non-linear device follows directly from the linear representation suggested earlier for the Clegg Integrator, and is illustrated with the system of Fig. 2.23. The equivalent linear representation is given in Fig. 2.24. The transfer-functions needed in the calculations are:

$$(i)\quad H(s) = \mathcal{L}h(t) \triangleq \frac{C(s)}{R(s)} = \frac{L(s)}{1+L(s)} \quad , \text{ with } L(s) = \frac{P(s)(1+b)}{s}$$

$$(ii)\quad V(s) = \mathcal{L}v(t) \triangleq \frac{Y(s)}{R(s)} = \frac{1}{s}\left(\frac{1}{1+L(s)}\right)$$

$$(iii)\quad H_a(s) = \mathcal{L}h_a(t) \triangleq \frac{C(s)}{A(s)} = \frac{1}{1+b}\left(\frac{L(s)}{1+L(s)}\right) = \frac{H(s)}{1+b} = \mathcal{L}\frac{h(t)}{1+b}$$

$$(iv)\quad V_a(s) = \mathcal{L}v_a(t) \triangleq \frac{Y(s)}{A(s)} = \frac{1}{s}\left[\frac{1+\frac{P(s)b}{s}}{1+L(s)}\right] = \frac{V(s)}{1+b} + \frac{b}{s(1+b)}$$

$$= \mathcal{L}\left(\frac{v(t)+b}{1+b}\right) \quad .$$

The following equations, derived in the manner of Equations (2.5) and (2.6), describe the time-response in this case:

$$c(t) = \int_o^t r(p)h(t-p)dp - \sum_i y_i h_a(t-t_i) \qquad (2.13a)$$

$$= \int_o^t r(p)h(t-p)dp - \frac{1}{1+b}\sum_i y_i h(t-t_i) \qquad (2.13b)$$

$$y(t) = \int_o^t r(p)v(t-p)dp - \sum_i y_i v_a(t-t_i) \qquad (2.14a)$$

$$= \int_o^t r(p)v(t-p)dp - \frac{1}{1+b}\sum_i y_i\left[b+v(t-t_i)\right] \qquad (2.14b)$$

where, as before,

$$y_i \triangleq \lim_{t\to t_i-} y(t) \quad .$$

Equations (2.13a) and (2.14a) differ from Equations (2.5) and (2.6) only in the appearance of $h_a(t)$ and $v_a(t)$, in place of $h(t)$ and $v(t)$, in the summation on the right-hand side. When $b = 0$, of course, Equations (2.13) and (2.14) reduce to Equations (2.5) and (2.6), since, in that case, $v(t) \equiv v_a(t)$ and $h(t) \equiv h_a(t)$.

2.6 Second-Order Non-Linear Step- and Disturbance-Response

Applying Equations (2.13) and (2.14) to the second-order case shown in Fig. 2.15, we now derive an expression for the maximum overshoot in the step-response, which occurs between t_1 and t_2, the first and second resets of the Clegg Integrator.

With $k_e \triangleq k(1+b)$,

$$H(s) \triangleq \frac{C(s)}{R(s)} = \frac{k_e}{s^2+as+k_e} \quad , \text{ and}$$

$$h(t) = \frac{\omega_n}{\sqrt{1-\delta^2}} \; e^{-\omega_n \delta t} \sin\left(\omega_n \sqrt{1-\delta^2}\; t\right) \quad ,$$

where $\omega_n = \sqrt{k_e}$

$$\delta = \frac{a}{2\sqrt{k_e}} \quad .$$

$$t_1 = \frac{\pi - \cos^{-1}\delta}{\omega_n \sqrt{1-\delta^2}} \tag{2.15}$$

Using Equations (2.13), (2.14) and (2.15), the step-response, for $t_1 \leq t \leq t_2$, is given by

$$c(t) = 1 - \left[\frac{b - 2\delta e^{\frac{\delta}{\sqrt{1-\delta^2}}(\pi - \cos^{-1}\delta)}}{(1+b)\sqrt{1-\delta^2}} \right] e^{-\omega_n \delta t} \sin\left(\omega_n \sqrt{1-\delta^2}\, t + \cos^{-1}\delta\right),$$

$$t_1 \leq t \leq t_2 \quad .$$

Setting $\frac{dc}{dt} = 0$, we find that the maximum of c(t) occurs at

$$t_{max} = \frac{\pi}{\omega_n \sqrt{1-\delta^2}} \quad , \quad \text{and}$$

$$c(t_{max}) = 1 + \left[\frac{b - 2\delta e^{\frac{\delta}{\sqrt{1-\delta^2}}(\pi - \cos^{-1}\delta)}}{1+b} \right] e^{-\frac{\pi\delta}{\sqrt{1-\delta^2}}} \quad .$$

Thus, $M_n(\delta, b) \triangleq$ the maximum overshoot in the non-linear step-response

$$= \left[\frac{b - 2\Delta e^{\frac{\delta}{\sqrt{1-\delta^2}}(\pi - \cos^{-1}\delta)}}{1 + b} \right] e^{-\frac{\pi\delta}{\sqrt{1-\delta^2}}} \qquad (2.17)$$

Since $M_L(\delta) \triangleq$ the overshoot in the corresponding linear step-response

$$= e^{-\frac{\pi\delta}{\sqrt{1-\delta^2}}} \qquad (2.18)$$

we note that for $b > 0$, $M_n(\delta, b) < M_L(\delta)$. Expression (2.17) can be negative in certain cases, showing that in those cases, the non-linear step-response has <u>undershoot</u> instead of overshoot.

In fact, $\frac{\partial M_n(\delta,b)}{\partial \delta} < 0$ for $0 \leq \delta < 1$ (see Appendix) and, therefore, for fixed b, the <u>maximum undershoot</u> occurs when $\delta = 1$ (critical damping), and is given by

$$\text{Maximum undershoot} = -M_n(1,b) = \frac{2e^{-1}}{1+b} = \frac{0.736}{1+b} \qquad (2.19)$$

For later use in non-linear design, we collect the following results on the second-order, non-linear step-response of the one-degree-of-freedom structure of Fig. 2.15:

(i) Maximum overshoot $= \left[\frac{b - 2\delta e^{\frac{\delta}{\sqrt{1-\delta^2}}(\pi - \cos^{-1}\delta)}}{1+b}\right] e^{-\frac{\pi\delta}{\sqrt{1-\delta^2}}}$ (2.17)

(ii) Maximum undershoot (occurs when $\delta = 1$) $= \frac{0.736}{1+b}$ (2.19)

The δ here, of course, refers to the damping in the corresponding linear transfer-function, and the maximum undershoot in the non-linear response occurs when the corresponding linear response is critically damped.

It may also be noted that expressions (2.17) and (2.19) also apply to the disturbance-response of the one-degree-of-freedom structure of Fig. 2.15, since, for this structure

disturbance-response = 1 - (step-response) .

Equations (2.17) and (2.18) compare the overshoots in the disturbance-responses of the corresponding non-linear and linear systems of Figures 2.15 and 2.17. We note that for a

given damping in the linear system, the non-linear response has less overshoot than the corresponding linear response; in consequence, for a given overshoot in the disturbance-response, the non-linear system can be designed with a smaller damping (in the corresponding linear system) than is possible in a linear design.

This is the principle that is applied later to show that in a two-degree-of-freedom design to meet specifications on step-response and disturbance-response, a non-linear design is possible which has a smaller bandwidth of (the corresponding linear) loop-transmission and transmits less feedback sensor-noise to the plant than the optimal linear design of Horowitz and Sidi.

In order to establish this result, we next consider the noise-response of the Clegg Integrator.

2.7 Noise-Response of the Clegg Integrator and the Modified Non-Linear Device

An input $x(t)$ to the Clegg Integrator produces the output $y(t)$ given by

$$y(t) = \int_{t_z}^{t} x(p)dp \qquad (2.1)$$

where t_z is the instant of the last zero-crossing of x prior to t. Let $T(t) \triangleq t - t_z$

= the interval between t and the last zero-crossing of x prior to t;

hence, $t_z = t - T(t)$, and thus

$$y(t) = \int_{t-T(t)}^{t} x(p)dp$$

When $x(t)$ is a stationary random process, the interval $T(t)$ is itself a stationary random process (or, for fixed t, a random variable). In principle, the statistics of T may be determined from those of $x(t)$, but such calculations have been possible only for a few processes[5], owing to the mathematical difficulties that arise. Even if the statistics of T are known, calculating the statistics of the output $y(t)$ is a formidable task, since this requires finding the expected value of a stochastic integral, one of whose limits is a random process whose statistics, in turn, depend on the integrated process.

It is known[5], however, that for a zero-mean Gaussian Markov process $x(t)$, the mean and variance of T tend to zero as the process $x(t)$ becomes more and more uncorrelated. This suggests an approximation that simplifies the problem and enables us to calculate the power spectrum of the output. In the expression $\int_{t-T}^{t} x(p)dp$, the random variable T in the lower limit is replaced by its mean value T_m. We then have the approximate relation

$$y(t) = \int_{t-T_m}^{t} x(p)dp \qquad (2.20)$$

which is a stochastic integral with <u>deterministic</u> limits.

(i) Let x_m and y_m be the expected values of the stationary processes $x(t)$ and $y(t)$ respectively. Using E to denote expected value, we have, from Equation (2.20),

$$y_m = E\{y(t)\}$$

$$= E\left\{\int_{t-T_m}^{t} x(p)dp\right\}$$

$$= \int_{t-T_m}^{t} E\{x(p)\}dp$$

$$= T_m x_m \quad ;$$

in particular, $y_m = 0$ if $x_m = 0$.

(ii) Let F denote Fourier Transform and let

$R_{xx}(\tau) \triangleq$ auto-correlation of $x(t)$

$R_{yx}(\tau) \triangleq$ cross-correlation of $y(t)$ and $x(t)$

$R_{yy}(\tau) \triangleq$ auto-correlation of $y(t)$

$S_{xx}(\omega)$ = spectral density of $x(t)$ = $F\{R_{xx}(\tau)\}$

$S_{yx}(\omega)$ = cross-spectral density of $y(t)$ and $x(t)$ = $F\{R_{yx}(\tau)\}$

$S_{yy}(\omega)$ = spectral density of $y(t)$ = $F\{R_{yy}(\tau)\}$.

We have

$$R_{yx}(\tau) = E\{y(t+\tau)x(t)\}$$

$$= E\left\{\int_{t+\tau-T_m}^{t+\tau} x(p)x(t)dp\right\}$$

$$= \int_{t+\tau-T_m}^{t+\tau} E\{x(p)x(t)\}dp$$

$$= \int_{t+\tau-T_m}^{t+\tau} R_{xx}(p-t)dp$$

$$= \int_{o}^{T_m} R_{xx}(\tau-T_m+v)dv \qquad (2.21a)$$

Taking Fourier Transforms on both sides,

$$S_{yx}(\omega) = \int_{o}^{T_m} F\{R_{xx}(\tau-T_m+v)\}dv$$

$$= \int_{o}^{T_m} S_{xx}(\omega)e^{j\omega(v-T_m)}dv$$

$$= S_{xx}(\omega)\int_{o}^{T_m} e^{j\omega(v-T_m)}dv$$

$$= S_{xx}(\omega)\left[\frac{1-e^{-j\omega T_m}}{j\omega}\right] \qquad (2.21b)$$

Then, using the technique of statistical linearization[6,7], we define $G(j\omega)$, the random-describing function of the Clegg Integrator, as follows:

$$G(j\omega) \triangleq \frac{S_{yx}(\omega)}{S_{xx}(\omega)} = \left[\frac{1-e^{-j\omega T_m}}{j\omega}\right] \qquad (2.21c)$$

It then follows[6,7] that, for the Clegg Integrator,

$$\frac{S_{yy}(\omega)}{S_{xx}(\omega)} = |G(j\omega)|^2 = \frac{4}{\omega^2}\sin^2\left(\frac{\omega T_m}{2}\right) \qquad (2.21d)$$

For a linear integrator, the corresponding relation is

$$\frac{S_{yy}(\omega)}{S_{xx}(\omega)} = \frac{1}{\omega^2} \qquad (2.22)$$

Using the relation

$$y_{rms} = \left[\frac{1}{2\pi}\int_{-\infty}^{\infty} S_{yy}(\omega)d\omega\right]^{1/2} ,$$

Equations (2.21d) and (2.22) enable us to conclude that the Clegg Integrator in cascade with a pure attenuation of 0.5 gives a smaller noise output than a linear integrator $\frac{1}{s}$, regardless of the actual value of T_m, so long as Equation (2.20) constitutes a reasonable approximation to Equation (2.1).

Turning to the modified non-linear device of Fig. 2.14, the input x(t) and the output y(t) are related by

$$y(t) = b\int_{-\infty}^{t} x(p)dp + \int_{t-T}^{t} x(p)dp \qquad (2.23)$$

where, as before, (t-T) is the instant of the last zero-crossing of x before t. Approximating T by T_m, as before,

$$y(t) = b\int_{-\infty}^{t} x(p)dp + \int_{t-T_m}^{t} x(p)dp \qquad (2.24)$$

Writing $y(t) = y_1(t) + y_2(t)$, where $y_1(t) = b\int_{-\infty}^{t} x(p)dp =$

= output of the linear integrator $\frac{b}{s}$,

$$y_2(t) = \int_{t-T_m}^{t} x(p)dp = \text{output of the Clegg Integrator,}$$

we obtain,

$$S_{yx}(\omega) = S_{y_1x}(\omega) + S_{y_2x}(\omega)$$

$$= S_{xx}(\omega)\left[\frac{b}{j\omega} + G(j\omega)\right], \text{ where}$$

$$G(j\omega) = \frac{1-e^{-j\omega T_m}}{j\omega}$$

Thus, $G_1(j\omega) \triangleq \dfrac{S_{yx}(\omega)}{S_{xx}(\omega)}$

= describing-function of the modified non-linear device

$$= \left[\frac{b+1-e^{-j\omega T_m}}{j\omega}\right] \qquad (2.25a)$$

and $$\frac{S_{yy}(\omega)}{S_{xx}(\omega)} = |G_1(j\omega)|^2$$

$$= \frac{b^2 + 4(1+b)\sin^2\frac{\omega T_m}{2}}{\omega^2} \qquad (2.25b)$$

For the corresponding linear transfer-function $\frac{(b+1)}{s}$, we have

$$\frac{S_{yy}(\omega)}{S_{xx}(\omega)} = \frac{(b+1)^2}{\omega^2} = \frac{b^2+(1+b)+b}{\omega^2} \qquad (2.26)$$

Once again, comparison of Equations (2.25b) and (2.26) shows that the non-linear device in cascade with an attenuation of 0.5 will give a smaller noise output than the corresponding

linear element $\frac{(b+1)}{s}$, regardless of the actual value of T_m, so long as Equation (2.24) is a reasonable approximation to Equation (2.23).

Fig. 2.25 is a record of the square of the noise output (instantaneous noise power) of the linear and Clegg integrators produced by an input of zero-mean noise, and the results are in agreement with the above conclusions.

Let us now consider the effect of zero-mean sensor-noise n(t) on the output c(t) (in the absence of command input), in the linear and non-linear systems shown in Figures 2.26 and 2.27 respectively.

We have,

$$N_1(\omega) \triangleq \left| \frac{S_{cc}(\omega)}{S_{nn}(\omega)} \right|_{\text{linear system}}$$

$$= \left| \frac{\frac{(b+1)}{j\omega} P_1(j\omega)}{1 + \frac{(b+1)P_1(j\omega)}{j\omega}} \right|^2$$

$$\approx \frac{(b+1)^2}{\omega^2} |P_1(j\omega)|^2 \qquad (2.27)$$

at high frequencies where $\left| \frac{P_1(j\omega)}{j\omega} \right| << 1.$

$$N_2(\omega) \triangleq \left| \frac{S_{cc}(\omega)}{S_{nn}(\omega)} \right|_{\text{non-linear system}}$$

$$= \left| \frac{\frac{(b+1)-e^{-j\omega T_m}}{j\omega} P_2(j\omega)}{1+\frac{(b+1-e^{-j\omega T_m})P_2(j\omega)}{j\omega}} \right|^2$$

$$\approx \frac{[b^2+4(b+1)\sin^2(\frac{\omega T_m}{2})]}{\omega^2} |P_2(j\omega)|^2 \qquad (2.28)$$

at high frequencies where $\left|\frac{P_2(j\omega)}{j\omega}\right| << 1$. Thus,

$$\frac{N_2(\omega)}{N_1(\omega)} \approx \frac{[b^2+4(b+1)\sin^2(\frac{\omega T_m}{2})]}{(b+1)^2} \left|\frac{P_2(j\omega)}{P_1(j\omega)}\right|^2 \qquad (2.29)$$

at high frequencies where

$$\left|\frac{P_1(j\omega)}{j\omega}\right| << 1 \quad , \quad \left|\frac{P_2(j\omega)}{j\omega}\right| << 1 \quad .$$

We thus find that

$$\frac{N_2(\omega)}{N_1(\omega)} < 1 \quad \text{if} \quad |P_2(j\omega)| < \left|\frac{P_1(j\omega)}{2}\right| \text{ at high frequencies,}$$

i.e. if $|L_2(j\omega)|_{db} < |L_1(j\omega)|_{db} - 6$, at high frequencies where

$L_1(s) = \frac{(b+1)P_1(s)}{s}$ = the loop-transmission of the linear system of Fig. 2.26

$L_2(s) = \frac{(b+1)P_2(s)}{s}$ = the linear loop-transmission corresponding to the non-linear system of Fig. 2.27.

We shall show later that for given design specifications on the sensitivities of step- and disturbance-responses, the

use of the above non-linear device enables us to make a non-linear design in which the magnitude of $L_2(j\omega)$ is at least 6 db smaller, at high frequencies, than the magnitude of the loop-transmission $L_1(j\omega)$ in the optimal linear design for the same problem. This will show that, for given specifications, the non-linear design achieves a smaller transmission of high frequency noise than is possible in the linear design.

CHAPTER III

PROCEDURE FOR NON-LINEAR DESIGN

3.1 The Design Problem

We now examine the application of the non-linear device of Fig. 2.14 in the design of a closed-loop system. We wish to develop a procedure for such design and to compare the results with the optimal linear design obtained by Horowitz and Sidi's[1] method.

The design problem is stated as follows:

(a) The transfer-function P(s) of a linear, time-invariant minimum-phase plant is described by a set of parameters $a_1, \ldots, a_p$ (gain, poles and zeros). Each a_i $(i = 1,\ldots p)$ is known to lie within a given range $\alpha_i \leq a_i \leq \beta_i$ $(i = 1,\ldots p)$, but its precise value is not known. Thus P(s) is a particular, unknown member of a certain known family of functions.

(b) Compensation must be designed in the two-degree-of-freedom structure of Fig. 3.1, such that, for all possible conditions of the plant P(s), the step-response of the system lies within certain specified bounds, such as, for example, the envelope shown in Fig. 3.2.

(c) In addition, it is required that the response to a disturbance D at the output (Fig. 3.1) should satisfy certain damping requirements.

(d) The magnitude of the loop-transmission in the linear design, and that of the corresponding linear loop-transmission in the non-linear design, should have an asymptotic slope of

(-20q)db/decade, as ω tends to infinity, where q is a given positive integer. In the linear design, q is the excess of poles over zeros in the loop-transmission.

Also, the loop-transmission of the linear design and the loop-transmission corresponding to the non-linear design are both of Type-1.

(e) The object is to arrive at a design which meets the specifications on step- and disturbance-responses, and, at the same time, minimizes the effect of feedback-sensor-noise, when there is no command input. A linear design which is quasi-optimal in this sense is furnished by the method of Horowitz and Sidi[1].

It will be shown that, using the Clegg Integrator in parallel with a linear integrator, a non-linear design is possible which transmits less feedback noise to the output than the optimal linear design.

3.2 Design Procedure

The calculations that have been carried out for time-response with the non-linear device, and the results obtained, have been described in terms of the transfer-functions defined for the corresponding linear system. In keeping with this description of non-linear results in corresponding linear terms, we shall present the method of non-linear design as an adaptation of the method of linear design proposed by Horowitz and Sidi[1]. In fact, the method of non-linear design, for a given set of specifications, consists in obtaining

the corresponding linear transfer-functions as a linear design (by Horowitz and Sidi's method) for a less restrictive set of specifications. The method of linear design is treated at length by Horowitz and Sidi in Reference [1], and, therefore, in order to describe the method of non-linear design, it will be enough to give an outline of their method and to indicate how it is adapted for non-linear design.

3.2.1 Outline of Procedure for Linear Design[1]

The time-domain bounds, within which the step-response should remain for all possible plant conditions, are translated into corresponding bounds within which the function $|T(j\omega)| = |\frac{F(j\omega)L(j\omega)}{1+L(j\omega)}|$ should remain for all plant conditions. There is no rigorous method of obtaining such corresponding bounds, but Horowitz and Sidi propose a practical method of trial and error which produces bounds that lead to a successful design.

The upper and lower bounds on $|T(j\omega)|_{db}$, in turn, lead to a bound $\Delta(\omega)$db on the maximum variation that can occur, at fixed ω, in $|\frac{L(j\omega)}{1+L(j\omega)}|_{db}$ over all the possible plant conditions, since $|T(j\omega)|_{db} = |F(j\omega)|_{db} + |\frac{L(j\omega)}{1+L(j\omega)}|_{db}$ and the pre-filter $F(s)$ is fixed and independent of the plant.

Therefore, at each ω, the loop transfer-function $L(j\omega)$, considered at some chosen plant condition, should be such that the variation in $|\frac{L(j\omega)}{1+L(j\omega)}|_{db}$, due to changing plant conditions, should not exceed $\Delta(\omega)$db. The use of the Nichols

Chart is the obvious method of examining the variation in $\left|\frac{L(j\omega)}{1+L(j\omega)}\right|_{db}$ due to variation in $L(j\omega)$. Using templates of the variation of $P(j\omega)$ over the plant conditions, and the bounds $\Delta(\omega)$ on the corresponding variation in $\left|\frac{L(j\omega)}{1+L(j\omega)}\right|_{db}$, we obtain, for each ω, a locus on the Nichols Chart as the lower bound for $L(j\omega)$. At high frequencies, however, the variation $\Delta(\omega)$ that is permissible in $\left|\frac{L(j\omega)}{1+L(j\omega)}\right|$ is greater than the actual variation that occurs in $L(j\omega)$, and, as a result, the step-response bounds impose no conditions on $L(j\omega)$ at these frequencies, and there are no loci on the Nichols Chart.

However, we must also take into account the specification that sets a limit to the overshoot in the disturbance response, determined by the transfer-function $\frac{1}{1+L(s)}$. Using the second-order model $\frac{\omega_n^2}{s^2+2\delta\omega_n s+\omega_n^2}$ for $\frac{L(s)}{1+L(s)}$, Horowitz and Sidi translate this into a lower bound on the damping δ in the second-order model, and, in turn, into a closed boundary on $\left|\frac{L(j\omega)}{1+L(j\omega)}\right|$, for all frequencies and plant conditions, based on the second-order relation

$$\underset{\omega}{\text{Max}} \left| \frac{\omega_n^2}{\omega_n^2 - \omega^2 + j2\delta\omega\omega_n} \right| = \frac{1}{2\delta\sqrt{1-\delta^2}} \quad .$$

The disturbance-response specification thus limits the maximum value that $\left|\frac{L(j\omega)}{1+L(j\omega)}\right|$ may assume, over all frequencies and plant conditions; on the Nichols Chart this defines a contour V (in

the notation of Horowitz and Sidi) whose effect is to limit the phase-lag that $L(j\omega)$ can have until some frequency ω_x at which $|L(j\omega_x)|$ is sufficiently small. The smaller the permitted damping in the disturbance-response, the larger the phase-lag in $L(j\omega)$ that is allowed by the contour V. Fig. 4.1 in Chapter IV shows the contours V_1 and V_2 corresponding, respectively, to $\delta_1 = 0.5$ and $\delta_2 = 0.3$, for a 40 db. variation in the gain of the plant.

Thus, the specifications on step-response and disturbance-response, taken together, furnish a set of loci on the Nichols Chart as bounds on $L(j\omega)$ at all ω. A linear design that meets the specifications and is optimal, in the sense of minimizing k_h where $k_h \triangleq \lim_{s\to\infty} s^q L(s)$, is one in which $L(j\omega)$ lies on its corresponding locus at each ω. The existence of such an optimal $L(s)$ and the manner of its realization are shown in Horowitz and Sidi's paper[1].

3.2.2 Development of Procedure for Non-Linear Design Step-Response Specifications

The step-response $c(t)$ of the two-degree-of-freedom structure of Fig. 3.3, with the non-linear device (Clegg Integrator + $\frac{b}{s}$) situated at the error junction of the feedback-loop is described by Equations (2.13) and (2.14) when we set $R(s) = \frac{F(s)}{s}$. It is clear that the non-linear response is identical with the corresponding linear response till t_1, the instant of first reset of the Clegg Integrator (in particular, if the Clegg Integrator is never reset, the linear and non-linear responses coincide for all t). This portion

of the non-linear response is thus determined by the corresponding linear transfer-function $T(s) = \frac{F(s)L(s)}{1+L(s)}$ and therefore, its sensitivity to plant variations is, in fact, determined by the sensitivity of the linear transfer-function $\frac{L(s)}{1+L(s)}$ (since F(s) is fixed and independent of the plant). We thus conclude that the variation of this portion, at least, of the non-linear step-response can be kept within the specified bounds by designing the corresponding linear loop-transmission L(s) as in a purely linear design.

As regards the response after the first reset, it is helpful to recall that a reset of the output y(t) of the Clegg Integrator at t_i from $y_i \triangleq y(t_i-)$, may be represented in the corresponding linear system by an impulse-input $-y_i\delta(t-t_i)$.

With the modified non-linear device (Clegg Integrator + $\frac{b}{s}$) situated at the error-junction, the response, after t_1 and until a possible second reset t_2, is found from Eqns. (2.13) and (2.14):

$$c(t) = c_L(t) - \frac{y_1}{1+b} h(t-t_1) \quad , \text{ where}$$

$r(t)$ = the output of the prefilter

$$c_L(t) = \int_o^t h(p)r(t-p)dp \quad , \text{ the linear response,}$$

$h(t)$ = impulse-response of $\frac{L(s)}{1+L(s)}$

$$y_1 = \int_o^{t_1} e(t)dt = \int_o^{t_1} [r(t)-c(t)]dt \quad .$$

Since a reset occurs at t_1, e(t) crosses zero at t_1 and changes sign. Consider the case when e(t) is positive for $0 < t < t_1$ and becomes negative after t_1, i.e.

$$c(t) < r(t) \quad \text{for} \quad 0 < t < t_1 \quad \text{and}$$
$$c(t) > r(t) \quad \text{for} \quad t_1 < t < t_2 \ .$$

Then $y_1 > 0$.

$$\text{Let } L(s) = \frac{A[s^{n-q} + \ldots.]}{[s^n + \ldots.]}$$

where q is the excess of poles over zeros in L(s), and $A > 0$ for minimum-phase L(s).

Then, from the initial value theorem of Laplace Transforms, we find

$$h^{(i)}(0) = \lim_{s\to\infty} s^{(i+1)} \frac{L(s)}{1+L(s)} = 0 \ , \quad i = 0,\ldots,(q-2),$$

and $h^{(q-1)}(0) = A > 0$.

Hence, $h(t) > 0$ over an open interval $(0,\Delta)$ and thus,

$$c(t) = c_L(t) - \frac{y_1}{1+b} h(t-t_1) < c_L(t)$$

over an open interval $(t_1, t_1+\Delta)$; i.e. the reset at t_1 tends to reduce the overshoot after t_1. This is illustrated in Fig. 3.4 . If a second reset occurs at t_2, similar arguments show that it tends to reduce the undershoot that occurs after t_2. If there is no reset after t_1, then $c(t) \geq r(t)$ for $t \geq t_1$, $c(t) - c_L(t) = -\frac{y_1}{1+b} h(t-t_1)$, $t \geq t_1$. Therefore,

$$\int_{t_1}^{\infty} [c(t)-c_L(t)]dt = -\frac{y_1}{1+b} \int_{t_1}^{\infty} h(t-t_1)dt$$

$$= -\frac{y_1}{1+b} \int_{o}^{\infty} h(t)dt$$

$$= -\frac{y_1}{1+b} \lim_{s\to 0} \frac{L(s)}{1+L(s)}$$

$$= -\frac{y_1}{1+b}$$

if L(s) is of Type-1 or higher, showing that, on the average, the response c(t) has less overshoot than $c_L(t)$ for $t > t_1$.

Thus, the effect of a reset is, in general, to reduce overshoot and undershoot in the non-linear response as compared to the corresponding linear response. In consequence, one expects the non-linear step-response, in general, to have smaller oscillations than the corresponding linear step-response, and, therefore, to remain within the same bounds as the corresponding linear step-response. An exception might occur for the plant condition in which the linear step-response corresponding to the non-linear design has near-critical damping. If the linear response has just enough overshoot to cause a reset in the non-linear response, the latter can have considerable undershoot, which might violate the lower bound of the step-response

specifications. Equation (2.19) gives an approximate* (second-order model) upper bound to such undershoot and enables b to be chosen so as to limit the undershoot to the desired value.

A general conclusion from these considerations is that the non-linear response tends to be less oscillatory than the linear response for quite general inputs, exceptions occurring when a reset occasioned by an overshoot causes exessive undershoot or vice versa. Examples of linear and non-linear response to general inputs are shown in Figures 4.11-a, b and c, for the linear and non-linear systems designed in Chapter IV.

---

* Equation (2.19) applies to the step-response without a pre-filter, or, equivalently, to the disturbance-response; however, if the step-response of the pre-filter is much faster than that of the feedback-loop for near-critical damping, the expression is a good approximation even for step-response with the pre-filter.

For instance, in the design example of Chapter IV, $\frac{kL_2}{1+kL_2}$ has near-critical damping for k = 1, and has then a bandwidth of about 4 rad/sec, while the pre-filter $F_2(s) = \frac{40}{s+40}$ has a bandwidth of 40 rad/sec. Figures 4.5-b and 4.6-b show that both the disturbance-response and step-response for k = 1 have the same undershoot.

We thus conclude that sensitivity specifications on step-response can be met in the non-linear design by designing the corresponding linear loop-transmission for the same low-frequency boundaries on the Nichols Chart as in a linear design, with special consideration for the largest undershoot that can occur.

Disturbance-Response Specifications

The benefits of the Clegg Integrator over the linear integrator are secured, in the main, in the design to meet the disturbance response specifications. In linear design, the specification on the overshoot in disturbance response is translated into a minimum damping δ_1 in a second-order model for the feedback-loop, and, in turn, into a boundary V_1 on the Nichols Chart, which limits, over a range of frequencies, the phase-lag allowable in the loop-transmission $L_1(j\omega)$ of the linear design.

It is seen from Equations (2.17) and (2.18) that, for the same overshoot in the disturbance-response, the non-linear feedback-loop can have a smaller damping (in the corresponding linear transfer-function) than in the linear design. If δ_2 is the damping corresponding to the non-linear design, equating the overshoots in the disturbance-responses of the linear and non-linear designs, we have

$$e^{-\frac{\pi\delta_1}{(1-\delta_1^2)^{1/2}}} = \left[\frac{b - 2\delta_2 e^{\frac{\delta_2}{(1-\delta_2^2)^{1/2}}(\pi-\cos^{-1}\delta_2)}}{1+b}\right] e^{-\frac{\pi\delta_2}{(1-\delta_2^2)^{1/2}}} \qquad (3.1)$$

which gives b as a function of δ_1 and δ_2.

Equation (2.19) shows that the choice of b also determines the maximum undershoot that can occur in the disturbance- and step-responses. If this expression is used to set a lower bound to b, then Equation (3.1) may be used to find the δ_2 that corresponds to a given δ_1, and we note that $\delta_2 < \delta_1$. For a given δ_1, the smaller the value of b, the smaller the value of δ_2. The non-linear design is then obtained by designing the corresponding linear loop-transmission $L_2(j\omega)$, using the boundary V_2 that corresponds to the δ_2 calculated from Equation (3.1). Since $\delta_2 < \delta_1$, V_2 allows a faster reduction of $|L_2(j\omega)|$ than is permissible in $|L_1(j\omega)|$.

Noise-Transmission

It has been shown in Section 2.7 that if $|L_2(j\omega)| < \frac{1}{2}|L_1(j\omega)|$ at high frequencies (i.e. at frequencies where $\frac{L(j\omega)}{1+L(j\omega)} \approx L(j\omega)$), the non-linear design transmits less feedback sensor-noise than the linear design, if the significant part of the noise-spectrum occurs at these high frequencies. The use of the boundary V_2 in the non-linear design in place of the boundary V_1 in the linear design usually enables us to make the ratio $\lim_{\omega\to\infty} |\frac{L_2(j\omega)}{L_1(j\omega)}|$ considerably smaller than $\frac{1}{2}$.

3.2.3 Steps in Non-Linear Design

The procedure for non-linear design may be summarized as follows:

1. The specifications on step-response are translated into bounds on the variation, at different frequencies, of the same minimum-phase transfer-function T(s) that would be used in Horowitz and Sidi's linear design.
2. Using these bounds and templates of plant-variation at the different frequencies, boundaries are derived on the Nichols Chart for the loop-transmission as in the linear design.
3. The damping δ_1, which would be used to derive the high-frequency boundary V_1 in the linear design is calculated from the disturbance-response specification. Values for b and δ_2 are then obtained from Equations (2.19) and (3.1), the choice of b influenced by the largest undershoot that can occur in the step and disturbance responses. The high-frequency boundary V_2 corresponding to δ_2 is then obtained.
4. The linear loop-transmission $L_2(s)$ corresponding to the non-linear design is obtained as a linear design for the boundaries derived in Step-2 and the high-frequency boundary V_2.
5. The series-compensation consists of the non-linear device (Clegg Integrator + $\frac{b}{s}$) at the error junction, followed by the linear transfer-function $\frac{L_2(s)}{P(s)[1 + \frac{b}{s}]}$, where P(s) is the plant transfer function corresponding to the plant-condition used in deriving the boundaries in Step-2.

6. The linear pre-filter $F_2(s)$ for the non-linear design is obtained from the equation

$$T(j\omega) = \frac{F_2(j\omega)L_2(j\omega)}{1 + L_2(j\omega)} \quad ,$$

where T(s) is the transfer-function derived in Step-1.

CHAPTER IV

A DESIGN EXAMPLE

4.1 The Problem

The method of non-linear design is illustrated, and linear and non-linear designs are compared in the following example.

Specifications:

(i) The plant has the transfer-function $P(s) = \frac{k}{s+4}$, where $1 \leq k \leq 100$.

(ii) A pre-filter and series compensation are to be designed in order to keep the step-response of the two degree-of-freedom system of Fig. 3.1 within certain bounds, for all values of k, $1 \leq k \leq 100$. We assume here that such time-domain bounds lead to the following bounds on the variation of the magnitude of the minimum-phase transfer-function $T(s) = \frac{F(s)L(s)}{1+L(s)}$ that would be used in a linear design.

$$\Delta(\omega) = \text{Max } |T(j\omega)|_{db} - \text{Min } |T(j\omega)|_{db}$$

$$= \text{Max} \left| \frac{L(j\omega)}{1+L(j\omega} \right|_{db} - \text{Min} \left| \frac{L(j\omega)}{1+L(j\omega)} \right|_{db} .$$

TABLE 4.1

Bounds On Variation in $|T(j\omega)|$

ω rad/sec	$\text{Max}\|T(j\omega)\|_{db}$	$\text{Min}\|T(j\omega)\|_{db}$	$\Delta(\omega)$db
1	0	-0.25	0.25
2	0.5	-0.5	1
4	1.0	-4.0	5
6	2.0	-9.0	11
10	2.0	-18.0	20
20	0.0	-30.0	30
40	0.0	-40.0	40

(iii) The response to a constant output-disturbance should go to zero in the steady-state, with a maximum overshoot of about 20% of the constant disturbance.

(iv) The loop-transmission $L_1(s)$ in the linear design, and the loop-transmission $L_2(s)$ corresponding to the non-linear design should both be of Type-1 and should have an excess of four poles over zeros.

4.2 Linear Design

Since the plant variation is a variation of pure gain by a factor of 100, the corresponding template on the Nichols Chart is a straight line of length 40 db, parallel to the magnitude-axis, for all frequencies. The bounds $\Delta(\omega)$ of Table 4.1 and the template of plant-variation together determine

the boundaries shown in Fig. 4.1 for $L_1(j\omega)$ at the different frequencies. k = 1 was used as the reference plant-condition in obtaining these boundaries.

Corresponding to the 20% overshoot allowed in the disturbance-response, $\delta_1 \approx 0.5$ and this leads to the high-frequency boundary V_1 shown in Fig. 4.1. Using these boundaries, the following loop-transmission $L_1(s)$ is obtained for the linear design.

$$L_1(s) = \frac{2.3\times10^7(s+11)(s+35)}{s(s+4)(s+30)(s+180)(s^2+216s+360^2)} \qquad (4.1)$$

Fig. 4.1 shows that $L_1(j\omega)$ lies quite close to its boundaries, and therefore, it is close to the optimal design in the sense of Horowitz and Sidi.

With $\frac{kL_1(j\omega)}{1+kL_1(j\omega)}$ known, for $1 \leq k \leq 100$, the following pre-filter $F_1(s)$ for the linear design is obtained with the help of Table 4.1 on pg. 49.

$$F_1(s) = \frac{70}{s+70} \qquad (4.2)$$

This completes the linear design, and the Bode plot of $L_1(s)$ is given in Fig. 4.2.

4.3 Non-Linear Design

The loop-transmission $L_2(j\omega)$ that corresponds to the non-linear design uses the same low-frequency boundaries as were obtained for $L_1(j\omega)$ (with the same reference

plant-condition). When $\delta_2 = 0.3$ is tried, Equation (3.1) gives b = 2.7 (the calculation is shown in the Appendix), which, from Equation (2.19), would limit the maximum undershoot to about 20%. The high-frequency boundary V_2 corresponding to $\delta_2 \simeq 0.3$ is shown in Fig. 4.1.

$L_2(s)$ is now obtained as a linear design with V_2 replacing V_1 as the high-frequency boundary, and is given by

$$L_2(s) = \frac{4.6\times10^6(s+18)(s+45)}{s(s+4)(s+50)(s+80)(s^2+208s+260^2)} \qquad (4.3)$$

With $\frac{kL_2(j\omega)}{1+kL_2(j\omega)}$ known, for $1 \leq k \leq 100$, the pre-filter $F_2(s)$ for the non-linear design is chosen so as to make $\frac{F_2(j\omega)kL_2(j\omega)}{1+kL_2(j\omega)}$ vary, as k varies from 1 to 100, between the limits given in Table 4.1 on pg. 49, over the range of frequencies listed in the Table. We choose

$$F_2(s) = \frac{40}{s+40} \qquad (4.4)$$

The non-linear device (Clegg Integrator + $\frac{2.7}{s}$) is situated at the error-junction of the feedback loop, followed by G(s), the linear part of the compensation and the plant P(s). G(s) is determined by the equation

$$L_2(s) = P(s)G(s)\frac{[1+b]}{s} = P(s)G(s)\frac{3.7}{s} \quad .$$

This completes the non-linear design and the Bode plot of $L_2(s)$ is given in Fig. 4.2. The Bode plots of $T_1 = F_1(s)\frac{kL_1(s)}{1+kL_1(s)}$

and $T_2(s) = F_2(s) \dfrac{kL_2(s)}{1+kL_2(s)}$, for k = 1 and k = 100, appear in Figs. 4.3 and 4.4, respectively.

4.4 Results

Figures 4.5 and 4.6 show the step- and disturbance-responses of the linear and non-linear designs, for several values of k, as well as the responses obtained when $L_2(s)$ is used as a linear design.

We note that the L_2-non-linear responses fall within the bounds of variation of the L_1-linear responses and meet the same specifications as the linear responses; the L_2-linear responses, however, violate those bounds.

The transmission of feedback sensor-noise to the output in the linear and non-linear designs is compared in Fig. 4.7, which is a record of the square of the actual noise output produced by zero-mean sensor noise (with a bandwidth of about fifteen times that of $\dfrac{100L_2(s)}{1+100L_2(s)}$), and is thus a record of instantaneous noise-power at the output. The noise at the output is seen to be much smaller in the non-linear design than in the linear design, and as a result, saturation of forward elements due to sensor-noise is much less of a problem in the non-linear design than in the optimal linear design.

Figures 4.8, 4.9 and 4.10 show linear and non-linear responses to sinusoidal and ramp inputs and to a combination of command- and disturbance-inputs. Figures 4.11-a,b,c compare linear and non-linear responses to some other input waveforms.

Though a Type-0 plant and pure gain-variation were considered in this example, the derivation of the procedure

for non-linear design has been quite general, with just one assumption made — that the device (Clegg Integrator + $\frac{b}{s}$) is situated at the error-junction; however, this imposes no restrictions on the design, and we see that it is also applicable to other kinds of plants and parameter-variations.

4.5 Conclusion

It has been shown that the non-linear device consisting of the Clegg Integrator in parallel with the linear integrator is a useful element to include in the compensation for a linear, minimum-phase plant with uncertain parameters, to achieve specified bounds on its response. For given plant-ignorance and bounds on response, it has been shown that, using this non-linear device, compensation can be designed in a two-degree-of-freedom structure in which there is less transmission of feedback sensor-noise to the plant and its output than is possible to achieve in a linear design. A method has been obtained which enables the non-linear design to be carried out in terms of an equivalent linear design by the method of Horowitz and Sidi.

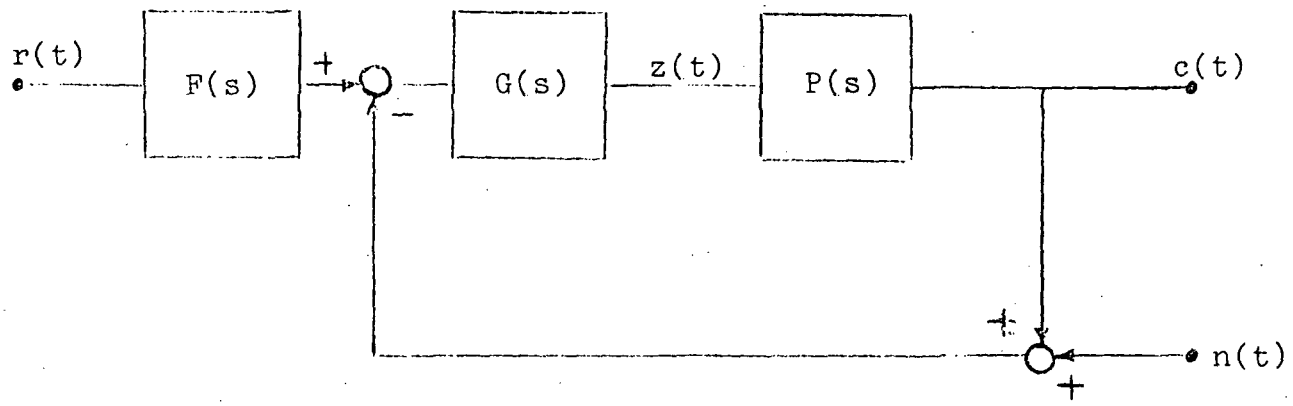

$$L(s) = P(s)G(s) \qquad T(s) = \frac{F(s)L(s)}{1+L(s)} \qquad B(s) = -\frac{1}{P(s)}\left[\frac{L(s)}{1+L(s)}\right]$$

Fig. 1.1: A Two-Degree of Freedom Feedback System

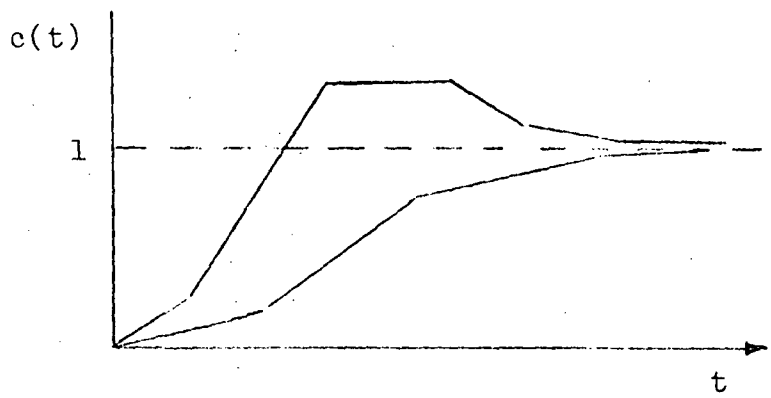

Fig. 1.2: Example of Bounds on Step-Response

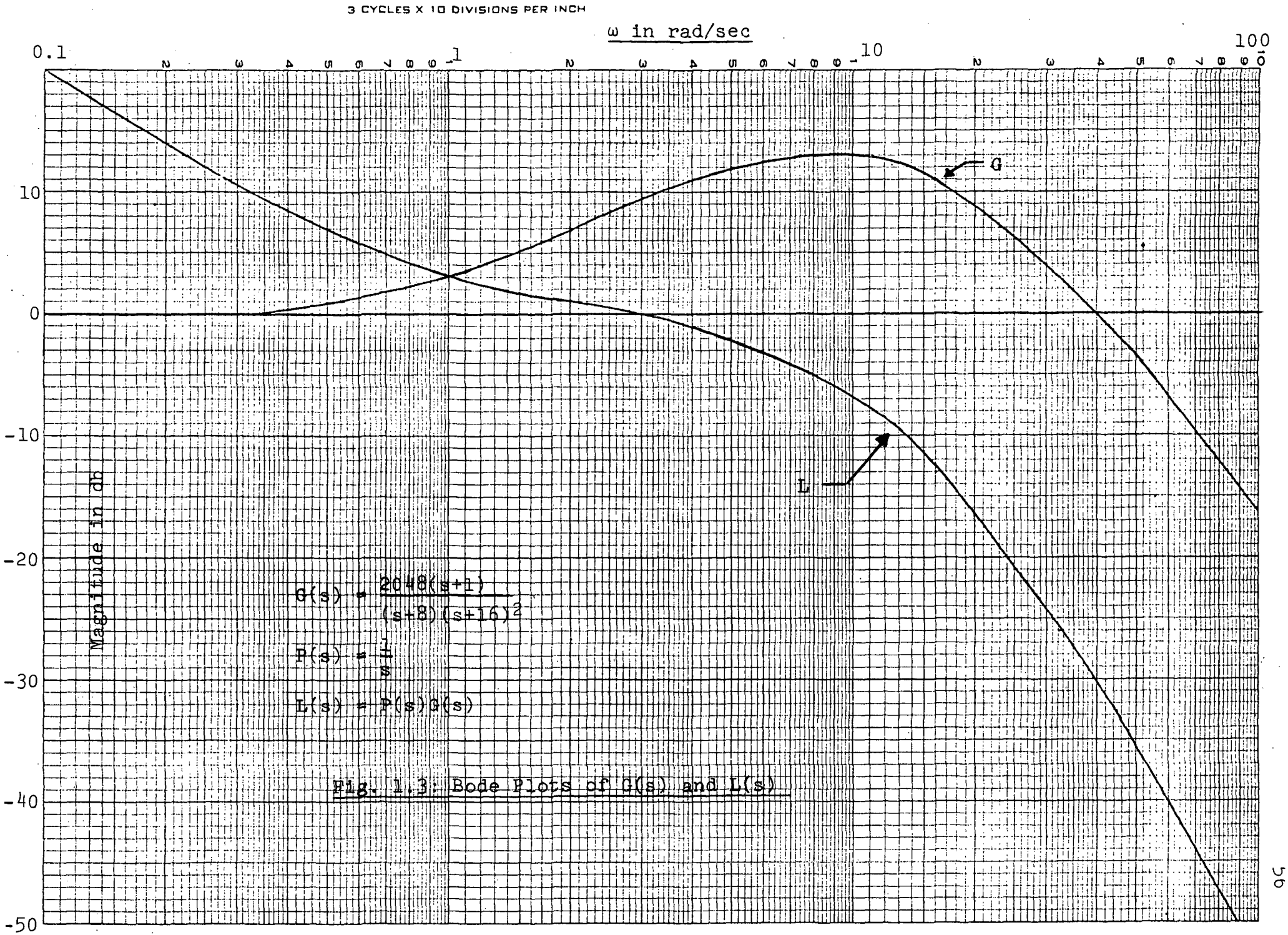

Fig. 1.3: Bode Plots of G(s) and L(s)

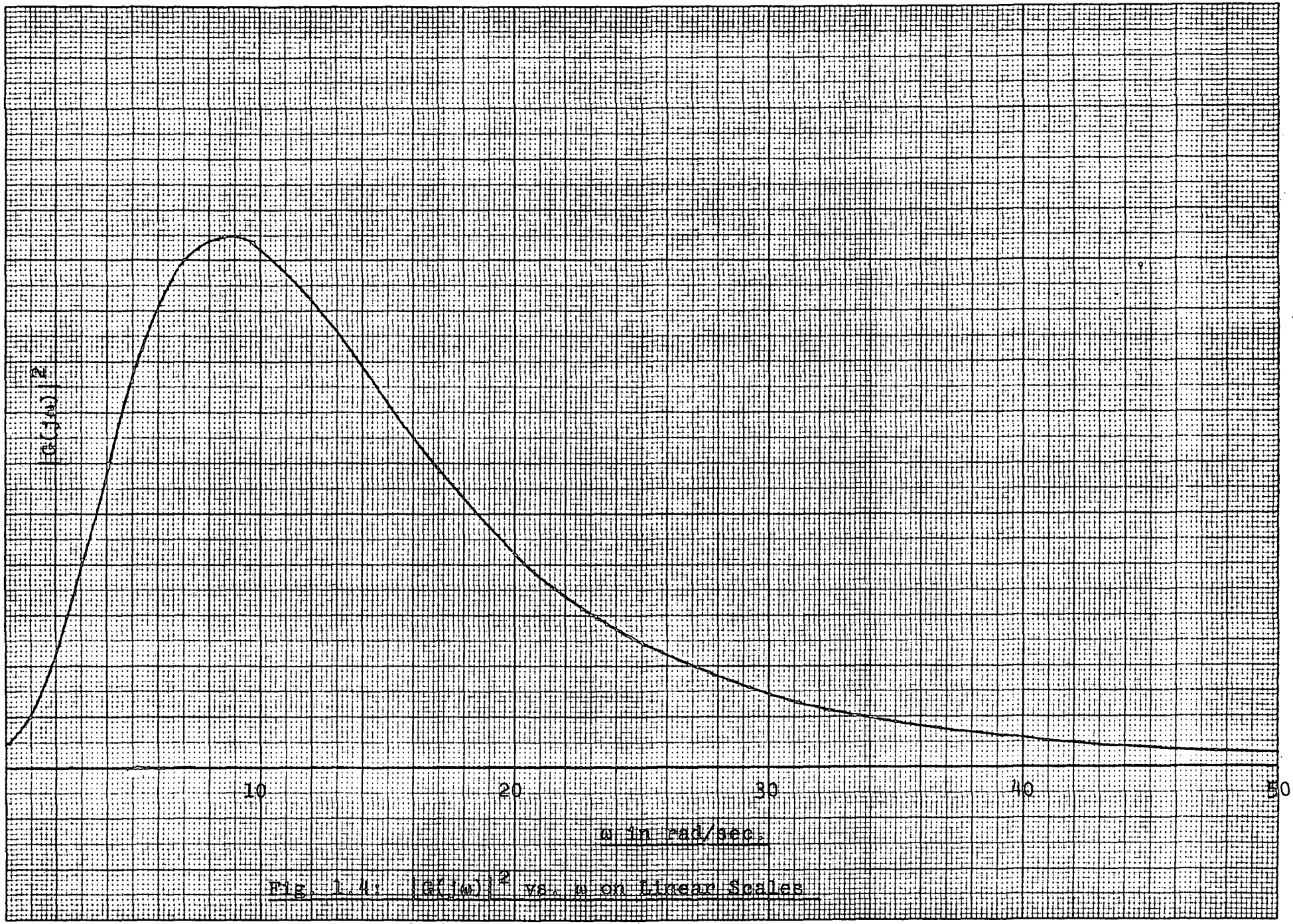

Fig. 1.4: $|G(j\omega)|^2$ vs. ω on Linear Scales

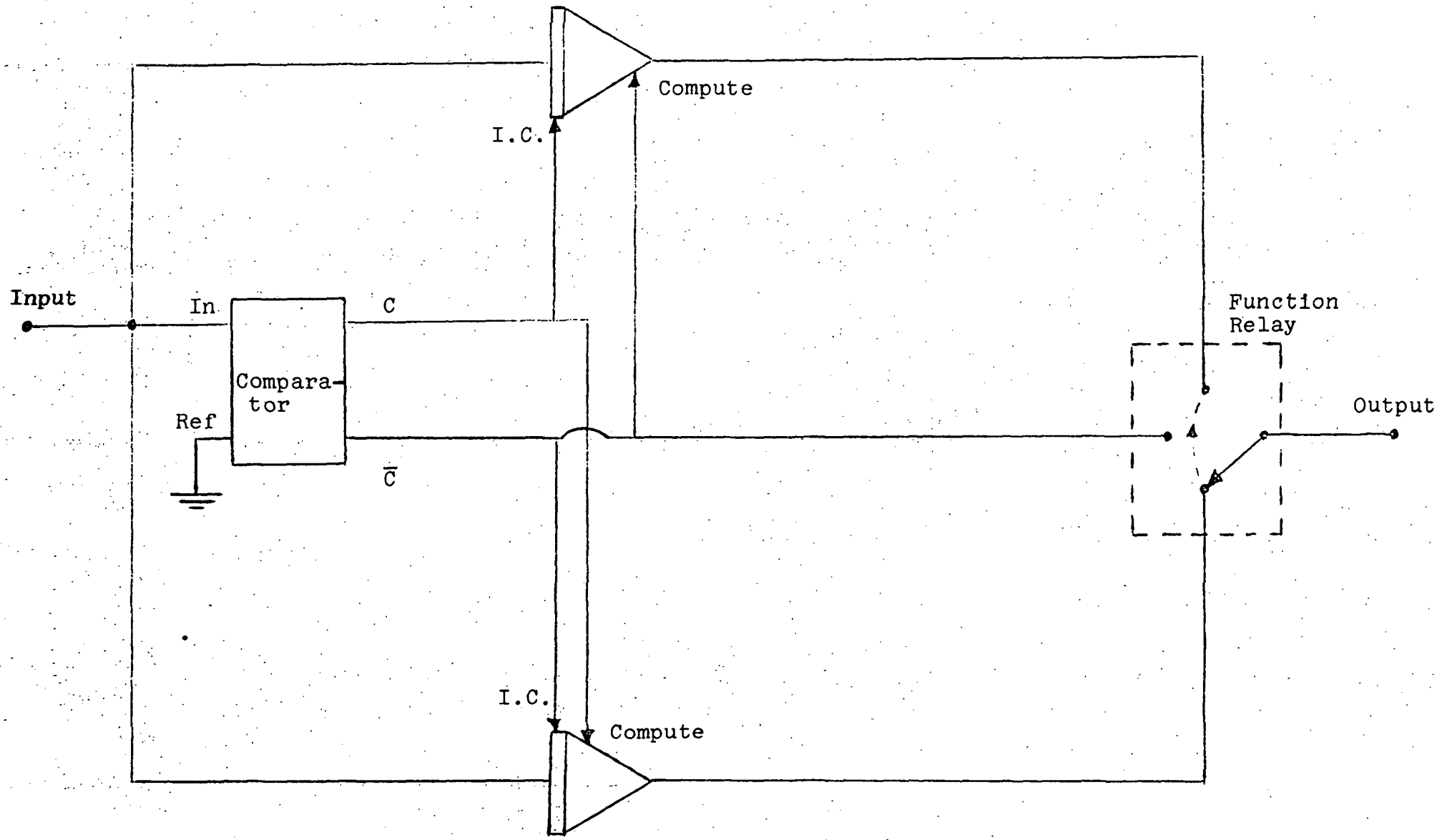

Fig. 2.1: Simulation of the Clegg Integrator

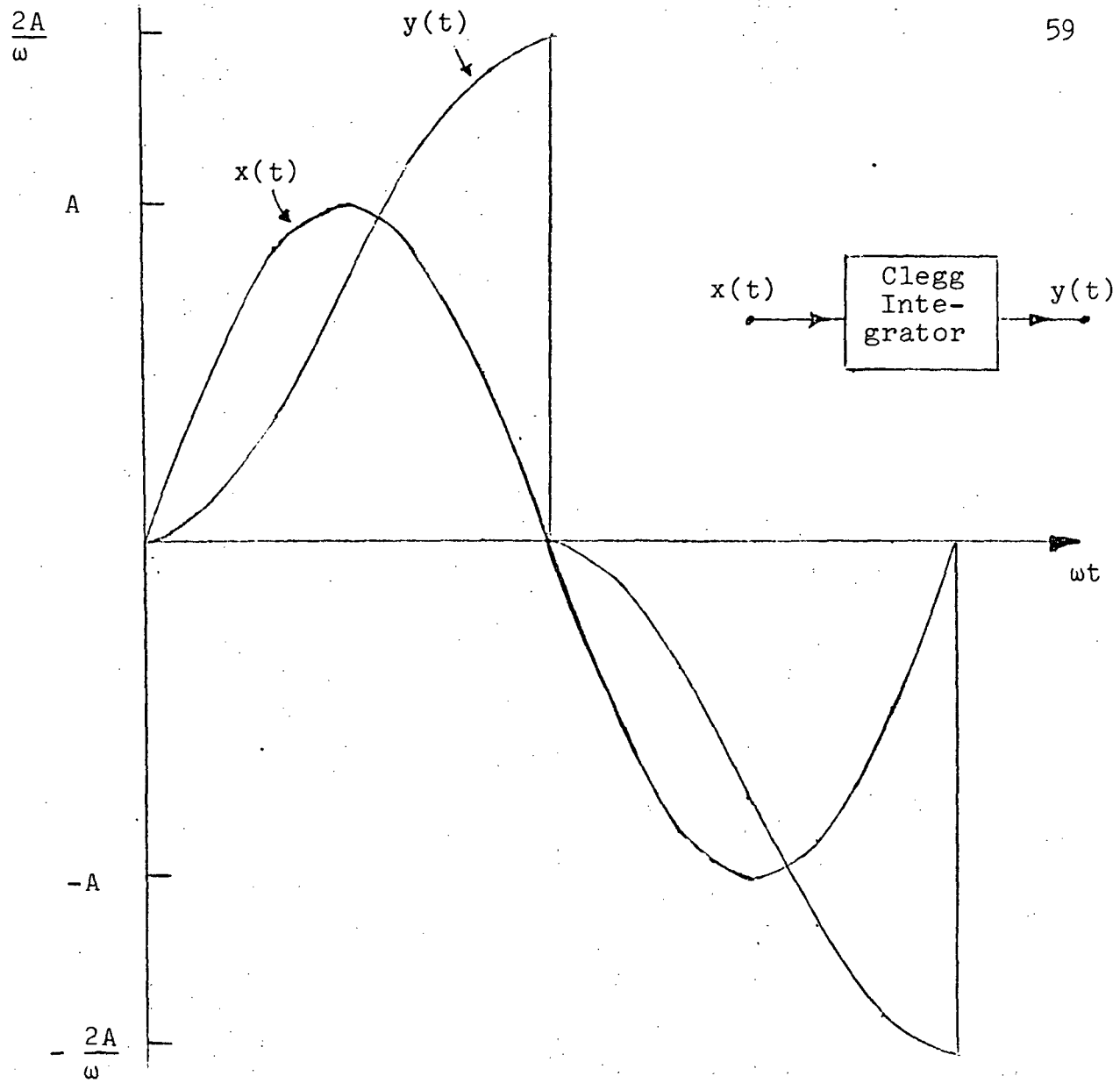

$$x(t) = A\sin\omega t$$

$$y(t) = \begin{cases} \frac{A}{\omega}(1-\cos\omega t), & 0 \leq \omega t < \pi \\ -\frac{A}{\omega}(1+\cos\omega t), & \pi \leq \omega t < 2\pi \end{cases}$$

Fig. 2.2: Sinusoidal Response of the Clegg Integrator

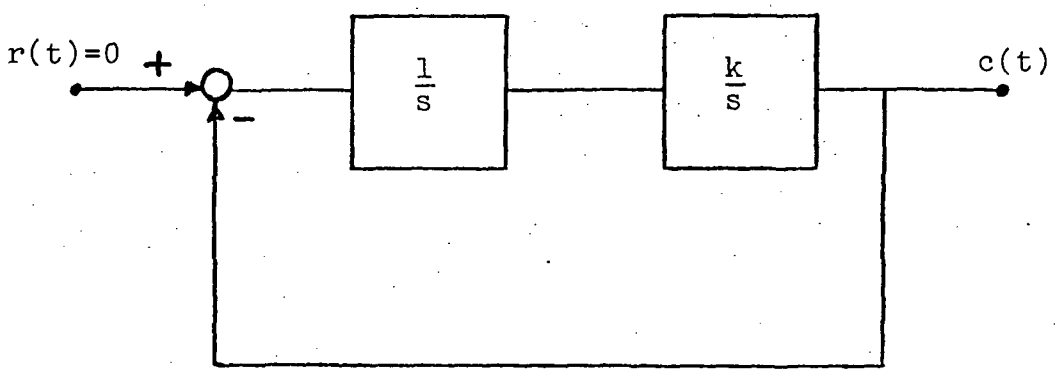

Fig. 2.3-a: A Closed-Loop Linear System

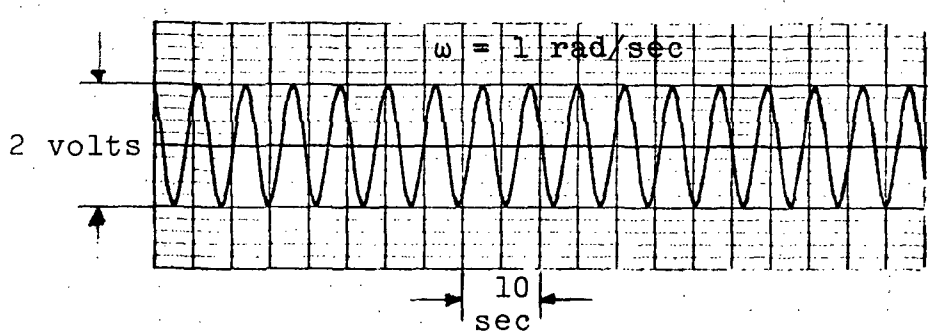

Fig. 2.3-b: Output of System of Fig. 2.3-a, for k = 1

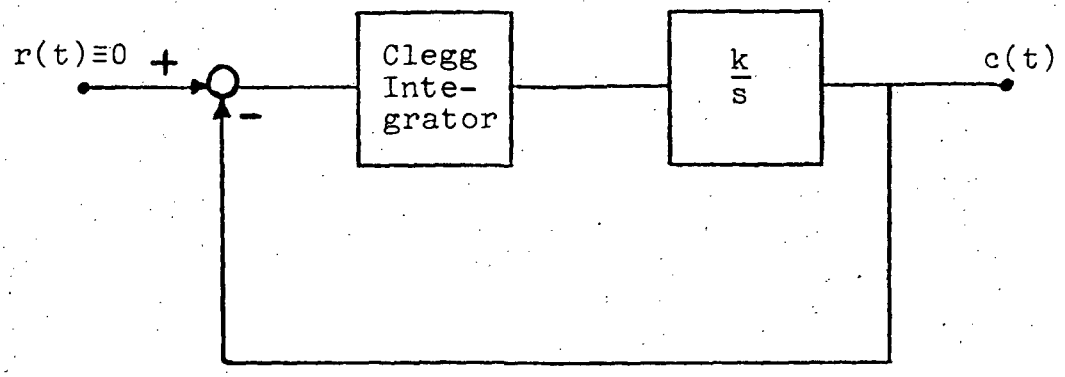

Fig. 2.4-a: A Closed-Loop Non-Linear System

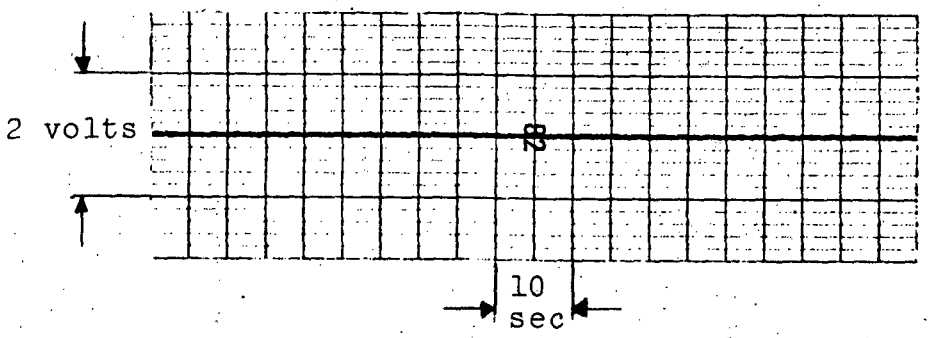

Fig. 2.4-b: Output of System of Fig. 2.4-a for k = 10

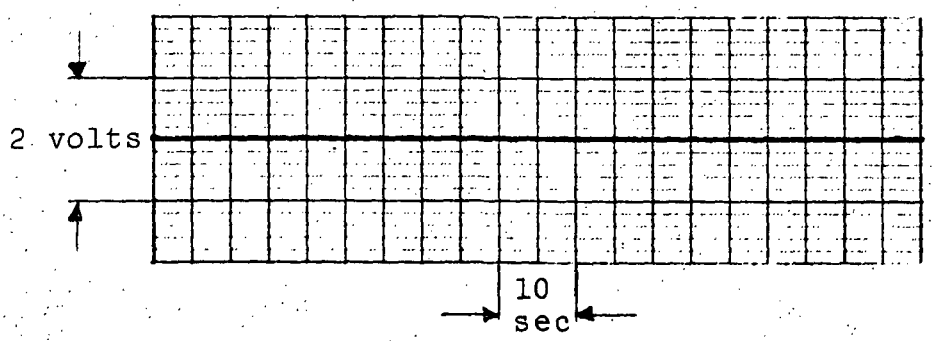

Fig. 2.4-c: Output of System of Fig. 2.4-a for k = 100

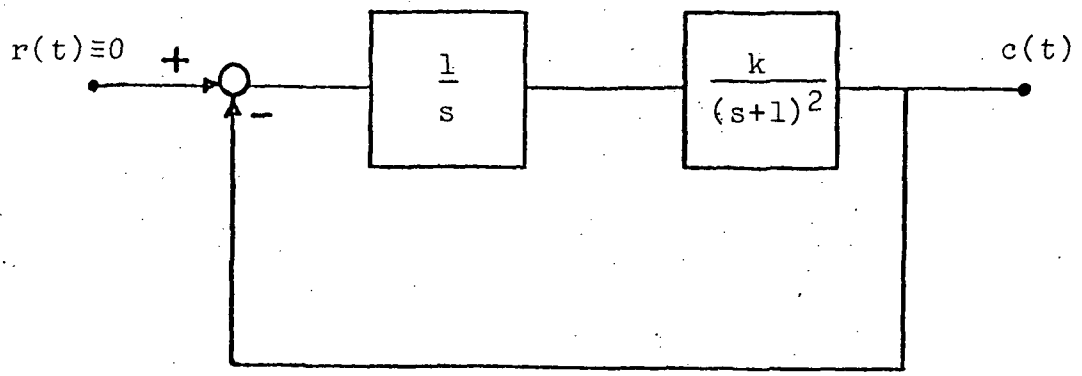

Fig. 2.5-a: A Closed-Loop Linear System

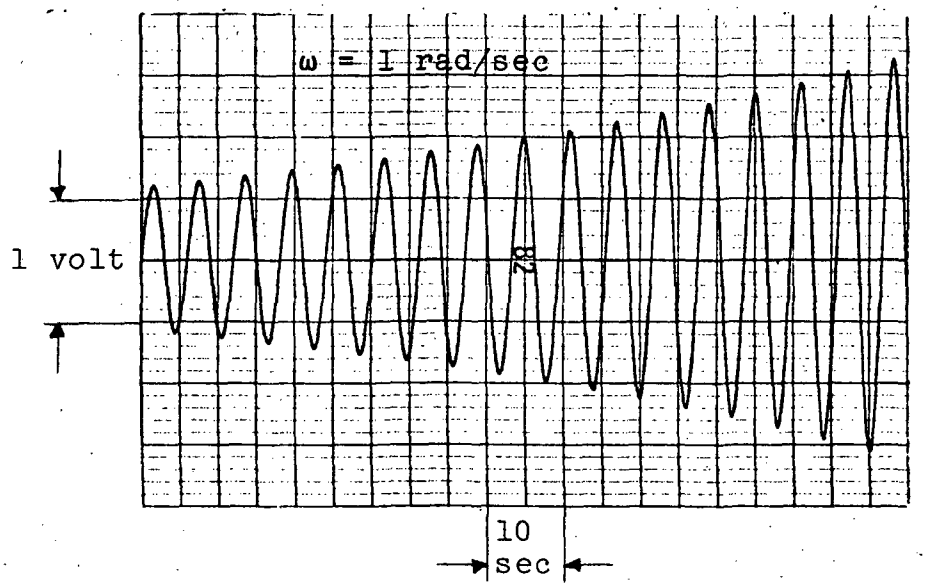

Fig. 2.5-b: Output of System of Fig. 2.5-a for k = 2.1

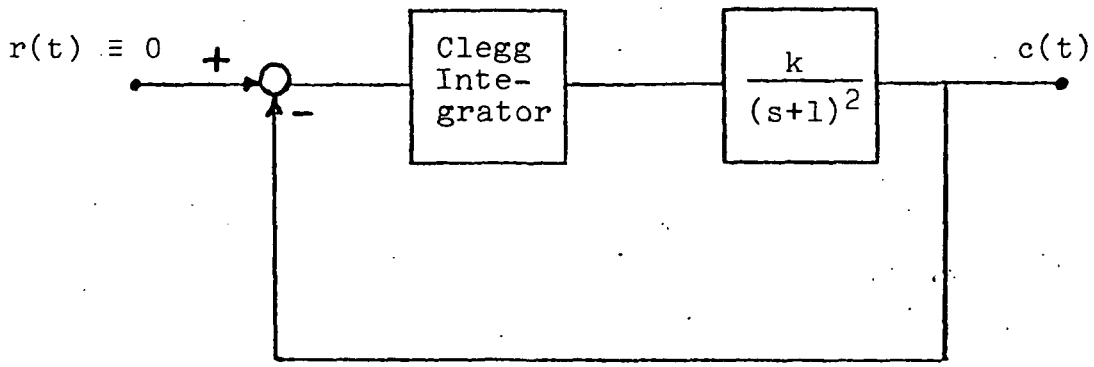

Fig. 2.6-a: A Closed-Loop Non-Linear System

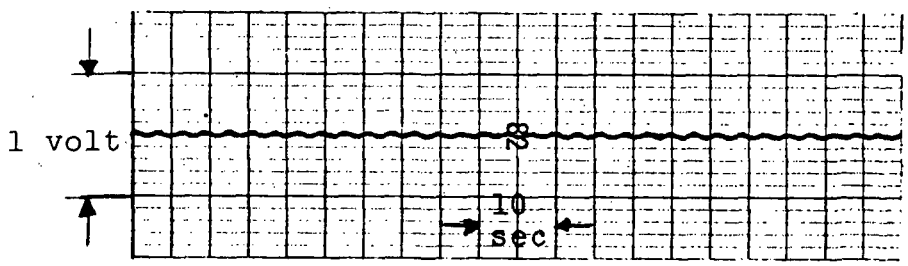

Fig. 2.6-b: Output of System of Fig. 2.6-a for k = 5

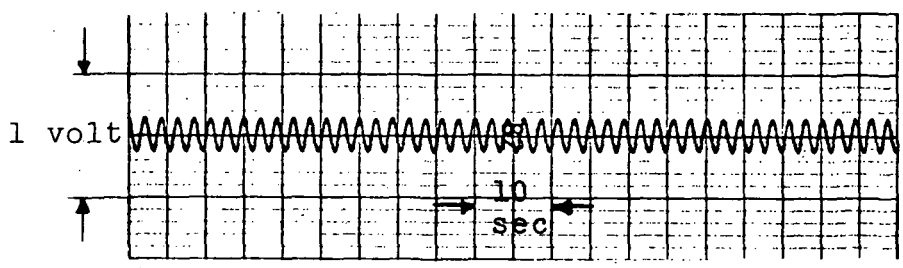

Fig. 2.6-c: Output of System of Fig. 2.6-b for k = 16

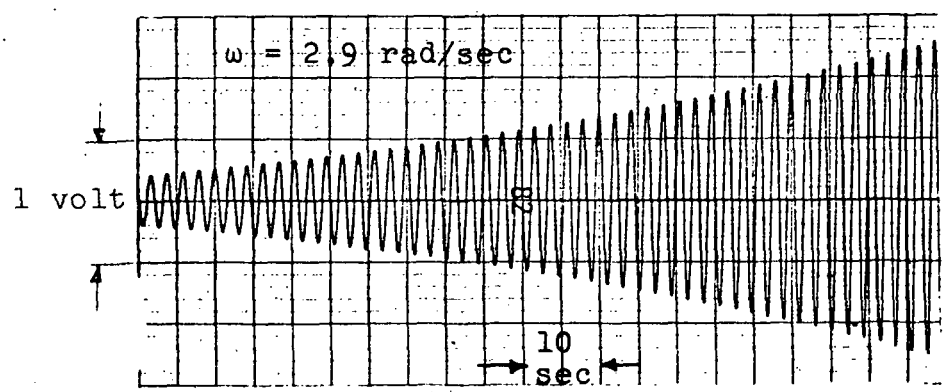

Fig. 2.7: Output of System of Fig. 2.6-a for k = 18

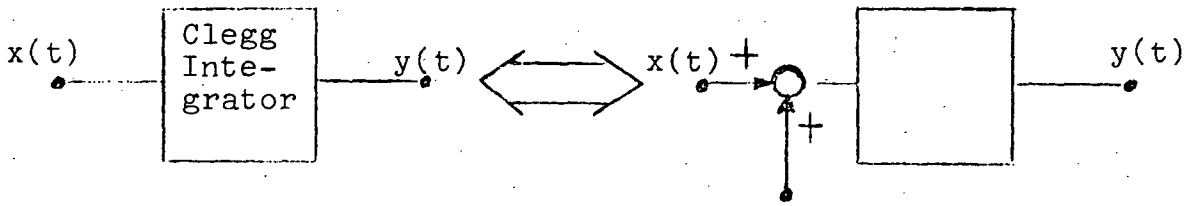

$$a(t) = -\sum_i y(t_i-)\delta(t-t_i)$$

$$x(t_i) = 0,\ i = 1,2,\ldots$$

Fig. 2.8: Linear Equivalent of the Clegg Integrator

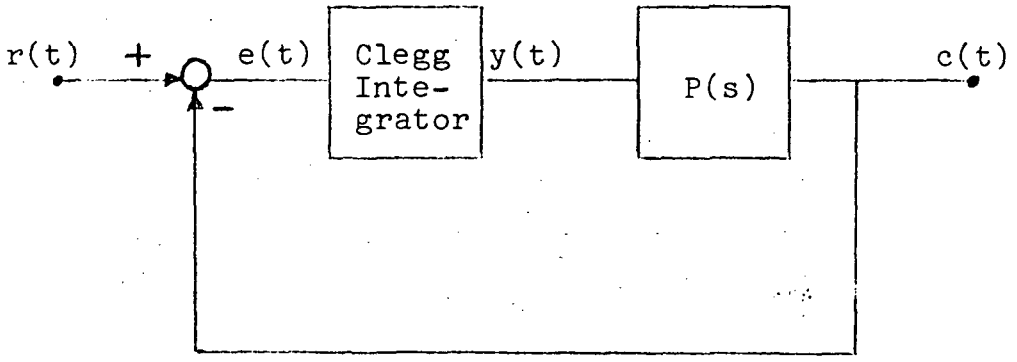

Fig. 2.9: A Closed-Loop Non-Linear System

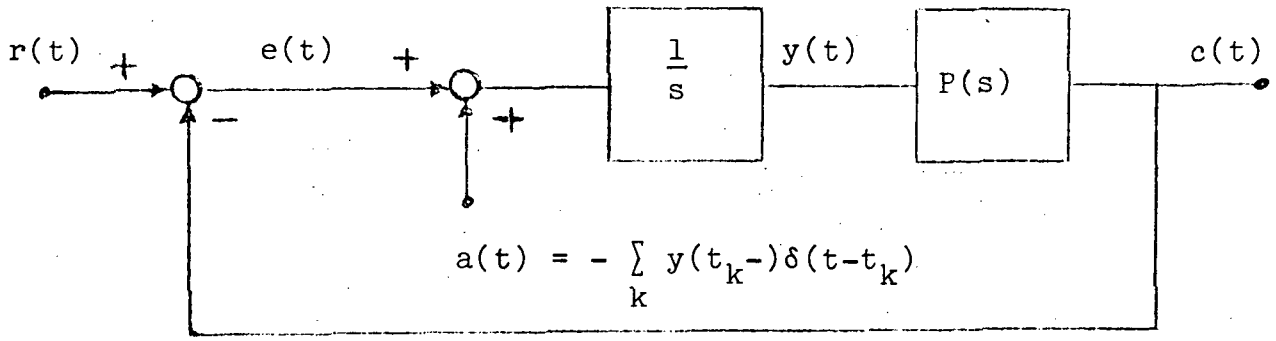

$$H(s) = \frac{C(s)}{R(s)} = \frac{C(s)}{A(s)} \qquad V(s) = \frac{Y(s)}{R(s)} = \frac{Y(s)}{A(s)}$$

Fig. 2.10: Linear Equivalent of System of Fig. 2.9

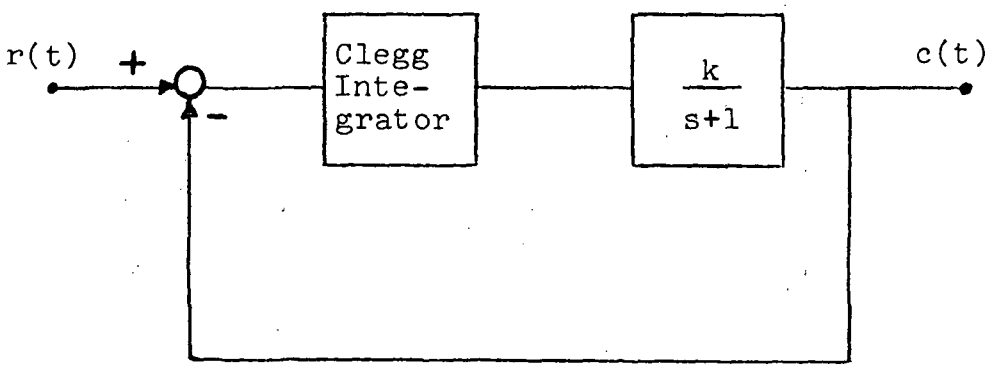

Fig. 2.11: A Closed-Loop Non-Linear System

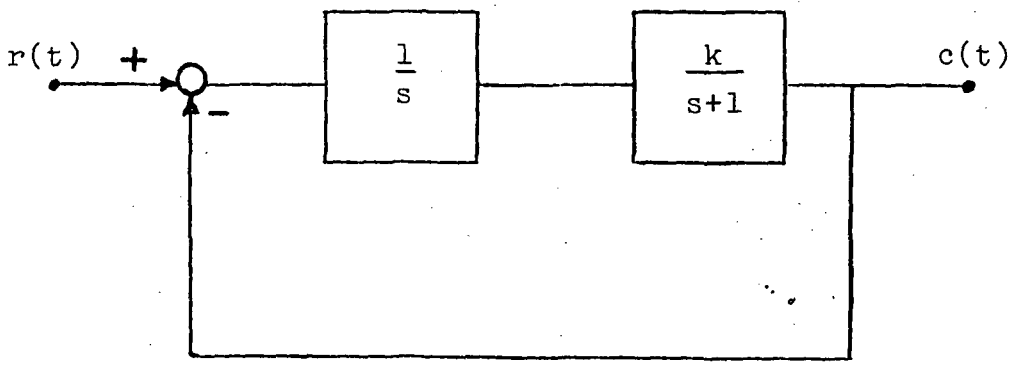

Fig. 2.12: The Linear System Corresponding to System of Fig. 2.11

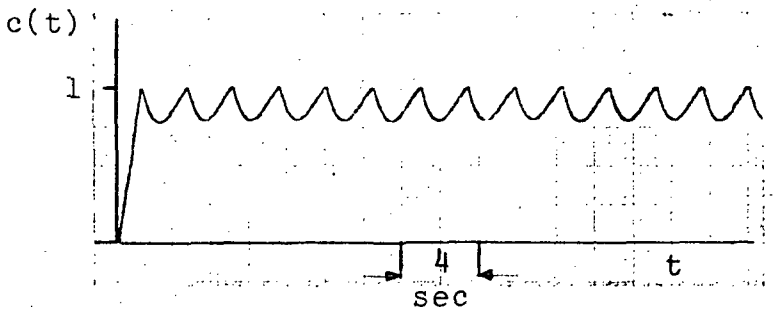

Fig. 2.13: Step-Response of System of Fig. 2.11, for k = 2

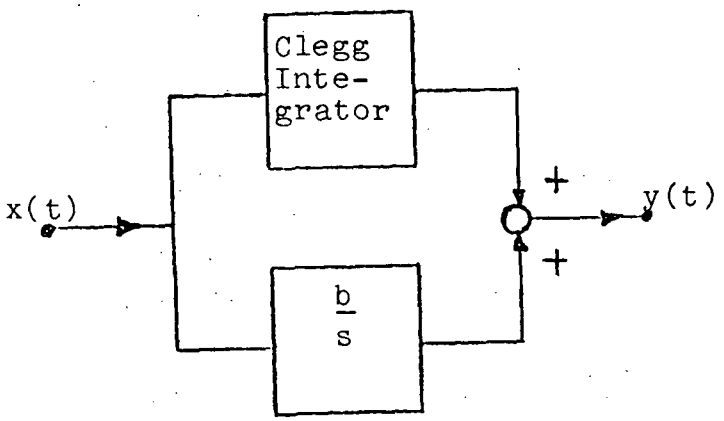

Fig. 2.14-a: Modified Non-Linear Device

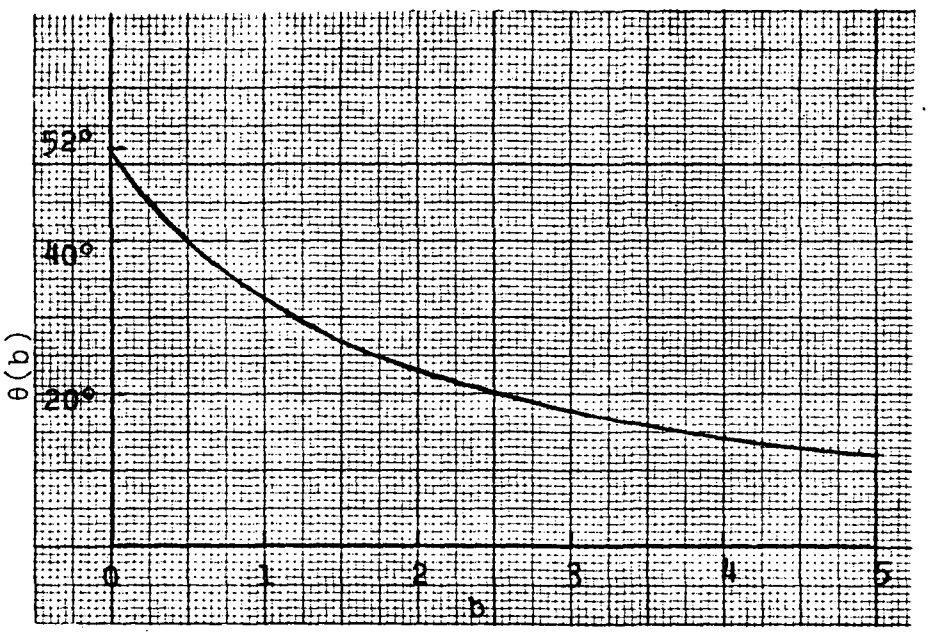

Fig. 2.14-b: $\theta(b) \triangleq \angle \frac{1.62\ e^{j52^\circ} + b}{1 + b}$ in degrees

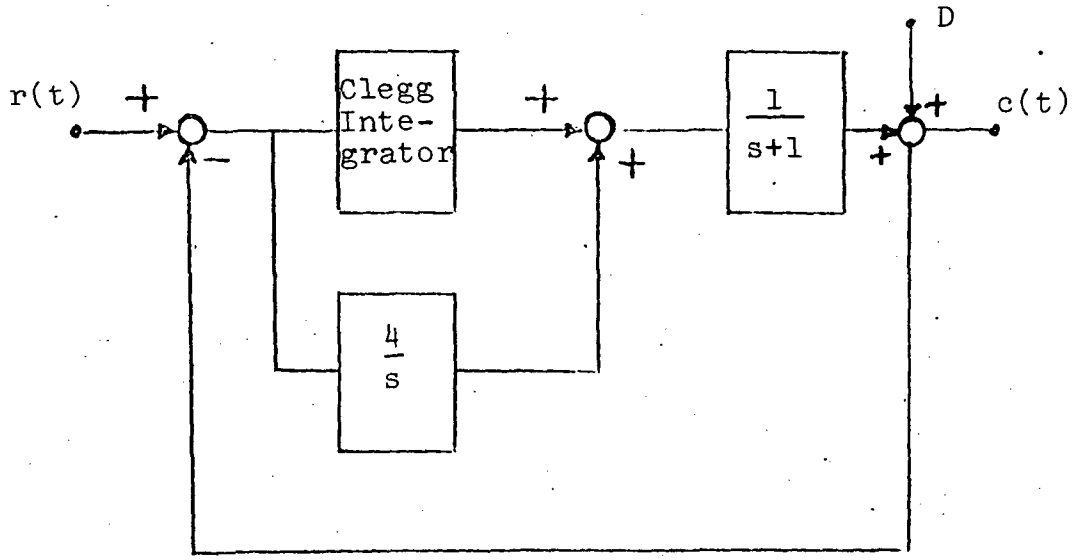

Fig. 2.15: A Closed-Loop Non-Linear System

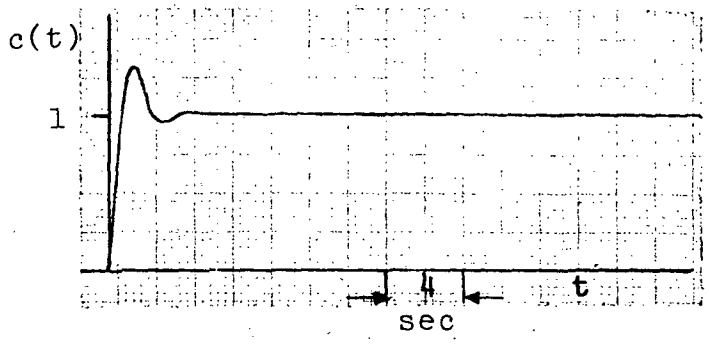

Fig. 2.16: Step-Response of System of Fig. 2.15

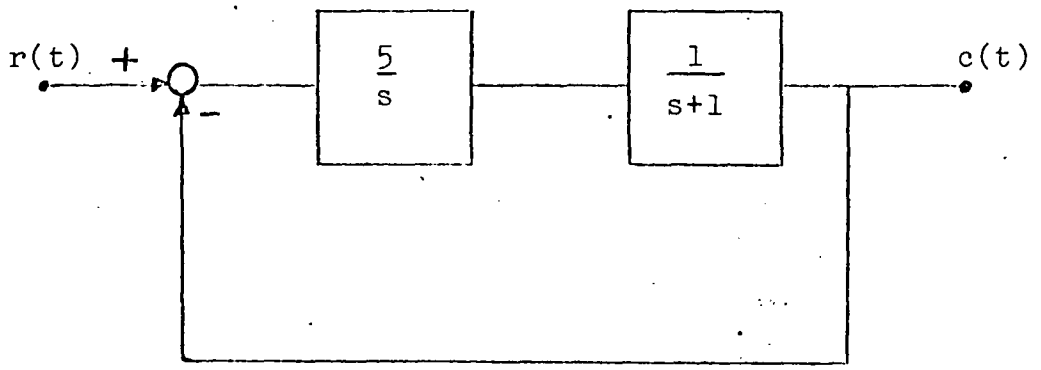

Fig. 2.17: Linear System Corresponding to System of Fig. 2.15

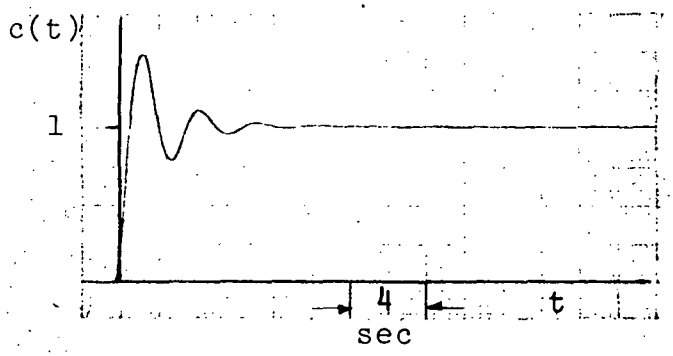

Fig. 2.18: Step-Response of System of Fig. 2.17

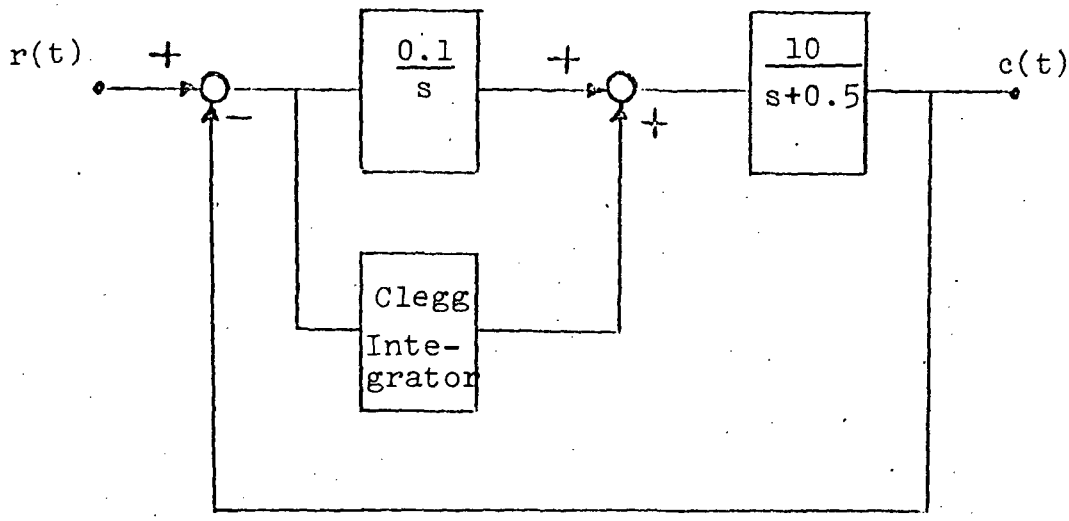

Fig. 2.19: A Type-1 Non-Linear System

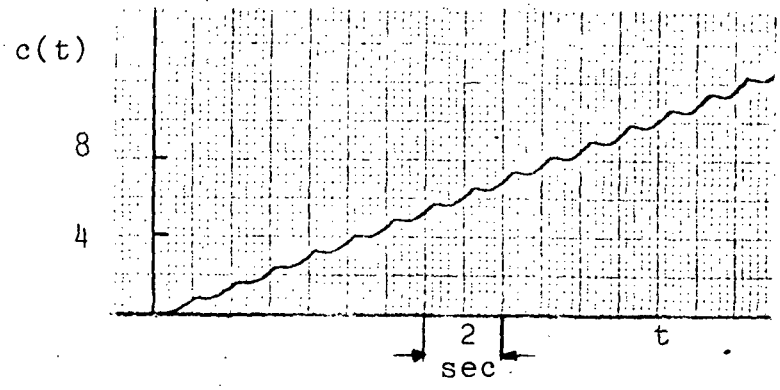

Fig. 2.20: Ramp-Response of System of Fig. 2.19

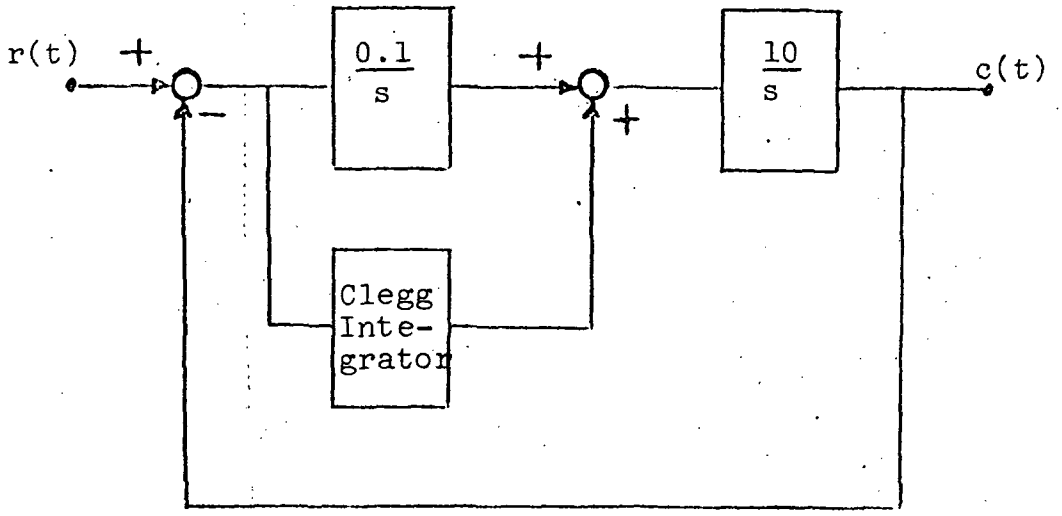

Fig. 2.21: A Type-2 Non-Linear System

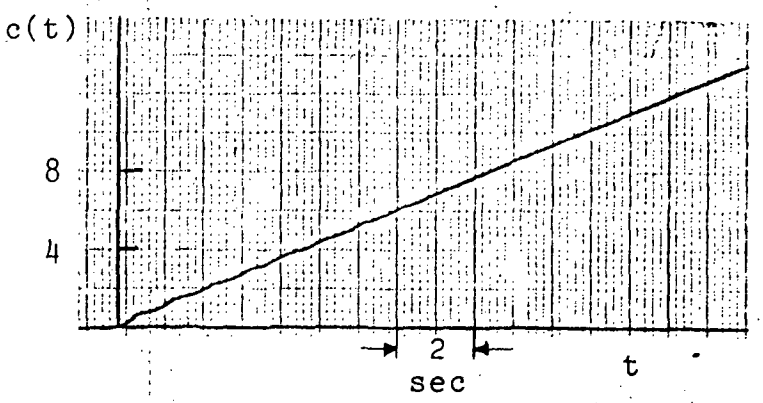

Fig. 2.22: Ramp-Response of System of Fig. 2.21

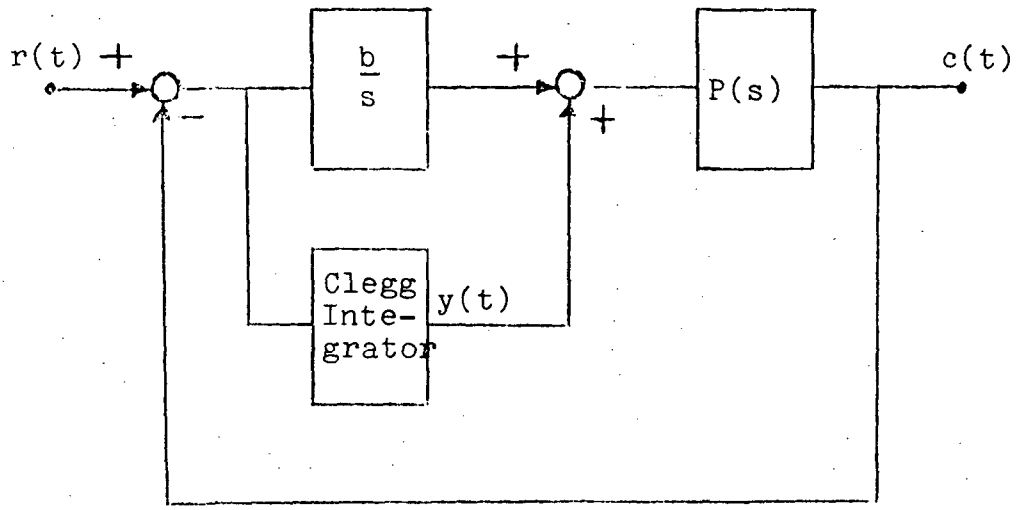

Fig. 2.23: A Closed-Loop Non-Linear System

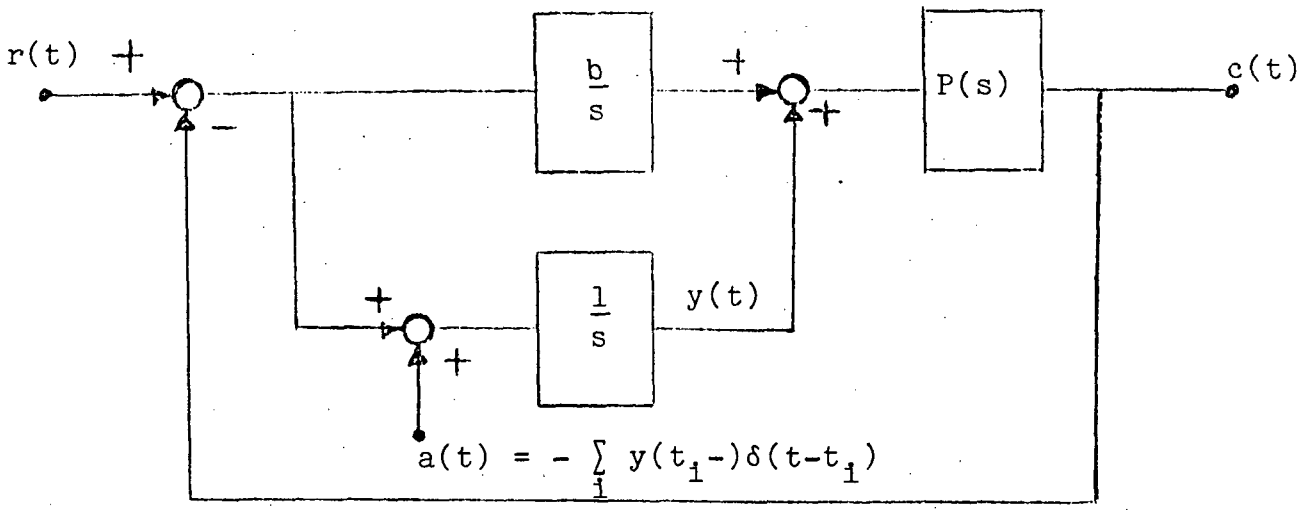

$$L(s) = P(s)\left(\frac{1+b}{s}\right) \qquad \frac{C(s)}{R(s)} = H(s) = \frac{L(s)}{1+L(s)}, \quad \frac{Y(s)}{R(s)} = V(s) = \frac{1}{s[1+L(s)]}$$

$$\frac{C(s)}{A(s)} = H_a(s) = \frac{H(s)}{1+b}, \quad \frac{Y(s)}{A(s)} = V_a(s) = \frac{1}{1+b}\left[V(s)+\frac{b}{s}\right]$$

Fig. 2.24: Linear Equivalent of Fig. 2.23

Bandwidth of noise ≈ 10 rad/sec

Peak-to-Peak value ≈ 160 volts

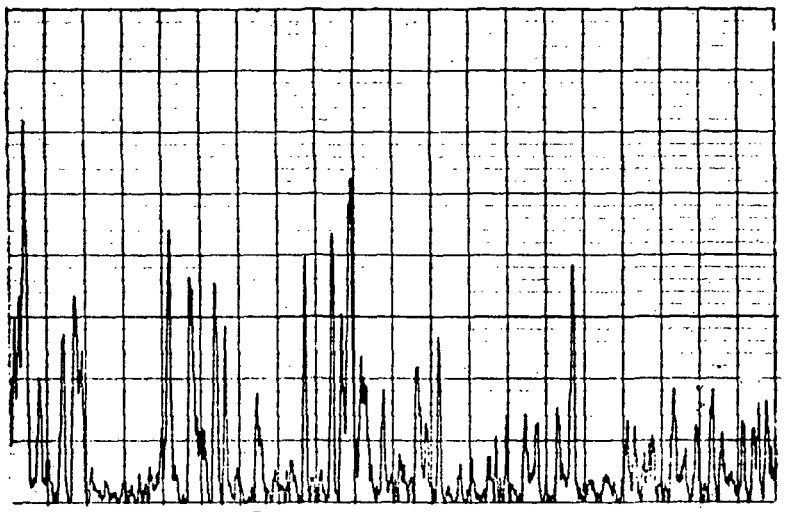

(output)^2 of Linear Integrator

All three figures have the same scales.

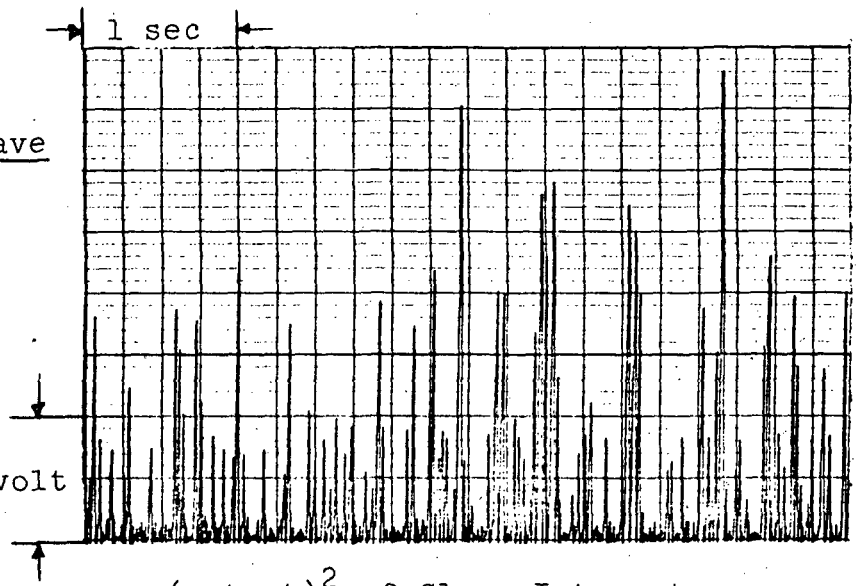

(output)^2 of Clegg Integrator

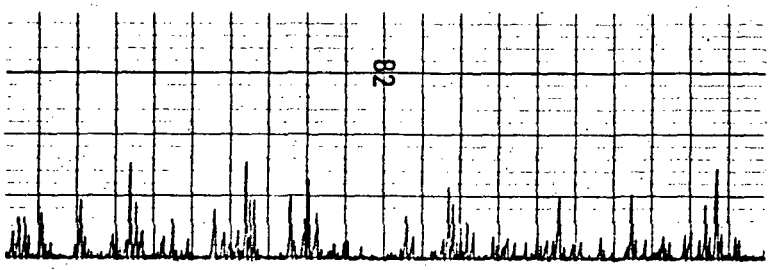

(output)^2 of 0.5 (Clegg Integrator)

Fig. 2.25: Output Noise-Power of Linear and Clegg Integrators with Zero-Mean Input Noise

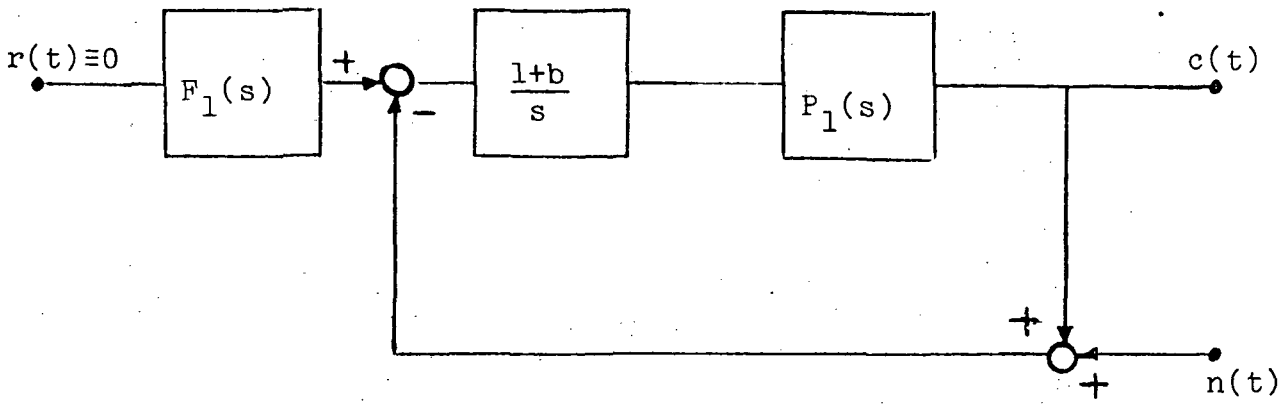

Fig. 2.26: Effect of Sensor-Noise —— Linear System

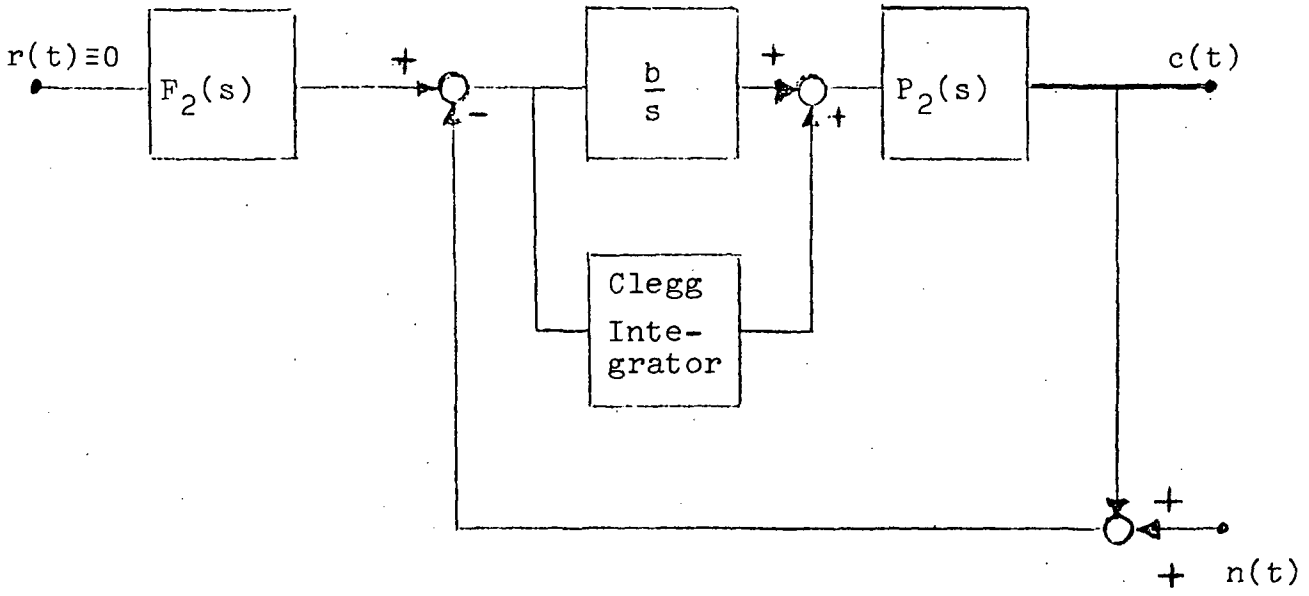

Fig. 2.27: Effect of Sensor-Noise —— Non-Linear System

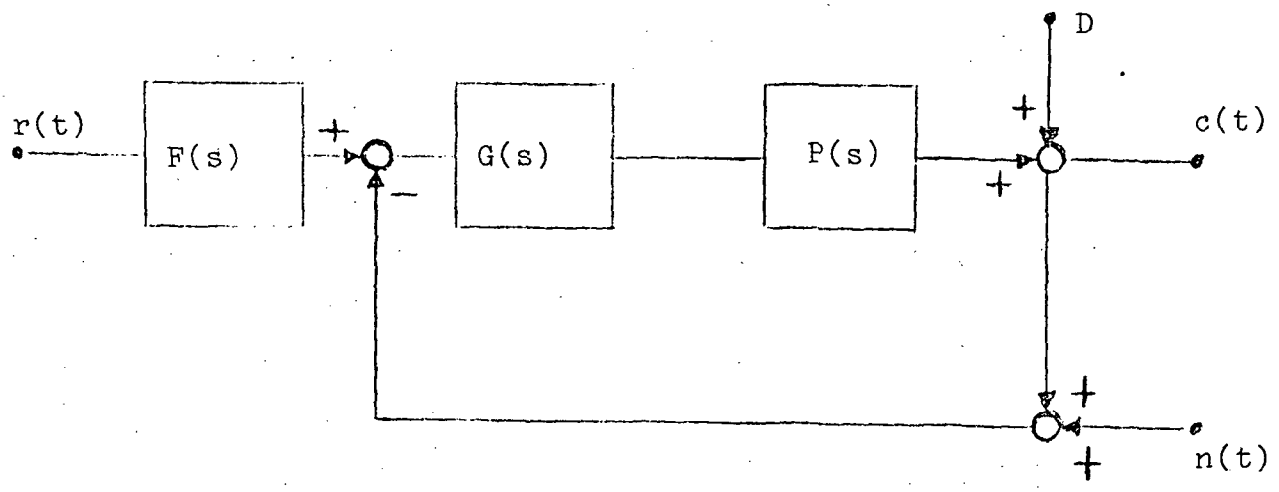

Fig. 3.1: Two-Degree-of-Freedom Structure for Linear Design

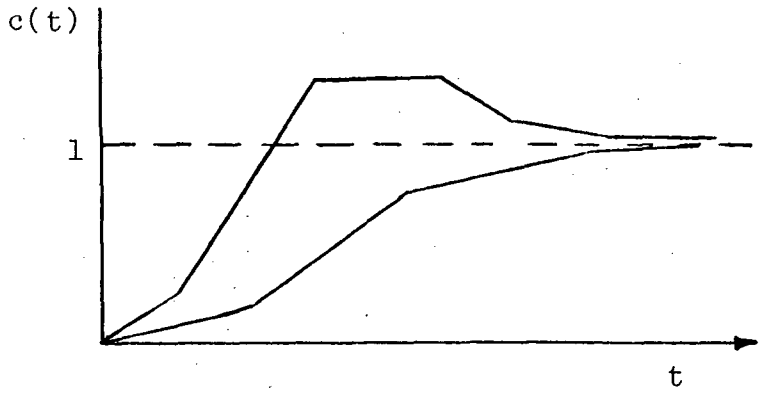

Fig. 3.2: Example of Bounds on Step-Response

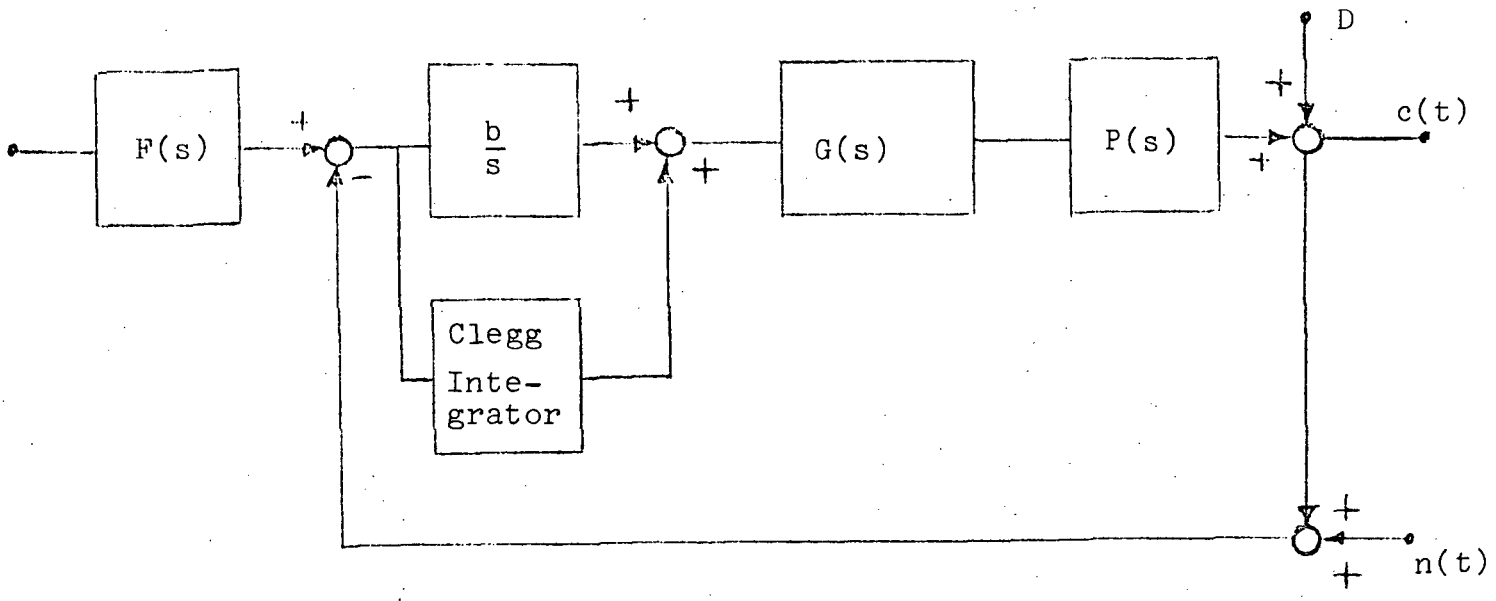

Fig. 3.3: Two-Degree-of-Freedom Structure for Non-Linear Design

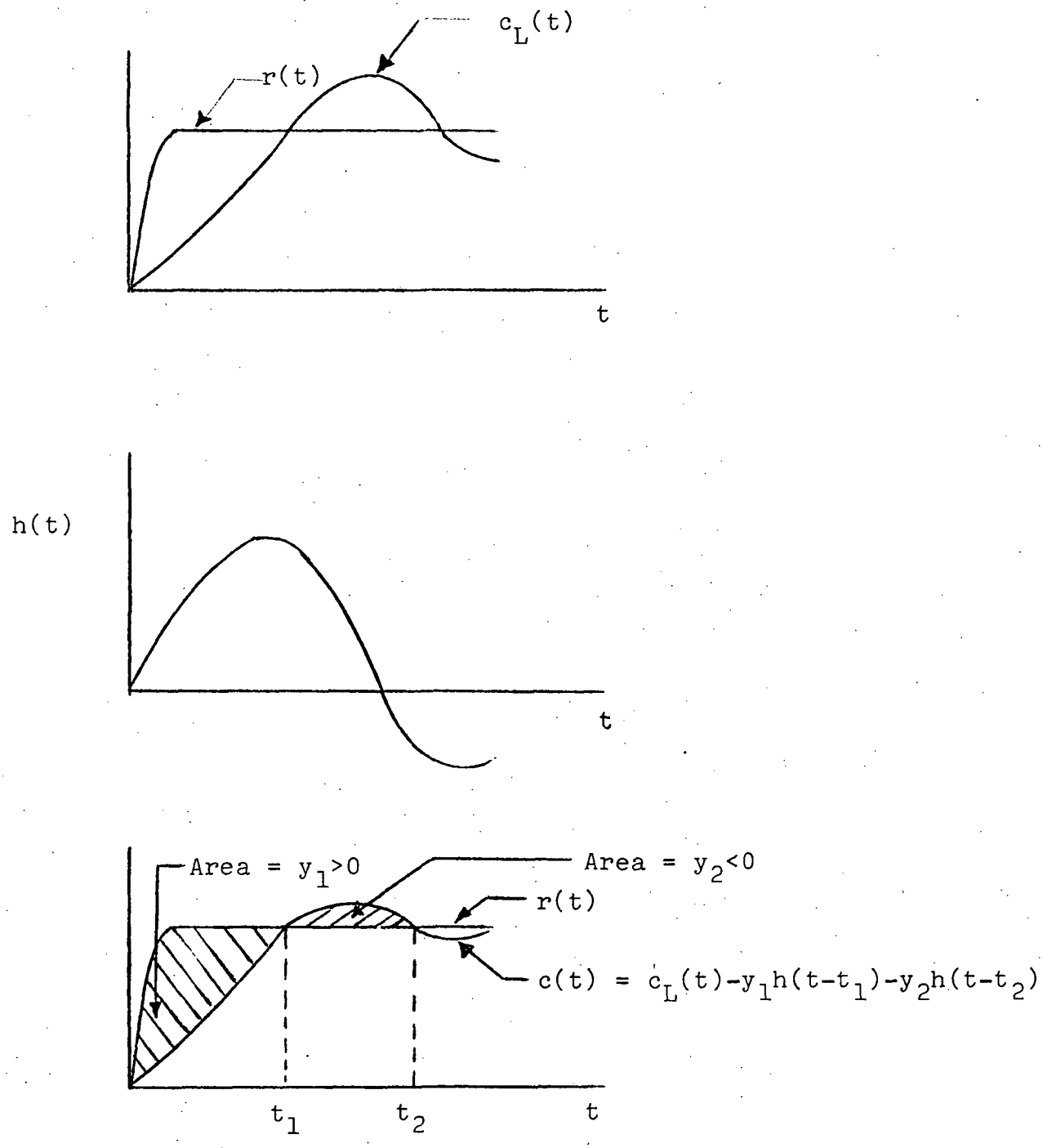

Fig. 3.4: Comparison of Linear and Non-Linear Responses

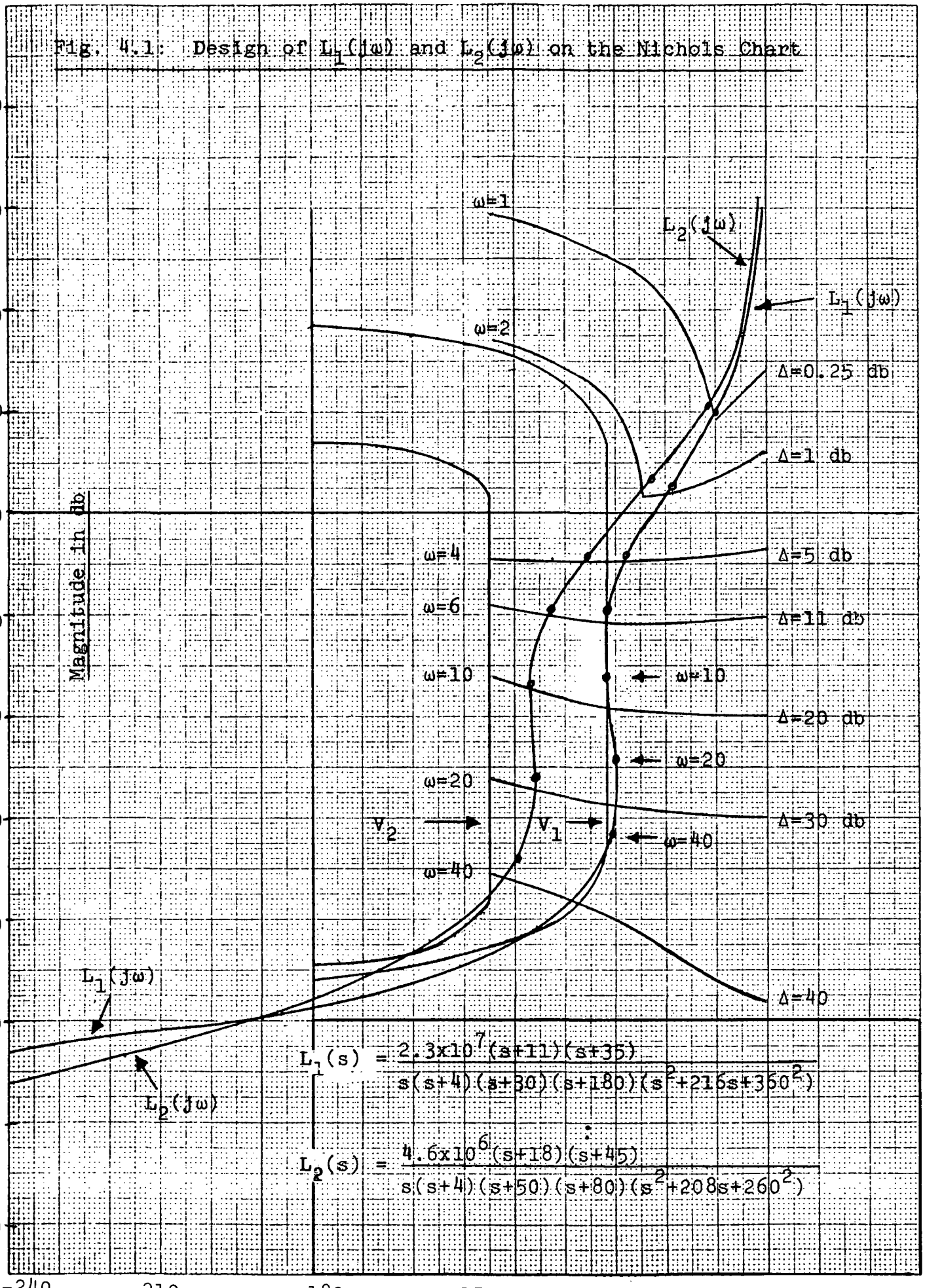
Fig. 4.1: Design of $L_1(j\omega)$ and $L_2(j\omega)$ on the Nichols Chart
Magnitude in db
Phase in Degrees
40
30
20
10
0
-10
-20
-30
-40
-50
-60
-70
-240
-210
-180
-150
-120
-90
ω=1
ω=2
ω=4
ω=6
ω=10
ω=20
ω=40
$L_2(j\omega)$
$L_1(j\omega)$
Δ=0.25 db
Δ=1 db
Δ=5 db
Δ=11 db
Δ=20 db
Δ=30 db
Δ=40
V_2
V_1
$L_1(s) = \frac{2.3\times10^7(s+11)(s+35)}{s(s+4)(s+30)(s+180)(s^2+216s+360^2)}$
$L_2(s) = \frac{4.6\times10^6(s+18)(s+45)}{s(s+4)(s+50)(s+80)(s^2+208s+260^2)}$

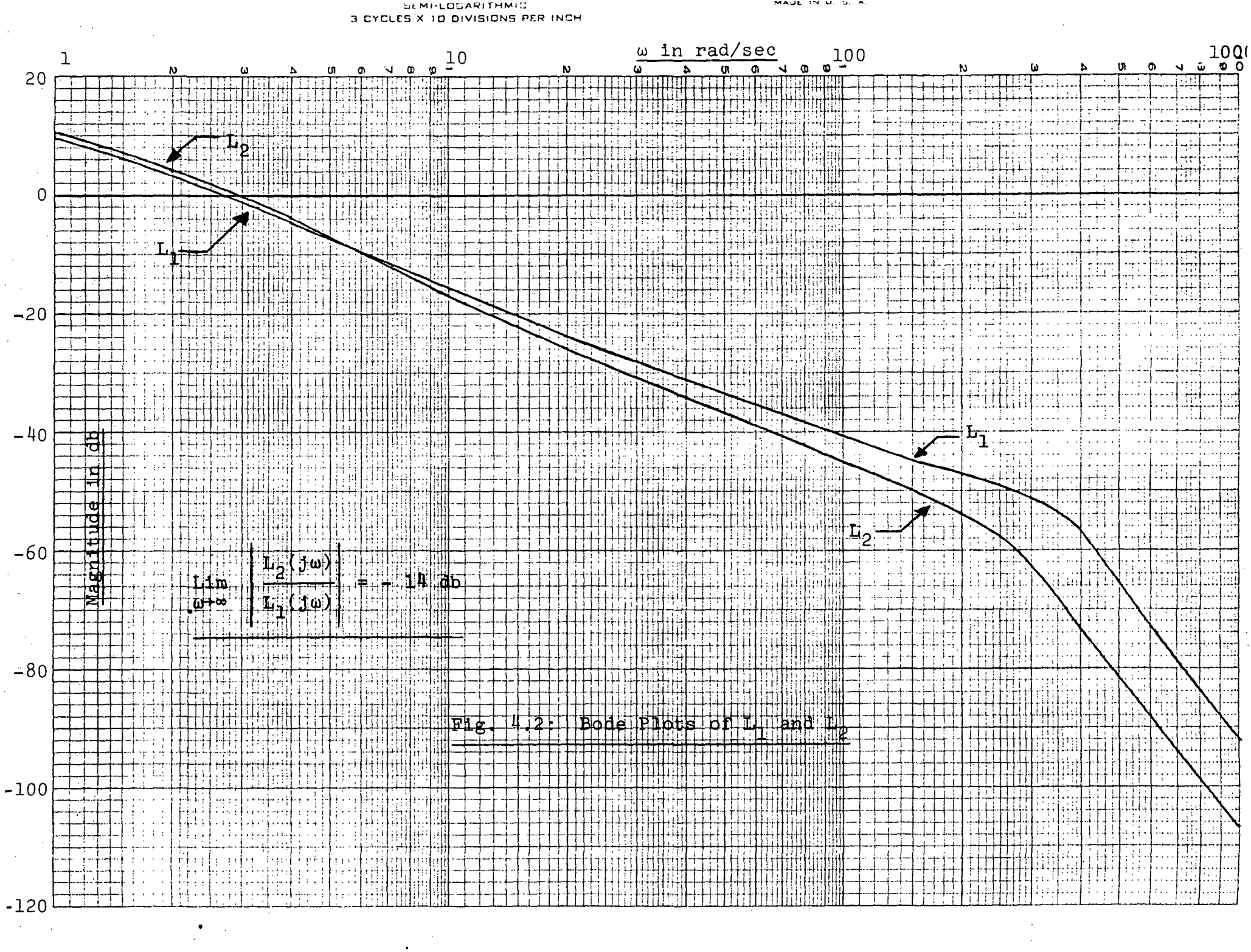

Fig. 4.2: Bode Plots of L_1 and L_2

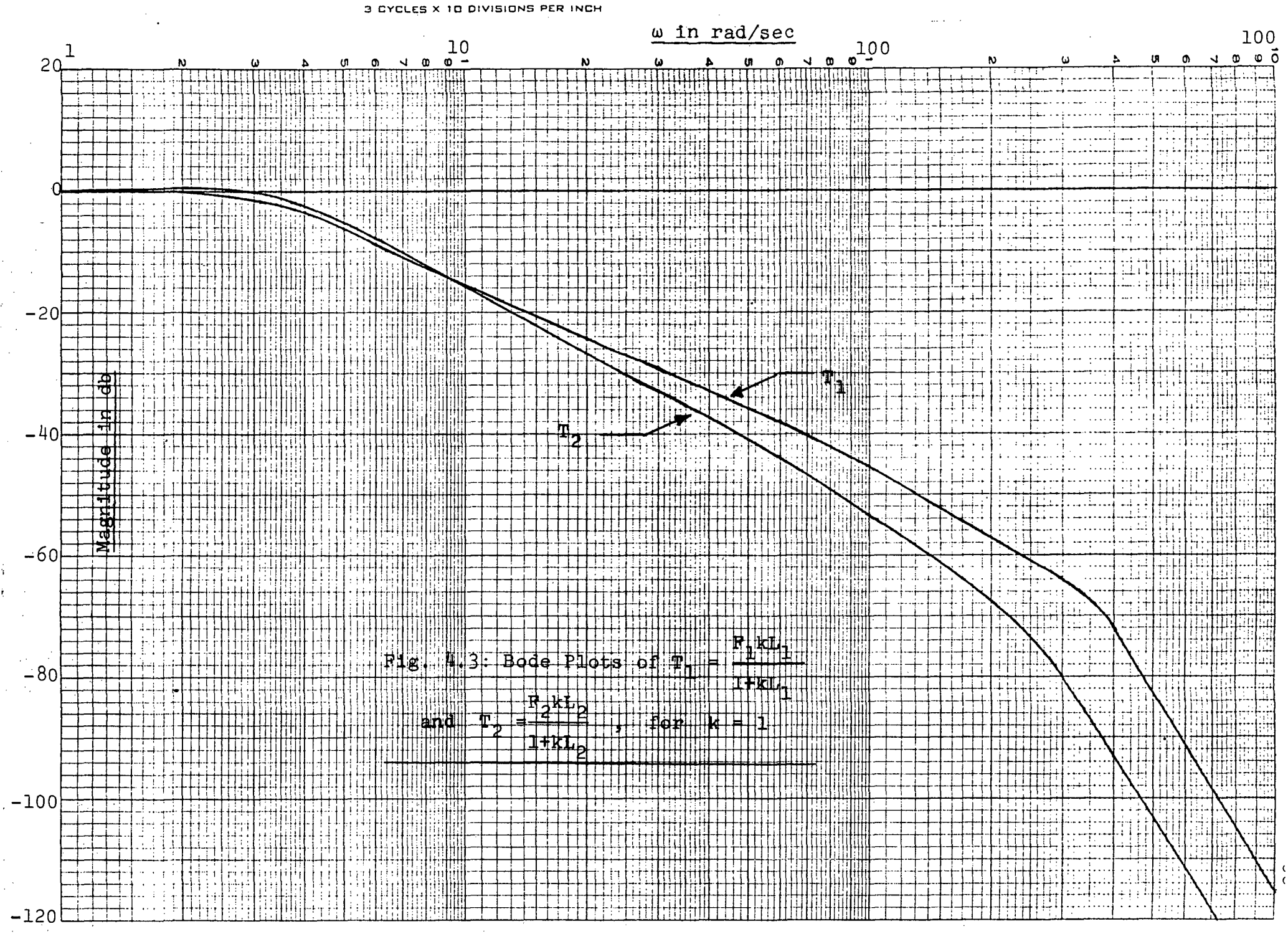

Fig. 4.3: Bode Plots of $T_1 = \dfrac{F_1 kL_1}{1+kL_1}$

and $T_2 = \dfrac{F_2 kL_2}{1+kL_2}$, for $k = 1$

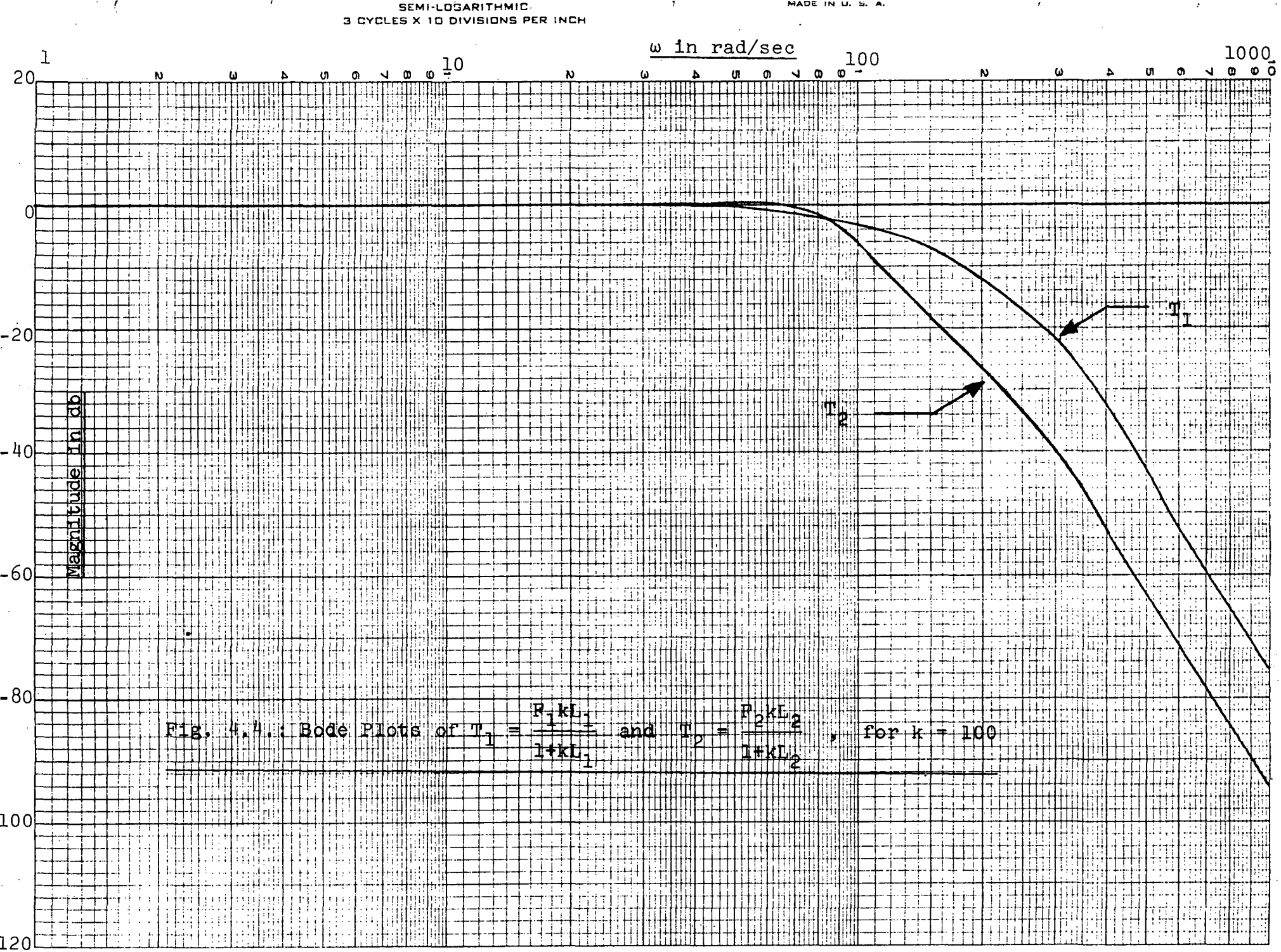

Fig. 4.4.: Bode Plots of $T_1 = \frac{F_1 kL_1}{1+kL_1}$ and $T_2 = \frac{F_2 kL_2}{1+kL_2}$, for $k = 100$

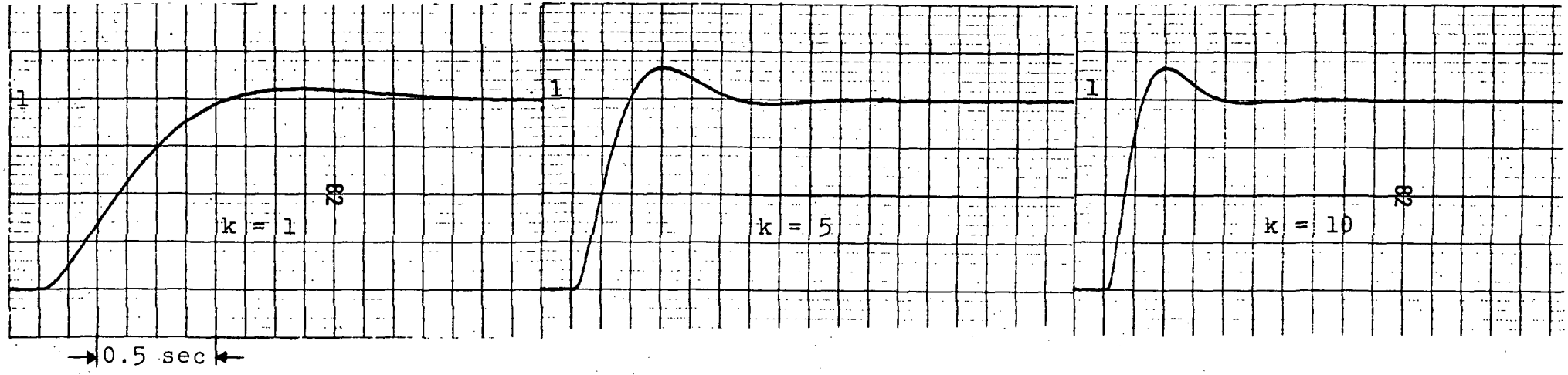

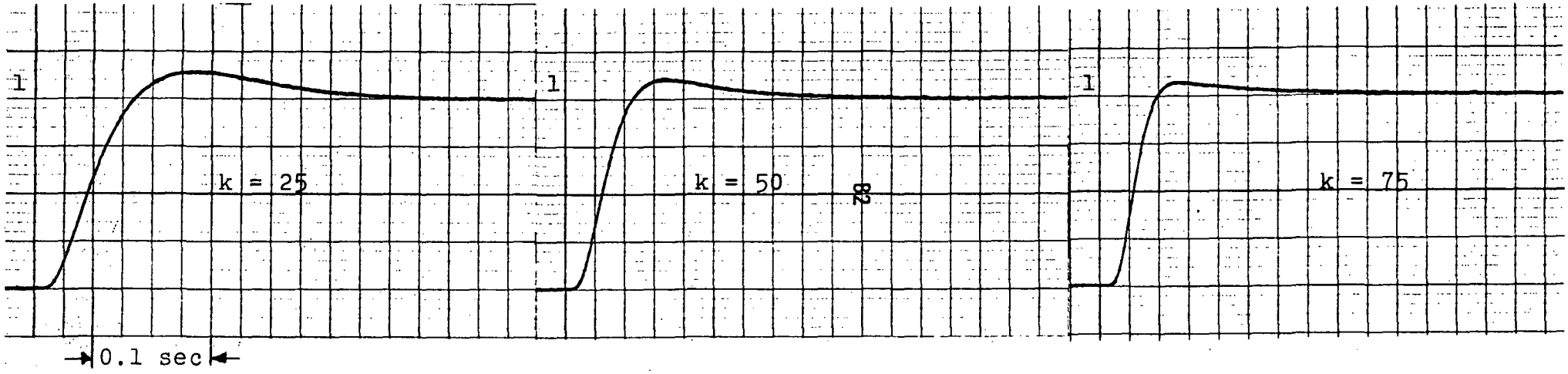

Time Scales

k = 1,5,10 : 1 cm = 0.25 sec.

k = 25,50,75,100: 1 cm = 0.05 sec.

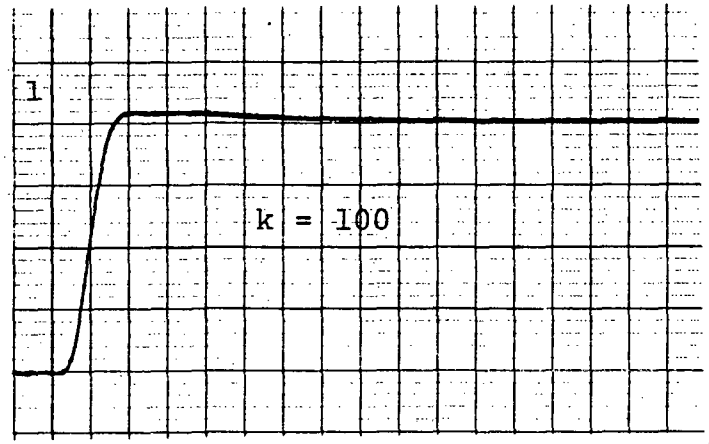

Fig. 4.5-a: Step-Responses of $T_1 = \frac{F_1 kL_1}{1+kL_1}$

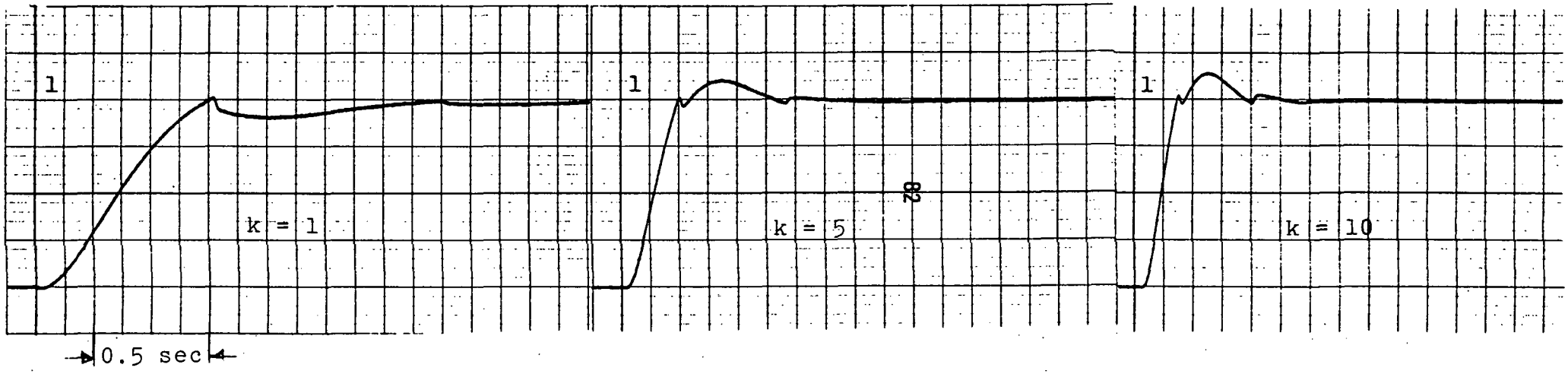

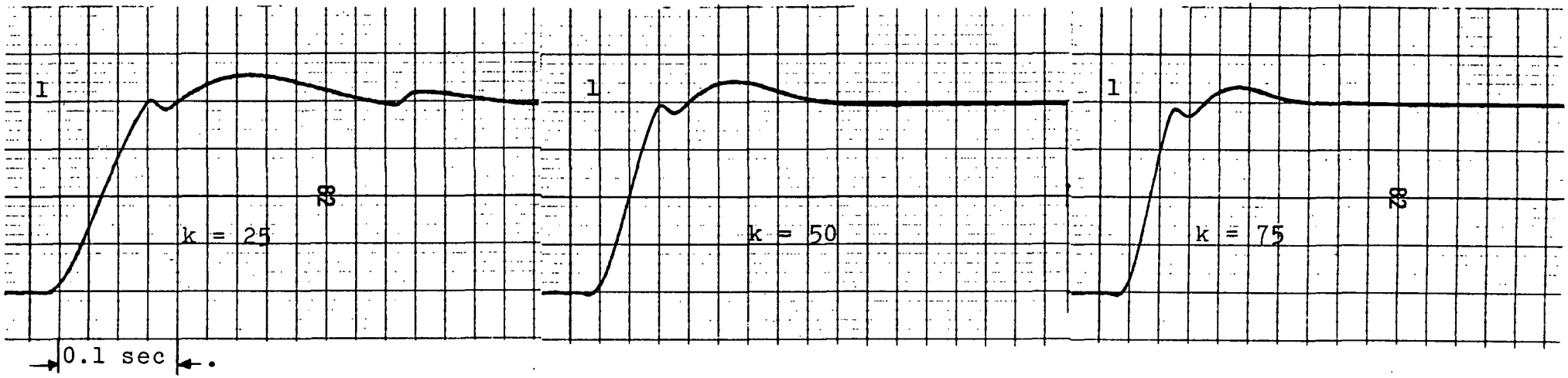

Time Scales

k = 1,5,10: 1 cm = 0.25 sec.

k = 25,50,75,100: 1 cm = 0.05 sec

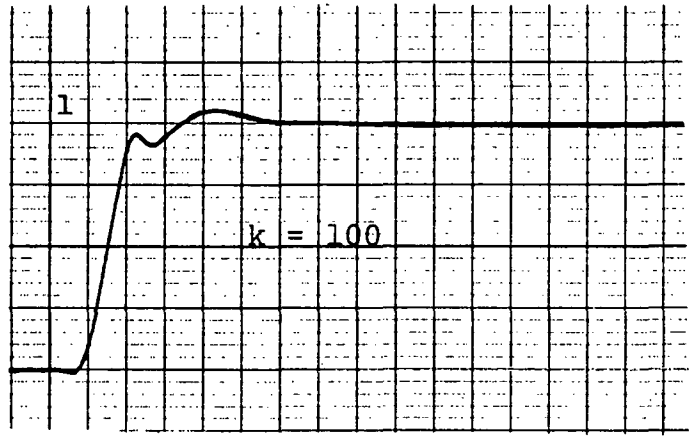

Fig. 4.5-b: Step-Responses of $T_2 = \frac{F_2 kL_2}{1+kL_2}$, Non-Linear

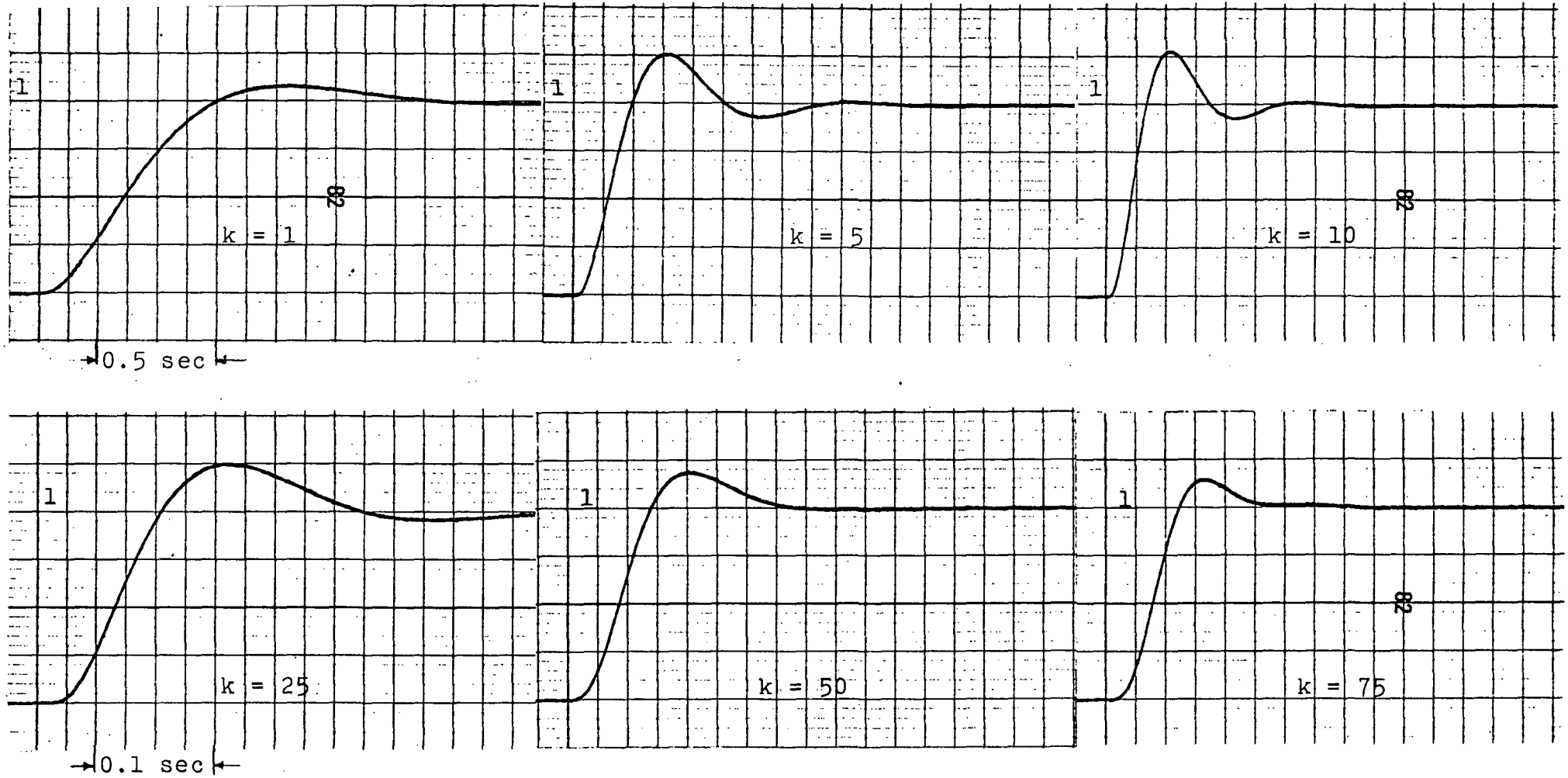

Time Scales:

k = 1,5,10: 1 cm = 0.25 sec.

k = 25,50,75,100: 1 cm = 0.05 sec

Fig. 4.5-c: Step-Responses of of $T_2 = \frac{F_2 k L_2}{1+kL_2}$, Linear

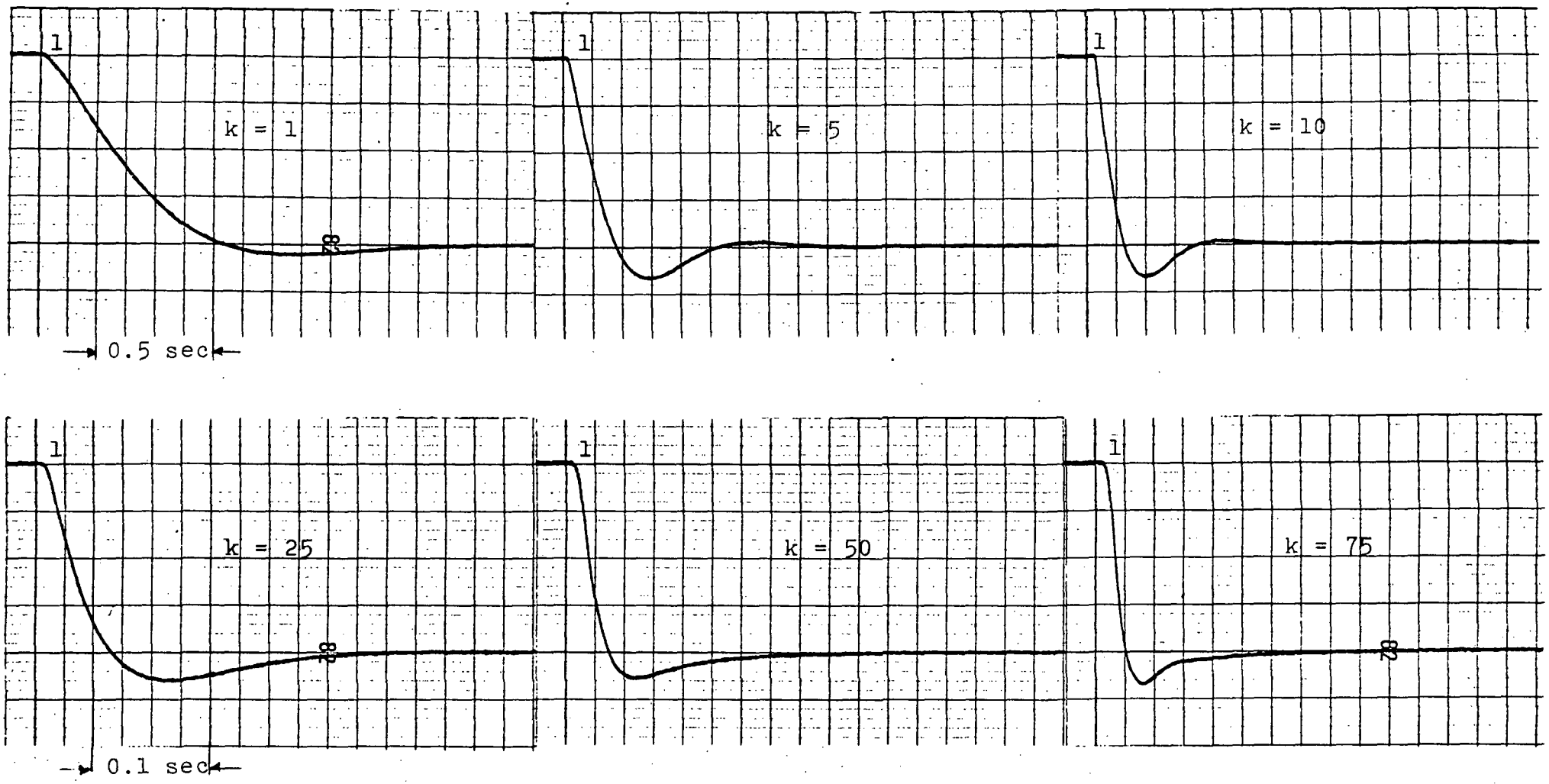

Time Scales:

k = 1,5,10: 1 cm = 0.25 sec.

k = 25,50,75,100: 1 cm = 0.05 sec.

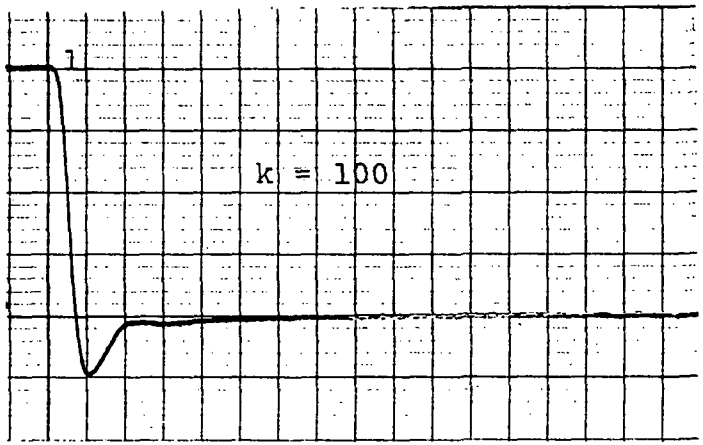

Fig. 4.6-a: Disturbance-Responses of $\frac{kL_1}{1+kL_1}$

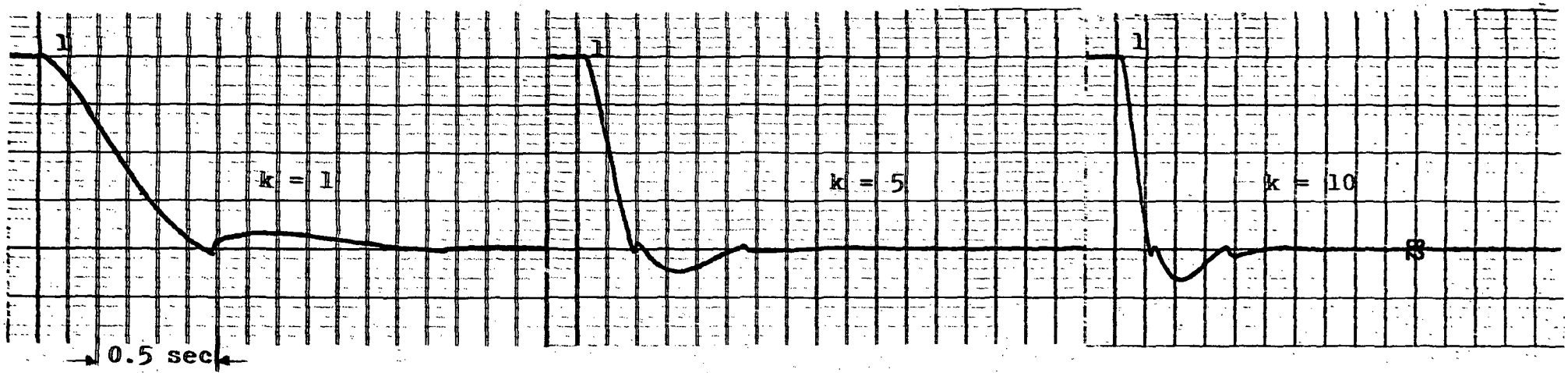

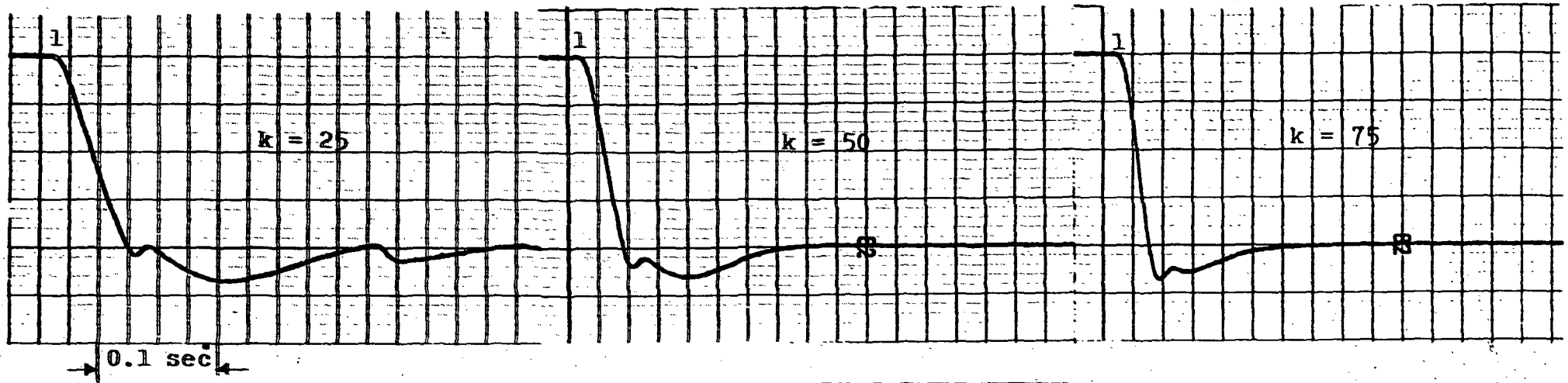

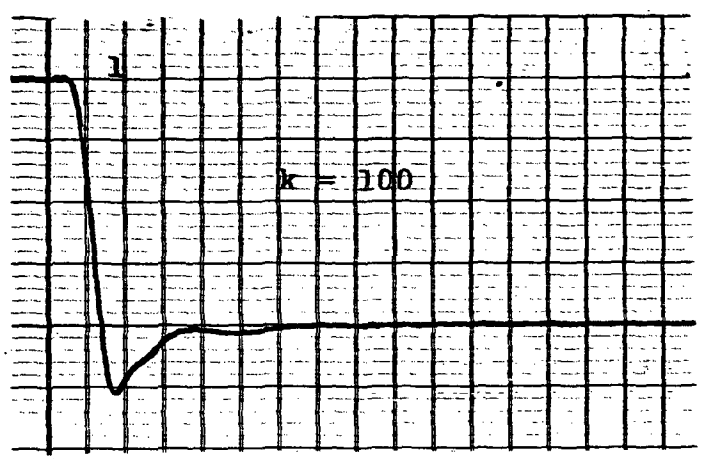

Time Scales

k = 1,5,10: 1 cm = 0.25 sec.

k = 25,50,75,100: 1 cm = 0.05 sec.

Fig. 4.6-b: Disturbance-Responses of $\frac{kL_2}{1+kL_2}$, Non-Linear

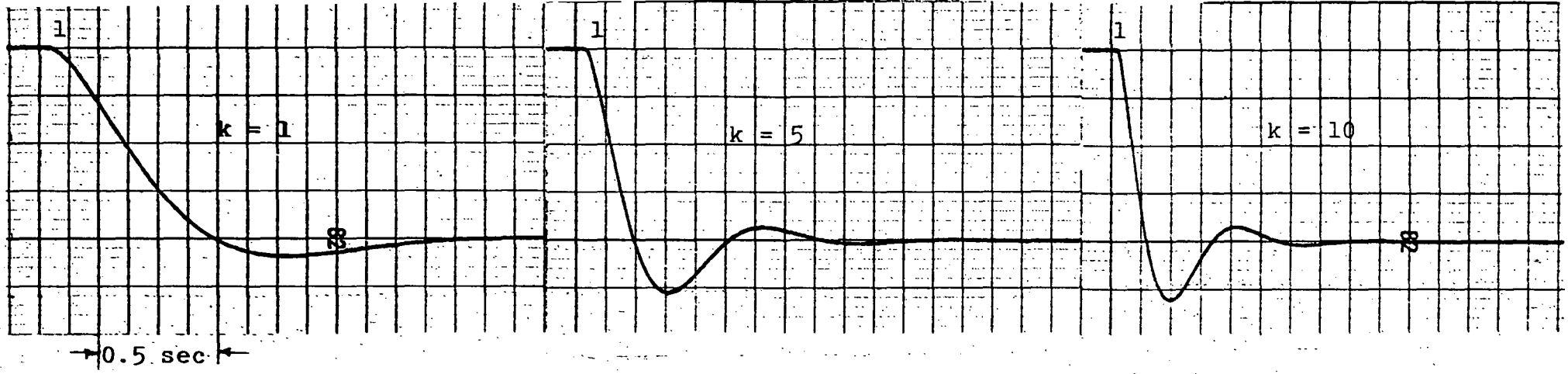

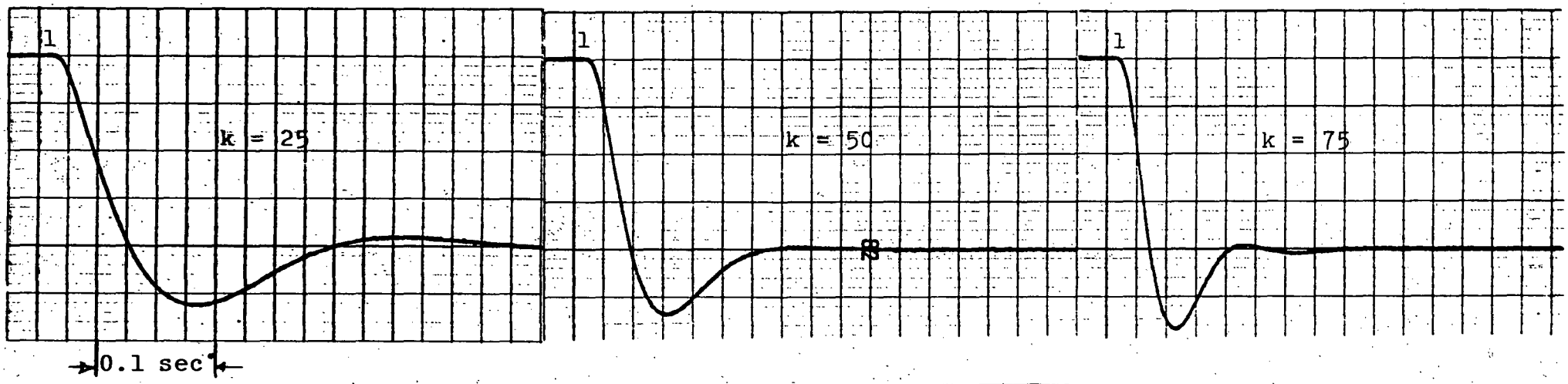

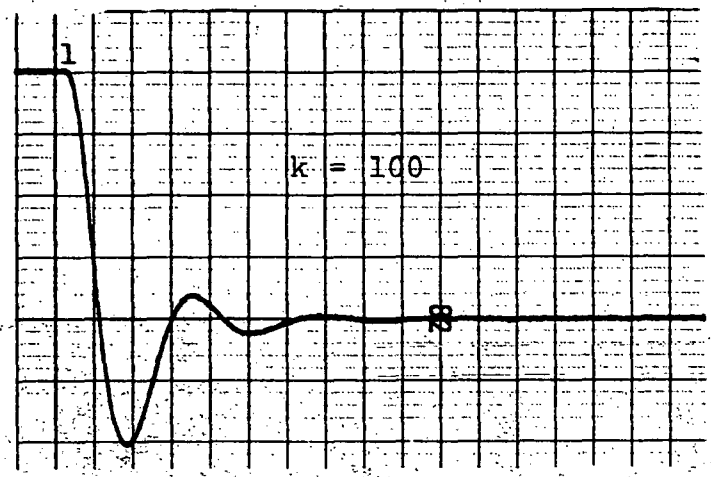

Time Scales:

k = 1,5,10: 1 cm = 0.25 sec.

k = 25,50,75,100: 1 cm = 0.05 sec.

Fig. 4.6-c: Disturbance-Responses of $\frac{kL_2}{1+kL_2}$, Linear

Bandwidth of Input Noise $\approx$ 15 * [Bandwidth of $(\frac{100L_2}{1+100L_2})$]

Peak-to-Peak Value of Noise $\approx$ 36 volts

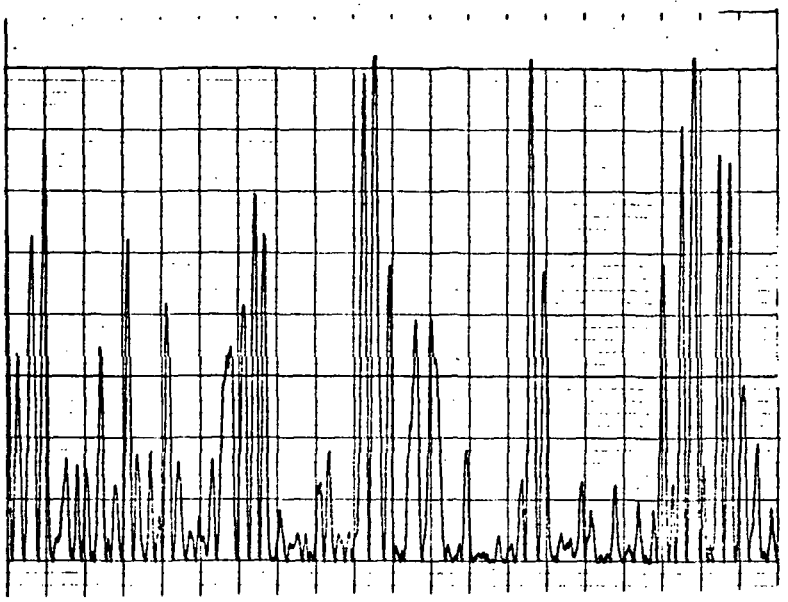

L_1

All three figures have the same scales

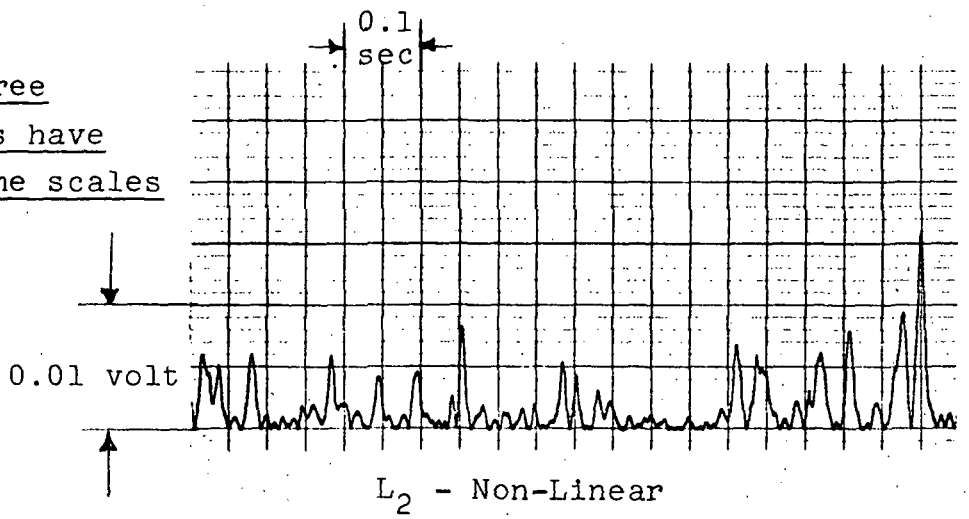

L_2 - Non-Linear

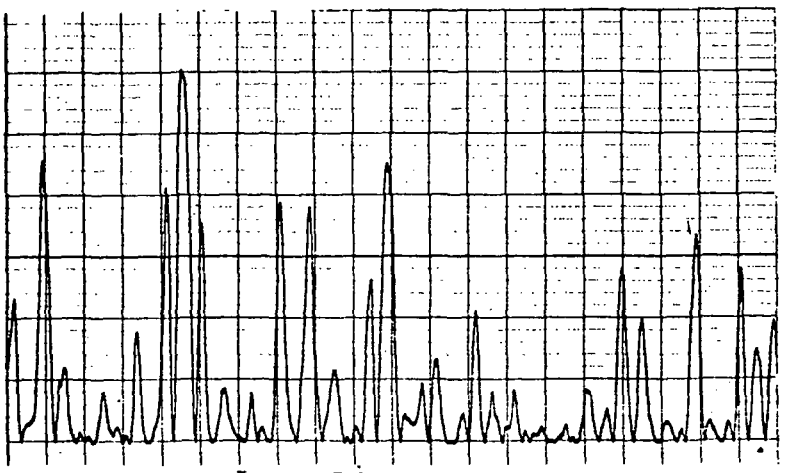

L_2 - Linear

Fig. 4.7: Output Noise-Power of $[\frac{100L}{1+100L}]$ with Zero-Mean Input Noise

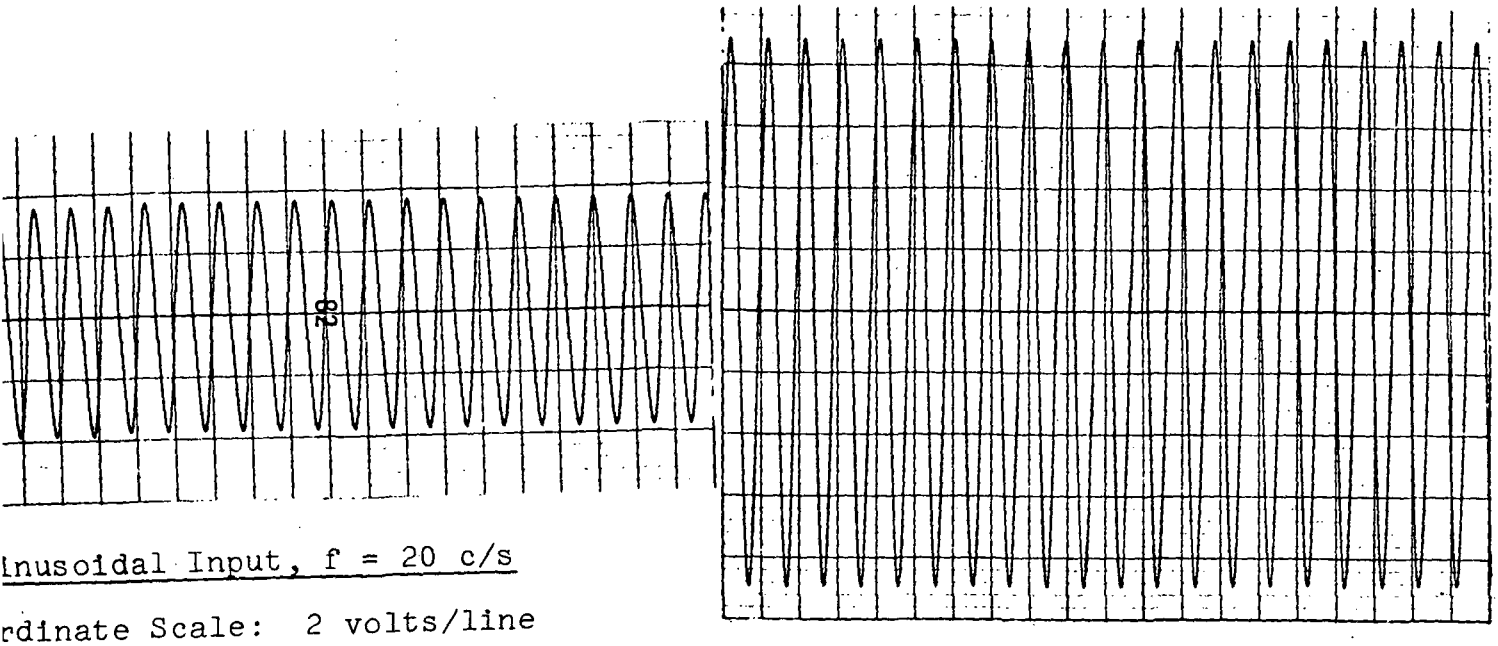

Inusoidal Input, f = 20 c/s

rdinate Scale: 2 volts/line

ime Scale: 1 cm = 0.1 sec.

T_1

esponse Scales (Same for all three responses)

rdinate: 0.5 volt/line

ime: 1 cm = 0.1 sec.

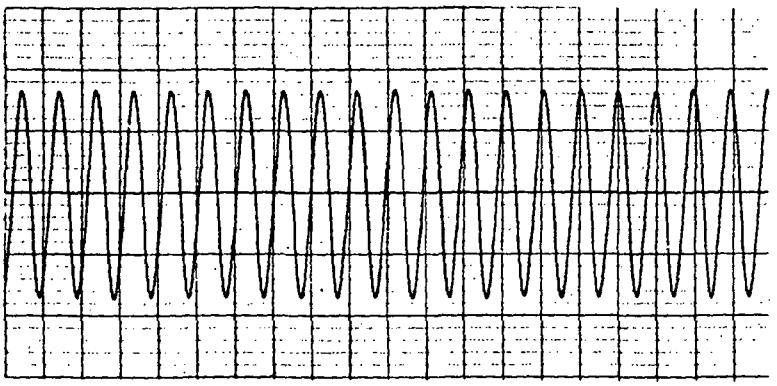

T_2 - Non-Linear

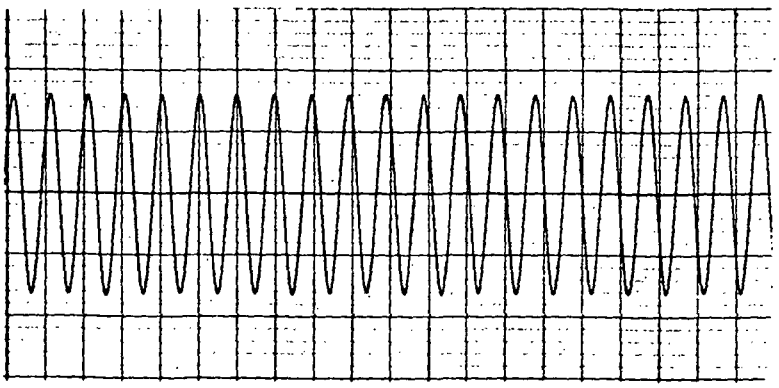

T_2 - Linear

Fig. 4.8: Sinusoidal Response of $T = F[\frac{100L}{1+100L}]$

Ramp - Input = 40 t

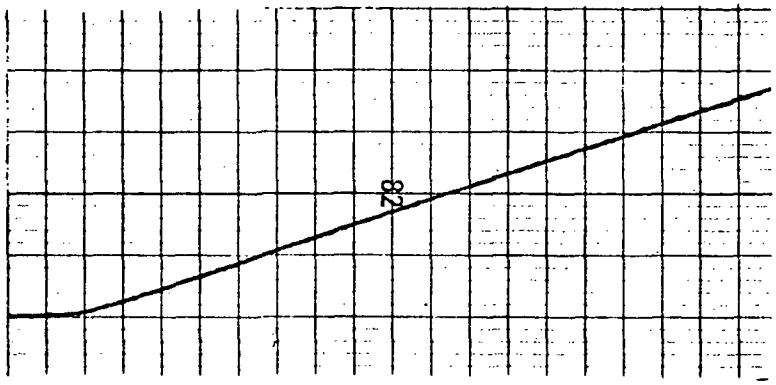

T_1

All three figures have the same scales

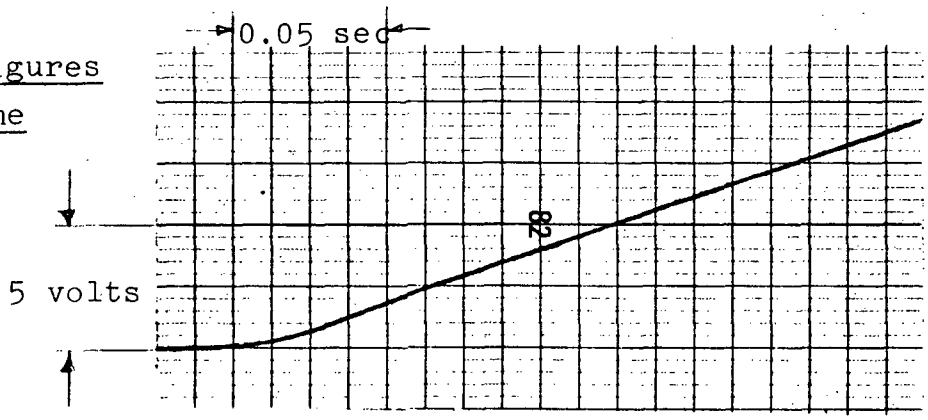

T_2 - Non-Linear

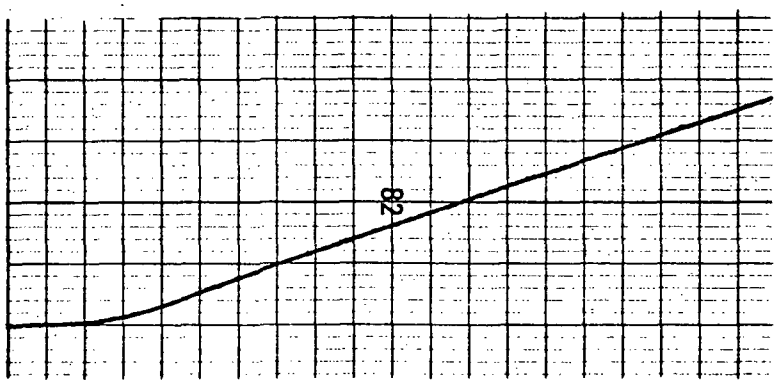

T_2 - Linear

Fig. 4.9: Ramp-Response of $T = F\left[\frac{100L}{1+100L}\right]$

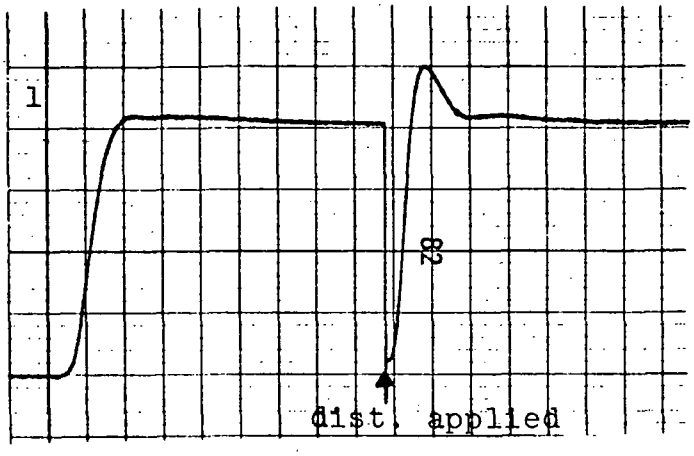

T_1

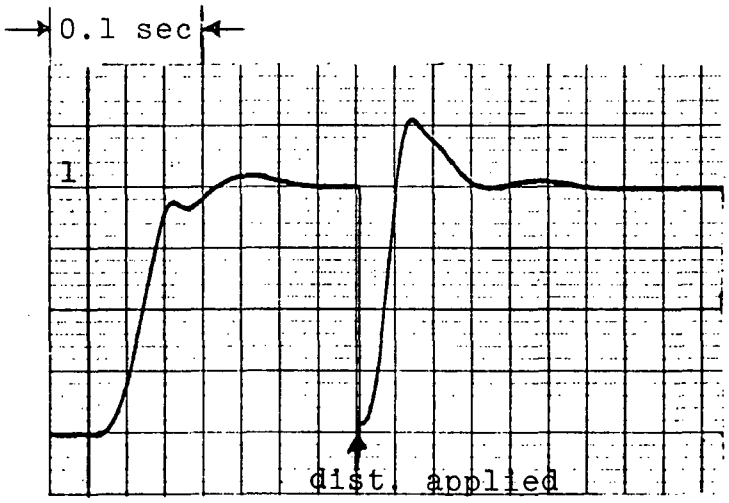

T_2 - Non-Linear

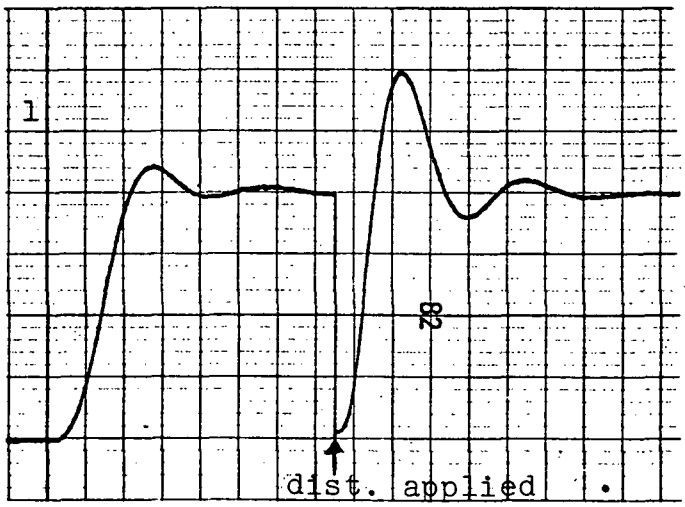

T_2 - Linear

Fig. 4.10: Response of $T = F\left[\frac{100L}{1+100L}\right]$ to Output Disturbance in Presence of Command-Step

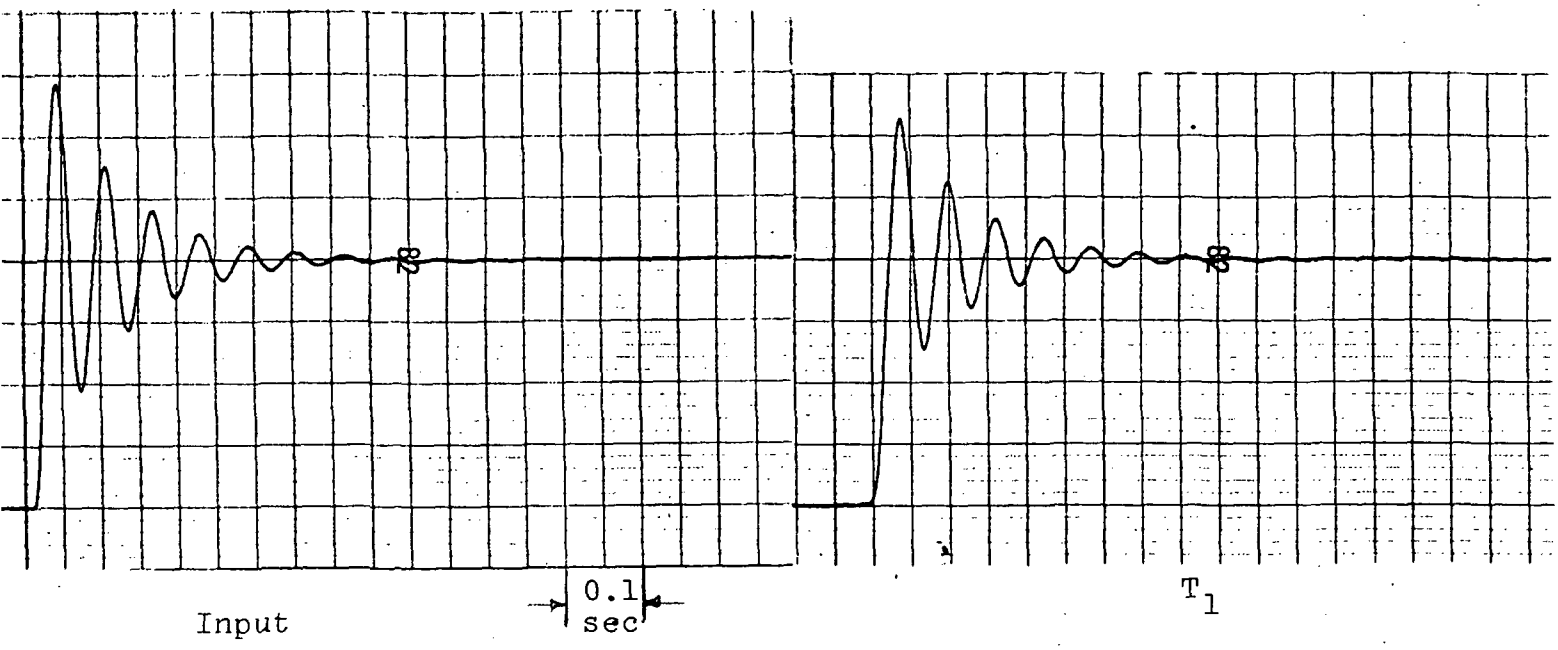

Scales (same for all four figures)

Ordinate: 2 volts/line

Time: 1 cm = 0.1 sec.

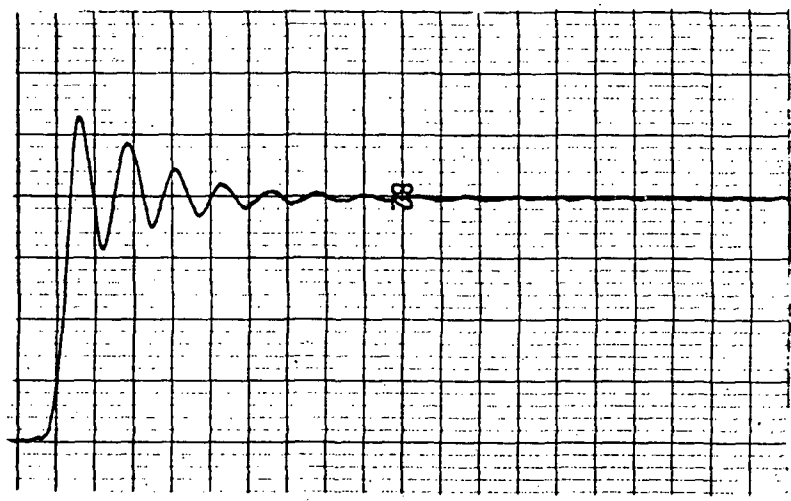

T_2 - Non-Linear

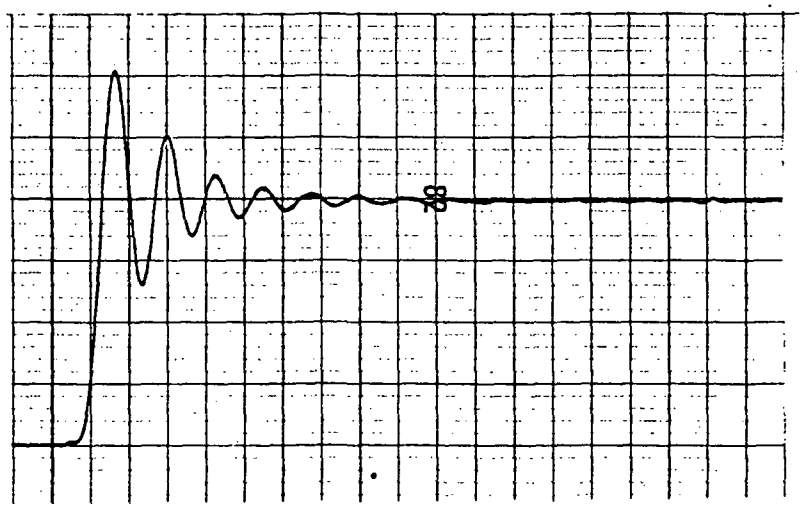

T_2 - Linear

Fig. 4.11-a: Linear and Non-Linear Responses

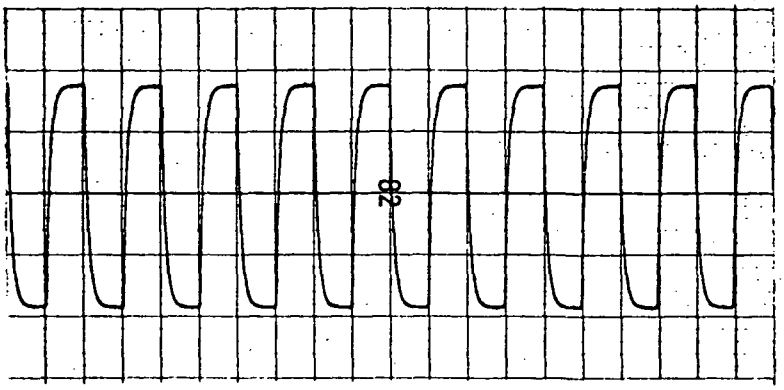

Input, f = 10 c/s

Scales for all 4 figs.

Ordinate: 2 volts/line

Time: 1 cm = 0.1 sec

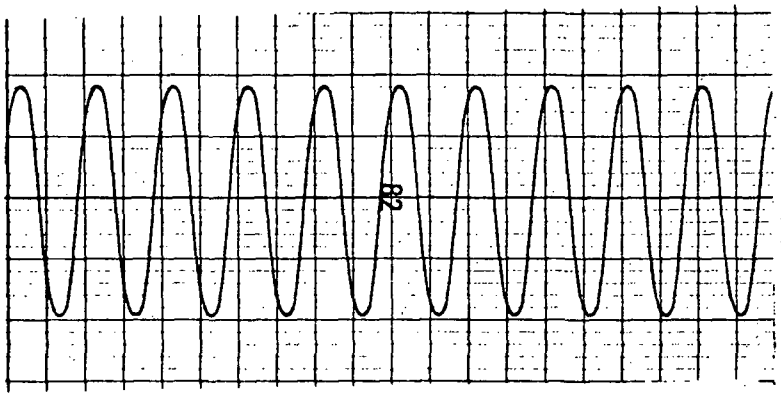

T_1

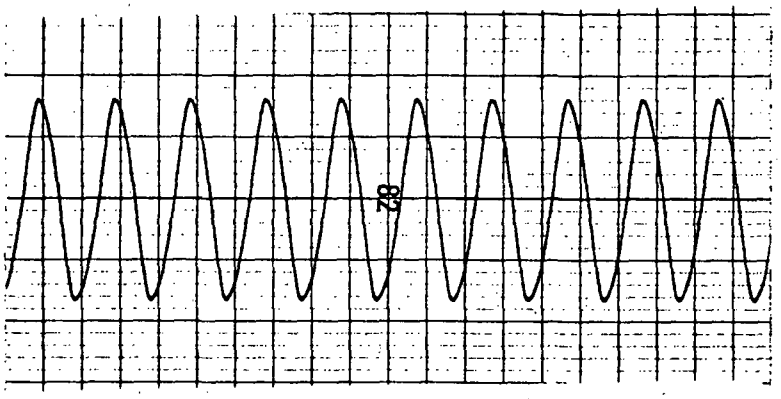

T_2 - Non-Linear

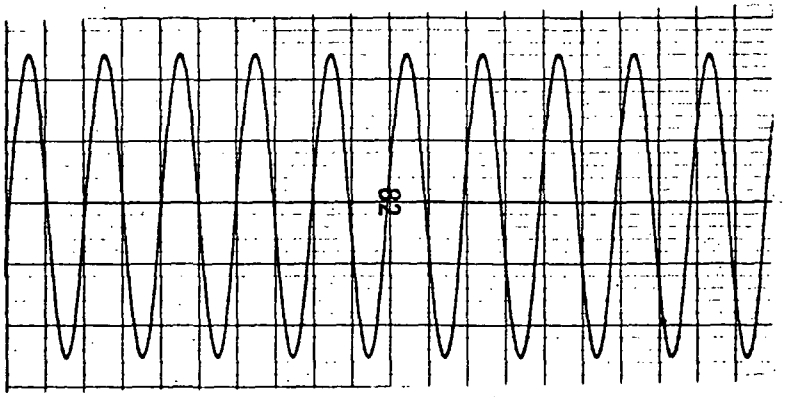

T_2 - Linear

Fig. 4.11-b: Linear and Non-Linear Responses

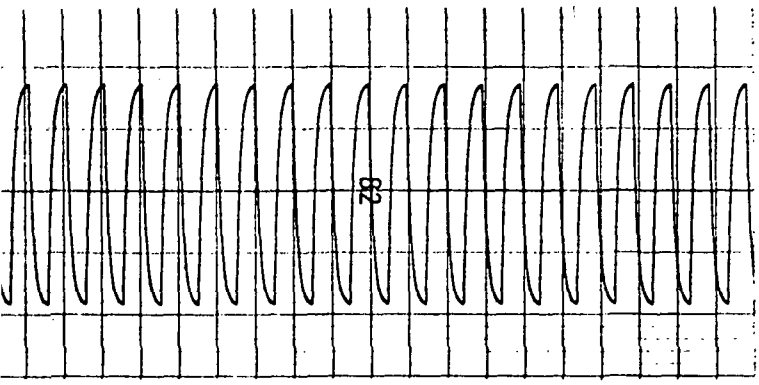

Input, f = 20 c/s

Ordinate: 2 volts/line

Time: 1 cm = 0.1 sec.

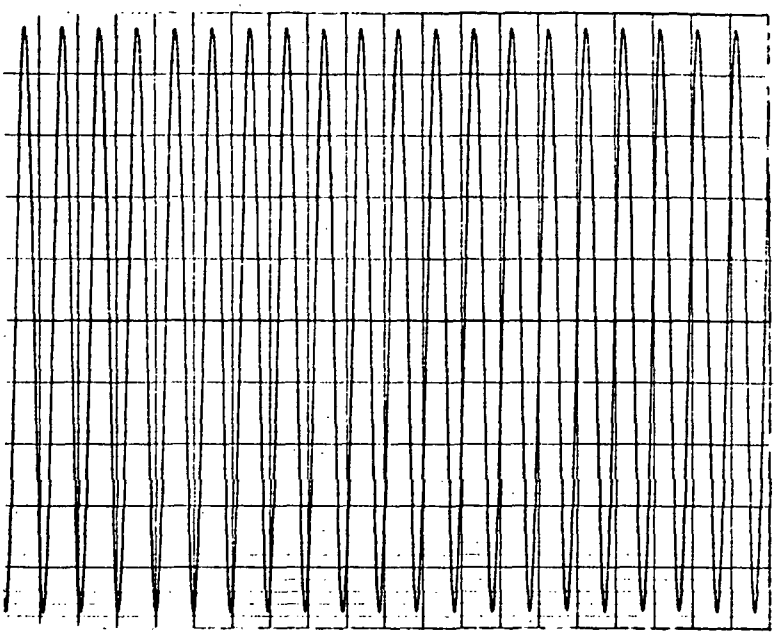

T_1

Response Scales (for all three responses)

Ordinate: 0.5 volt/line

Time: 1 cm = 0.1 sec.

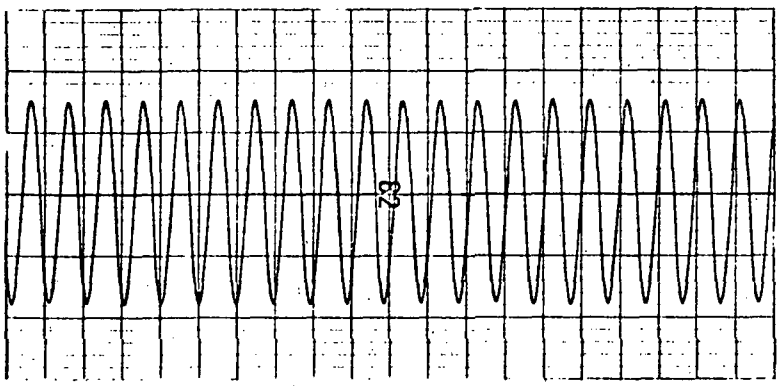

T_2 - Non-Linear

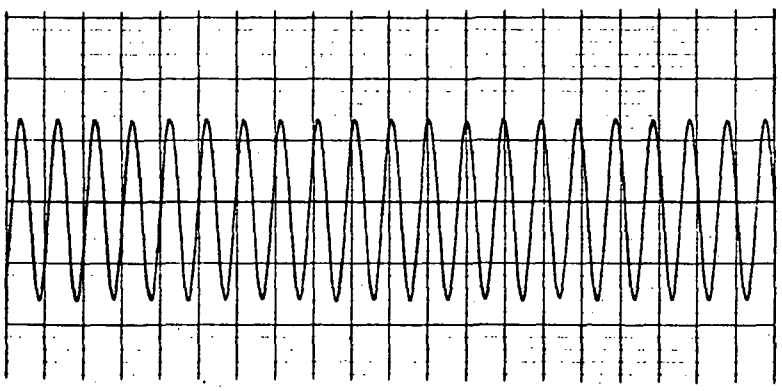

T_2 - Linear

Fig. 4.11-c: Linear and Non-Linear Responses

REFERENCES

1. I.M. Horowitz and M. Sidi, "Synthesis of Feedback Systems with Large Plant Ignorance for Prescribed Time Domain Tolerances," (To appear in International Journal of Control, 1972).

2. I.M. Horowitz, "Optimum Loop Transfer Function in Single-Loop Minimum Phase Feedback System," (To appear in International Journal of Control, 1973).

3. J.C. Clegg, "A Non-Linear Integrator for Servomechanisms," Trans. AIEE, Part II, Appl. Ind., vol. 77, March, 1958, pp. 41-42.

4. A. Gelb and W.E. Vander Velde, Multiple-Input Describing Functions and Non-Linear System Design, McGraw-Hill, 1968, pp. 79-81, 315-317.

5. D. Slepian, "The One-Sided Barrier Problem for Gaussian Noise," Bell System Technical Journal, Vol. 41, March, 1962, pp. 463-501.

6. A. Gelb and W.E. Vander Velde, Reference [4], pp. 366-367.

7. J.E. Gibson, Non-linear Automatic Control, McGraw-Hill, 1963, pp. 385-386.

APPENDIX

A.1 Calculation of $\frac{\partial M_n}{\partial \delta}(\delta, b)$

From Equation (2.17) on page 24, setting $\phi = \cos^{-1}\delta$,

$$M_n(\delta, b) = M_n(\cos\phi, b)$$

$$= \frac{b}{1+b} e^{-\pi\cot\phi} - \frac{2\cos\phi}{1+b} e^{-\phi\cot\phi}$$

$$\frac{\partial M_n}{\partial \phi} = \frac{b}{1+b}(\pi \operatorname{cosec}^2\phi e^{-\pi\cot\phi}) - \frac{2e^{-\phi\cot\phi}}{1+b}\{-\sin\phi+\phi\cos\phi\operatorname{cosec}^2\phi - \cos\phi\cot\phi\}$$

$$= \frac{1}{(1+b)\sin^2\phi}\left[\pi b e^{-\pi\cot\phi} + 2e^{-\phi\cot\phi}(\sin\phi - \phi\cos\phi)\right]$$

$$\geq 0 \quad , \quad 0 \leq \phi \leq \frac{\pi}{2} \quad (\text{i.e. } 0 \leq \delta \leq 1) .$$

Now,

$$\frac{\partial M_n}{\partial \delta} = \frac{\partial M_n}{\partial \phi}\frac{\partial \phi}{\partial \delta}$$

$$= \frac{\partial M_n}{\partial \phi}\frac{\partial(\cos^{-1}\delta)}{\partial \delta}$$

$$= -\frac{1}{\sqrt{1-\delta^2}}\frac{\partial M_n}{\partial \phi} \leq 0 \quad , \quad 0 \leq \delta < 1 .$$

A.2 Calculation of b in Non-Linear Design of Chapter IV

We use Equation (3.1) on page 44 with $\phi_1 \triangleq \cos^{-1}\delta_1$, $\phi_2 \triangleq \cos^{-1}\delta_2$.

$$e^{-\pi\cot\phi_1} = \frac{1}{1+b}\left[b - 2\delta_2 e^{\cot\phi_2(\pi-\phi_2)}\right] e^{-\pi\cot\phi_2}$$

$$= \frac{1}{1+b}\left[be^{-\pi\cot\phi_2} - 2\delta_2 e^{-\phi_2\cot\phi_2}\right]$$

From the linear design, $\delta_1 = 0.5$ and therefore, $\phi_1 = 60°$ and $e^{-\pi\cot\phi_1} = 0.164$. With $\delta_2 = 0.3$ in the non-linear design, $\phi_2 = 72.5° = 1.265$ radians, and $e^{-\pi\cot\phi_2} = 0.374$. $2\delta_2 e^{-\phi_2\cot\phi_2} = 0.403$. Thus,

$$0.164 = \frac{1}{1+b}\ [0.374b - 0.403]$$

$$b = \frac{0.403 + 0.164}{0.374 - 0.164} = \frac{0.567}{0.21} = 2.7 \quad .$$